AN EXPERIMENTAL AND THEORETICAL INVESTIGATION OF UNSTABLE FISCHER CHROMIUM CARBENE COMPLEXES

A thesis submitted in fulfilment of the requirements for the degree of

MASTER OF SCIENCE

Of

RHODES UNIVERSITY

By

Che Makanjee

December 2012

Abstract

This organometallic study involves the use organostannanes and organolithiums as precursors to chromium Fischer carbene complexes. Fischer carbenes are typically electrophilic and are stabilized by a single π-donor substituent, and contain low oxidation state metals (often but not always from Group 6). They are highly reactive and can give access to a range of biologically active compounds through cyclopropanations, insertions, coupling and photochemical reactions.

Synthesis and characterization of three MOM-protected α-alkoxy organostannanes was successfully carried out *via* a nucleophilic addition of tributylstannyllithium to suitable aldehydes, and immediate protection of the alcohol with MOM. Two *N*-BOC protected α-amino organostannanes were successfully synthesized and characterized *via* α-lithiation and tin-lithium exchange in the presence of TMEDA.

Tin-lithium transmetallation of the organostannanes allowed access to the organolithiums required for the synthesis of novel Fischer carbenes. Addition of chromium hexacarbonyl to the organolithiums formed the acylpentacarbonyl chromate salt which was alkylated with Meerwein salt, resulting in the Fischer carbene and a by-product, tetrabutyltin, which proved difficult to remove. Several Fischer carbenes were synthesized and characterized, some simple and known and some novel.

In silico work explored the reaction coordinate of the [2+2] cycloaddition towards the formation of β-lactams, and the photoactivation cycle that precedes this process. Computational work also showed the effect of the ligand on the stability and reactivity of the carbene. It was found that in some cases the oxygen on the ligand could negatively influence the stability of the carbene (when compared to a simple methyl carbene). A link between bond orders and back donation in Fischer carbenes was explored in an attempt to theoretically predict the stability of a range of carbenes.

Table of Contents

List of Figures

List of Tables

List of Abbreviations

AIM	atoms in molecules
B3	Becke's three-parameter hybrid functional
B3LYP	Becke (3-parameter), Lee, Yang, Parr functional
BLYP	Becke, Lee, Yang, Parr functional
BOC	*t*-butoxycarbonyl
BuLi	butyllithium
CI	configuration interaction
CO	carbonyl
DCD	Dewar-Chatt-Duncanson
DCM	dichloromethane
DEPT	Distortionless Enhancement by Polarisation Transfer
DFT	density functional theory
DMA	*N*,*N*-dimethylaniline
DMAP	*N*,*N*-dimethylaminopyridine
e	electron
Et_2O	diethyl ether
GEA	generalized expansion approximation
GGA	generalized gradient approximation
h	hour(s)
HK	Hohenberg-Kohn
HMQC	heteronuclear multiple bond correlation
HOMO	highest occupied molecular orbital
HSBC	heteronuclear single quantum coherence
HSE	Heyd, Scuseria, Ernzerhof functional
IR	infra-red
ISC	inter system crossing
KS	Kohn-Sham
L	ligand
LDA	local density approximation
LDA	lithium diisopropylamide
LF	ligand field
LST	linear synchronous transit
LUMO	lowest unoccupied molecular orbital

M	metal
MD	molecular dynamics
min	minute(s)
MLCT	metal-ligand charge transfer
MM	molecular mechanics
MOM-Cl	chloromethyl methyl ether
NHC	*N*,*N'*-heterocyclic carbene
NMR	nuclear magnetic resonance
PBE	Perdew, Burke, Ernzerhof functional
PM-IRRAS	polarization modulation infra-red reflection absorption spectroscopy
PNA	peptide nucleic acid
ppm	parts per million
PW91	Perdew & Wang 1991 functional
QST	quadratic synchronous transit
Rf	retardation factor
t-Bu	*tert*-butyl
THF	tetrahydrofuran
TLC	thin-layer chromatography
TMEDA	*N*,*N*,*N'*,*N'*-tetramethylethylenediamine
V-QMC	variational-quantum Monte-Carlo

Acknowledgements

The sincerest thanks go to my supervisor, Dr Rosa Klein for guiding and watching over me, and throwing light over the darkness in front of me, from my undergraduate years through to my postgraduate years. Her carefully worded emails and suggestions are always so well designed. Her insights extend far beyond the realms of chemistry and science, and will stay with me throughout life.

For all his help with the computer modelling, I give thanks to Dr Kevin Lobb. Always willing to help wherever possible, and with the ability and know-how to fix any computer, he brings a vast knowledge of chemistry and physics together, making it seem easier than it is.

The family of F22 created an effervescent atmosphere to work in, which I thank them for. Particular thanks must go to Annalene, for striving to make things seem possible, and Tope, for being just about the friendliest person I have ever met (and a walking chemistry textbook). A special mention must go to Mrs I (now Dr) and Lulama for occasionally igniting the effervescent atmosphere.

My friends, the people I am most proud to know, have helped me more than they imagine. By believing without doubt in what at times seemed the most impossible of tasks. This could not have been reached without inspiration and support from my friends. Each of you have a warm fuzzy place forever.

My family, for giving me these opportunities in life and picking me up when I felt the world had it out for me.

Finally, to the NRF for their gracious funding without which this would not have been remotely possible.

Chapter 1:Introduction

1.1. Organometallic Methods in Organic Synthesis

1.1.1. A Background to Organometallic Chemistry

Organometallic chemistry is often regarded as a subfield of inorganic chemistry, but since it incorporates strong elements of organic and materials chemistry, it enjoys wide-ranging applications, including in biological and analytical chemistry.[1] Generally defined, an organometallic molecule is one that contains a metal-carbon bond; hence organometallic chemistry also looks at the transformations of organic compounds using metals. This definition is not strictly followed by all chemists. Occasionally, a molecule might be referred to as organometallic if it is synthesized by or will be used in an organometallic reaction, and if the chemistry of the molecule can be thought of in terms of organometallic principles. Since many organometallic compounds are intermediates in reactions, the focus of research in the field is usually on understanding and tuning the reactivity.[1]

Credit for the first organometallic compound synthesized has been given to Louis Claude Cadet de Gassicourt, who prepared an organoarsenic compound in 1757. He did this by thermally inducing a reaction between arsenious oxide and potassium acetate (Equation 1).[2] This was called Cadet's Fuming Liquid.

$$As_2O_3 + 4CH_3COOK \longrightarrow [AsMe_2]_2$$

Equation 1: Reaction giving the first organometallic compound, an organoarsenide[2]

Soon after the discovery of Cadet's Fuming Liquid, William Zeise prepared a complex of platinum and ethylene by reaction of $PtCl_4$ with boiling ethanol. This is known as Zeise's salt (Figure 1a) and was one of the earliest examples demonstrating *hapticity* as a concept, since it has an η^2-ethylene ligand. It was only in the 20th century that the molecular structure of this compound was unequivocally determined *via* X-ray diffraction.

(a) (b)

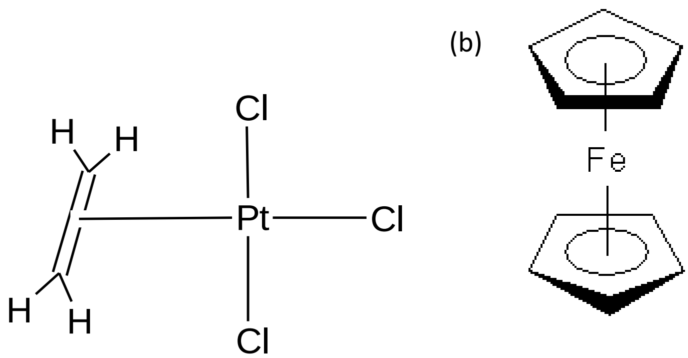

Figure 1: (a) Zeise's salt, showing η^2 hapticity, (b) Ferrocene, showing η^5 hapticity

Progress in organometallic chemistry increased rapidly from this point, with Charles Friedel and James Crafts preparing organochlorosilanes in 1863, Alfred Werner exploring the ideas of what we now know as coordination chemistry, and the preparation of the first Grignard reagents by Victor Grignard[3] (who was awarded the Nobel Prize in Chemistry[4] in 1912 for his work) in 1899. In 1917, Wilhelm Schlenk discovered organolithium compounds and later established the well-known Schlenk equilibrium equation for organomagnesium compounds (Equation 2).[2]

$$2RMgX \rightleftharpoons MgX_2 + MgR_2$$

Equation 2: Schlenk equilibrium for organomagnesium compounds[2]

A popular example in organometallic chemistry is the ferrocene molecule (Figure 1b), $Fe(C_5H_5)_2$. As with many discoveries, it was an accidental one. Pauson and Kealy reacted cyclopentadienyl magnesium bromide and ferric chloride[5] hoping to prepare fulvalene, but instead made a light orange powder. They assigned the large stability of the compound to the aromatic character of the negatively charged cyclopentadienyls, but did not solve the structure correctly. The sandwich structure and η^5 hapticity was later successfully deduced by Woodward and Wilkinson.[6] Ernst Fischer expanded the work to include other metallocenes, and in 1973, Fischer and Wilkinson shared the Nobel Prize in Chemistry, in part for their work on metallocenes.

The field of catalysis grew rapidly with the understanding and use of organometallic compounds. Karl Ziegler and Guilio Natta together developed what is known as the Ziegler-Natta catalyst, which is used in the synthesis of polymers.[7] This organometallic catalyst is essential for the commercial manufacture of various high molecular-weight polymeric materials. The pair was awarded the Nobel Prize in Chemistry in 1963 for this work.[4] The well-known, Nobel Prize-winning Heck reaction was discovered in 1968. It is a carbon-carbon bond-forming reaction between an unsaturated halide or pseudohalide with an alkene utilizing a palladium catalyst.[8] In general, main-group organometallics are typically used as reagents on a stoichiometric level, whereas transition-group organometallics are typically used as catalysts.

1.1.2. Chemistry of Organometallic Compounds

Organometallic compounds are characterized by a metal to carbon bond. The electronic character of the bond will generally depend on the electronegativity of the metal. Predominantly ionic complexes are formed with group one and two metals, while transition metal complexes exhibit more covalent character. Of course, there are exceptions; if the carbon-containing ligand exists as a stable carbanion, then the bond can be more ionic. This is significant, as it led to organolithium, -magnesium, -zinc and -aluminium compounds having a substantial impact on organic chemistry by providing stabilized but highly reactive carbanions able to act as nucleophiles or strong bases.[9]

An important aspect in metal-ligand (M-L) bonding in transition-group organometallics is the phenomenon of *back bonding*, especially with an unsaturated ligand. This is in addition to the donation of electron density from a filled orbital of a ligand to an empty orbital of a metal (σ-bond), and comprises the donation of electron density from a d-orbital of the metal into the empty π*-antibonding orbital of the ligand (Figure 2).[10] This allows low-valence metals with filled *d*-orbitals to form stable complexes with ligands.

Spectroscopic and theoretical studies have shown that for the CO ligand, π-back donation is usually similar or greater in size than the CO→metal electron donation from the σ-bond. This facilitates bonding of CO molecules to transition metals, but also reduces the bond order of the carbon-oxygen bond, which results in a weaker bond. This can be seen on infrared spectroscopy by a decrease in the frequency of the ν_{CO} band from that of free CO, sometimes by as much as 200 cm^{-1}.[10]

Complex	**$Ti(CO)_6^{-2}$**	**$V(CO)_6^{-1}$**	**$Cr(CO)_6$**	**$Mn(CO)_6$**	**CO**
ν_{CO} (cm^{-1})	1748	1859	2000	2100	2143

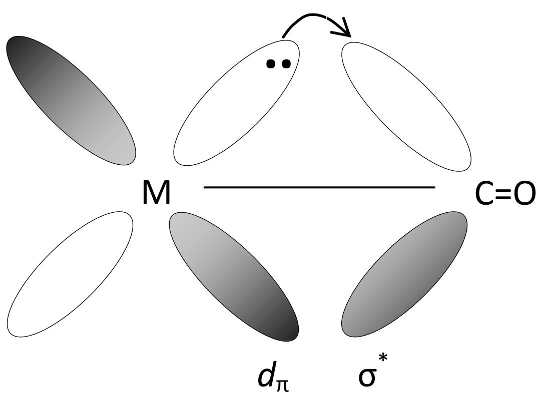

Figure 2: Back bonding between empty *d*-orbitals of a metal and π* orbitals of CO

Oxidative Addition

Perhaps the most common reaction process in organometallic chemistry is *oxidative addition*.[9] This is a process in which the oxidation state of a metal centre is increased, along with the coordination number of the centre, by the addition of one or two ligands. This mechanism is often seen in catalytic cycles along with the reverse process, *reductive elimination*, a decrease in oxidation state and coordination number (Equation 3). This is facilitated by the elimination of a coordinated ligand (often, this ligand will be the product in a catalytic cycle). Since oxidative addition requires a vacant coordination site, it is most common on four- or five-coordinate complexes.

$$\underset{16e}{L_nM} + A\text{-}B \;\underset{\textit{reductive elimination}}{\overset{\textit{oxidative addition}}{\rightleftharpoons}}\; \underset{18e}{L_nM}\begin{matrix} ^{\diagup}\,A \\ \\ _{\diagdown}\,B \end{matrix}$$

Equation 3: Oxidative addition and its reverse process, reductive elimination[9]

In most applications of oxidative addition, the electron count increases by two, implying that a vacant 2*e* site is required on the metal. If need be, a vacant site on an 18*e* complex can be opened by the loss of a ligand. It is also required that the metal undergoing oxidation has a stable oxidation state two units above the initial state. Similarly, reductive elimination requires that the metal has a stable oxidation state two units below the initial state. Binuclear oxidative addition is possible in the case of a 17*e* complex or a binuclear M-M 18*e* complex, which can dissociate into a 17*e* complex:

$$\underset{17e}{2L_nM} \;\; (\text{or } \underset{18e}{L_nM\text{-}ML_n}) + A\text{-}B \longrightarrow \underset{18e}{L_nM\text{-}A} + \underset{18e}{L_nM\text{-}B}$$

Equation 4: Binuclear oxidative addition[9]

There are four major oxidative addition mechanisms. Although each is different in implementation, the outcome is the same: an increase in coordination number, electron count and oxidation state.

i) *<u>Concerted, or three-centre, oxidative addition mechanism</u>*

In a concerted mechanism, the incoming ligand first binds as a σ-complex. If this σ-complex is stable, the reaction will stop at that point. If the back donation from the metal into the ligand σ^*-orbital is sufficiently strong, however, the A-B bond may dissociate, being replaced by M-A and M-B. Non-polar reagents, such as H_2 or hydrocarbons, tend to react *via* this mechanism. A well-known example is the addition of H_2 to Vaska's Complex (Figure 3). This is a 16*e* square planar d_8 species, $IrCl(CO)(PPh_3)_2$.

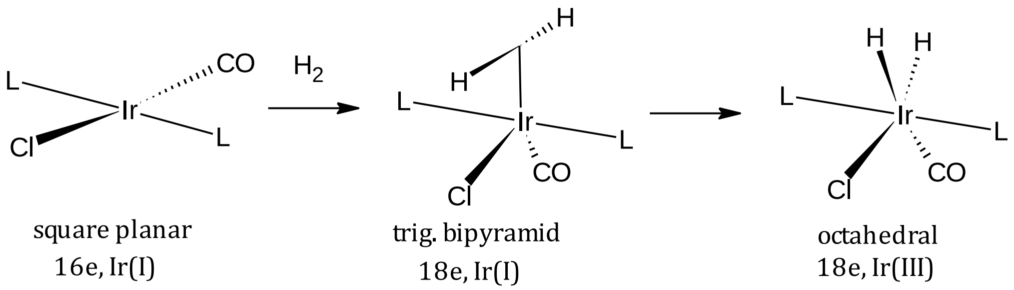

Figure 3: Concerted oxidative addition of H_2 to Vaska's complex[9]

Two of the ligands move from a *trans* to a *cis* relationship when the dihydride is formed, before the dihydrogen dissociates. Although addition takes place in a *cis* manner, the two hydrogen ligands can rearrange. For reductive elimination, however, the two ligands would need to be *cis* to one another.

ii) *<u>S_N2 mechanism</u>*

The S_N2 pathway is preferred for polarized A-B ligands, such as alkyl halides. The metal electron pair of L_nM attacks the ligand σ*-orbital at the least electronegative atom to give L_nMA^+ and B^- fragments. This is a second-order reaction and is accelerated in polar solvents. This is analogous to the bimolecular nucleophilic substitution (S_N2) reaction found in organic chemistry. Figure 4 illustrates this mechanism for the addition of methyl iodide to Vaska's complex.

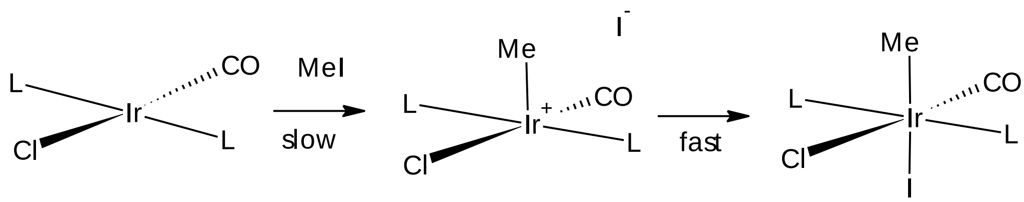

Figure 4: Oxidative addition of MeI to Vaskas's complex *via* the S_N2 reaction mechanism[9]

The first step involves oxidation of the metal without a change in electron count, while the second step increases the electron count by 2*e* without changing the oxidation state. Together, these two steps result in the full oxidative addition. Several factors can influence reactivity in S_N2 additions. In general, reactivity increases with increasing metal nucleophilic character or a better leaving group on the alkyl moiety, while steric hindrance at carbon slows the reaction.[9]

iii) Radical mechanism

The radical mechanism indicates the addition of a radical under oxidative conditions. This is well illustrated by Hill and Puddephatt's photochemically initiated oxidative addition of isopropyl iodide to dimethyl(1,10-phenanthroline)platinum(II).[11] Initiation is required to provide a supply of radicals. The metal complex is excited by irradiation at 473 nm into the MLCT. This excited complex abstracts an iodine atom from *i*-PrI. A second abstraction gives the di-iodide substituted metal complex, along with two free Pr· radicals (Figure 5).

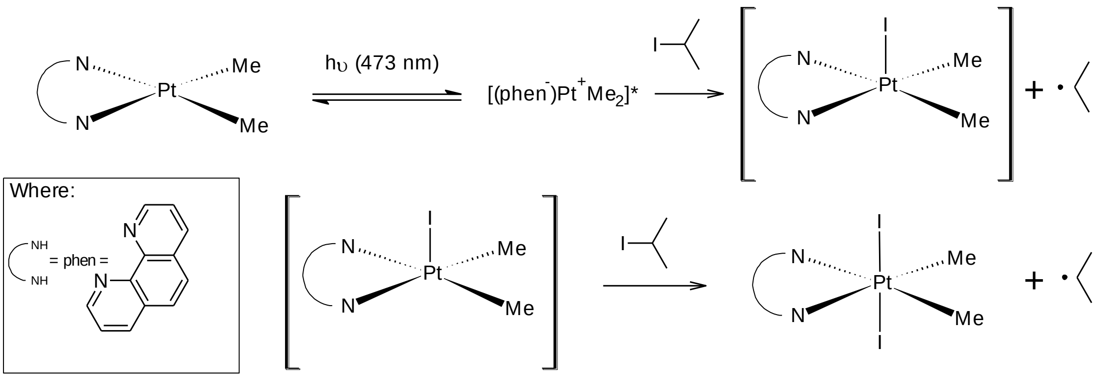

Figure 5: Initiation step of the free chain radical oxidative addition mechanism

The reaction is then propagated by these Pr· radicals coordinating to a metal complex, which in turn abstracts an iodine atom from *i*-PrI, resulting in the product complex and another Pr· radical, and so on (Figure 6).[11]

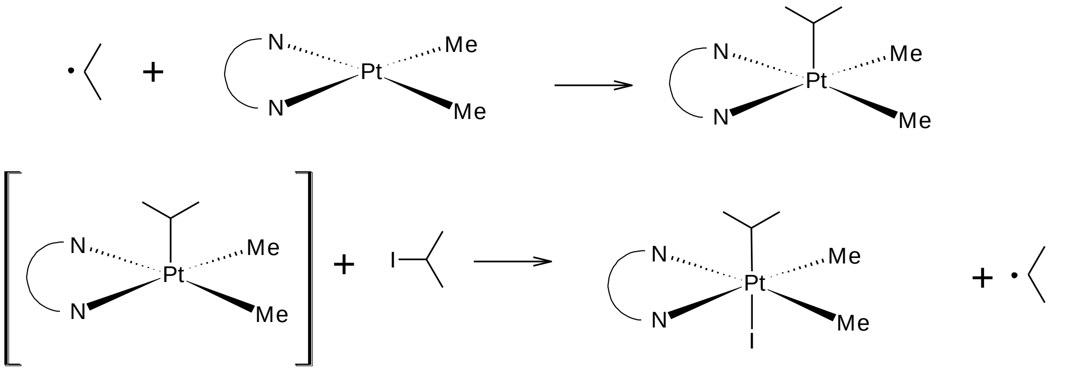

Figure 6: Propagation step of the free chain radical oxidative addition mechanism

The initiation step is encouraged by a triplet sensitizer (benzophenone) and retarded by a triplet quencher (pyrene), suggesting a predominantly triplet character of [(phen$^-$)Pt$^+$Me$_2$]*, while a free radical scavenger reduced the quantum yield by a factor of 1000. Oxidative additions of binuclear complexes often occur *via* radical mechanisms because they involve 1*e* rather than 2*e* changes at the metals.[11]

iv) Ionic mechanism

The ionic mechanism is similar to the S_N2 mechanism, with the main difference being that the former involves substrates that are dissociated in solution prior to interaction with the metal centre. This is common for hydrogen halides, such as HCl, which readily dissociate. There are two variations for addition, depending on the basicity of the metal complex. Most commonly, sufficiently basic complexes will protonate first, after which the anion binds to give the final product (Figure 7). For less basic metal complexes, the halide ion attacks first, followed by protonation to give the product.[9]

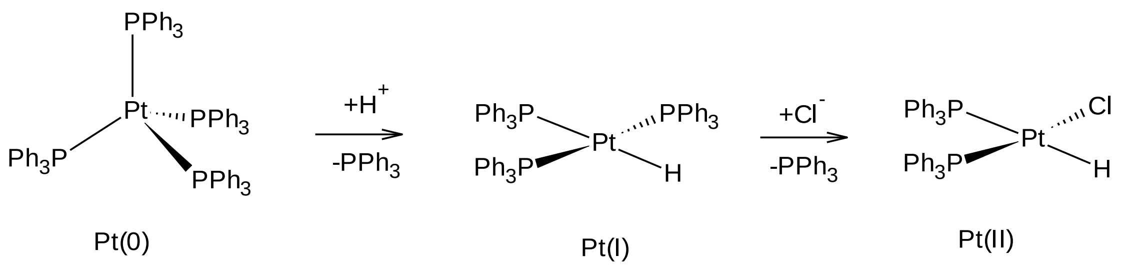

Figure 7: Ionic mechanism for protonation followed by "anionation"

The first process is favoured by polar solvents, basic ligands and a low oxidation-state metal, while the second is favoured by electron-acceptor ligands and cases where there is a net positive charge on the complex.

For low-spin transition metal complexes, using the concepts of oxidative addition and/or reductive elimination in combination with the *18-electron rule* (more of a preference than a rule), it is sometimes possible to predict the stability of reaction products or intermediates. The 18-electron rule is similar to the octet rule used in "traditional" organic chemistry, which involves simple counting of electrons that may be accommodated by the valence orbitals. With the inclusion of five *d*-orbitals, the octet rule is expanded to 18 electrons and can allow for some basic predictions about the mechanism of reaction, as well as possible reactivity of organometallic compounds. These can be thought of as applications of the above oxidative addition reaction mechanisms.

Transmetallation

Transmetallation is an exchange of ligands between two metal centres:

$$\mathbf{R'}\text{-}M + R\text{-}\mathbf{M'} \longrightarrow \mathbf{R'\text{-}M'} + R\text{-}M$$

This process is commonly found in catalysis, such as in the well-known Stille and Negishi coupling reactions.[9] In the case of the palladium catalyzed Stille reaction, an organotin compound is coupled to an sp^2-hybridized organic halide:

$$R\text{-Sn(R)}_3 + \mathbf{R'}\text{-X} \longrightarrow R\text{-}\mathbf{R'} + \text{X-Sn(R)}_3$$

Metal-halogen exchange

This is a similar concept to transmetallation, but here we are replacing a halogen with a metal centre:

$$R\text{-X} + \mathbf{R'}\text{M} \longrightarrow R\text{-M} + \mathbf{R'}\text{-X}$$

This exchange process can be used to synthesize *in situ* formulations of functionalized organolithium reagents from simple organolithiums (*n*BuLi, *s*Buli, MeLi etc).[9] As these are equilibrium reactions, the desired organolithium will only be formed if the corresponding carbanion is more stable than that of the initial lithium reagent.[9]

1.2. Organostannane Chemistry

1.2.1. History of Organostannanes

Organotin compounds are versatile reagents in organometallic chemistry. When used as an intermediate, they are relatively stable and can be easily stored for extended periods. The first documented organotin compound discovered is attributed to Frankland, and was presented to the world in 1849.[12] This was a reaction of ethyl iodide with elemental tin to produce diethyltin diiodide (Equation 5).

$$2EtI + Sn \longrightarrow Et_2SnI_2$$

Equation 5: Frankland's diethyltin diiodide first synthesized in 1849[12]

In 1859, an "indirect" method of synthesis was devised by Buckton, who obtained tetraethyltin by reaction of Frankland's diethylzinc and tin tetrachloride (Equation 6).[13]

$$2EtI + 2Zn \longrightarrow 2EtZnI \longrightarrow Et_2Zn + ZnI_2$$

$$2Et_2Zn + SnCl_4 \longrightarrow Et_4Sn + 2ZnCl_2$$

Equation 6: Indirect synthesis of tetraethyltin by Buckton in 1859[13]

This method was improved in various ways, and in 1900, there were around 37 published papers on organotin compounds.[13] In 1903, Pope and Peachy prepared several simple and mixed tetralkylstannanes and tetraphenyltin from newly developed Grignard reagents and tin tetrachloride and alkyltin halides.[14] In 1962, Kuivila showed that the reaction of trialkyltin hydrides with alkyl halides (Equation 7) was a radical chain reaction involving the short-lived trialkyltin radical $R_3Sn\cdot$.[15]

$$R_3SnH + R'X \longrightarrow R_3SnX + R'H$$

Equation 7: Radical chain reaction of trialkyltin hydrides with alkyl halides by Kuivila in 1962

Organotin compounds have found extensive applications in industry, agriculture and medicine. Use of these compounds in the environment has been reduced considerably due to the (now well-known) negative impact of organotin pollution. Industry uses include stabilization of poly(vinyl chloride) and catalysis of polyurethane formation.[16]

1.2.2. Chemistry of Organostannanes

1.2.2.1. Synthesis of Organostannanes

Organostannane synthesis has been well explored over the decades from the time that the first organotin was synthesized. The possible reaction pathways available can be separated depending on the oxidation state of the tin centre. An overview of these is given in Schemes 1, 2 and 3, which relate to tin(IV), tin(III), and tin(II).[16]

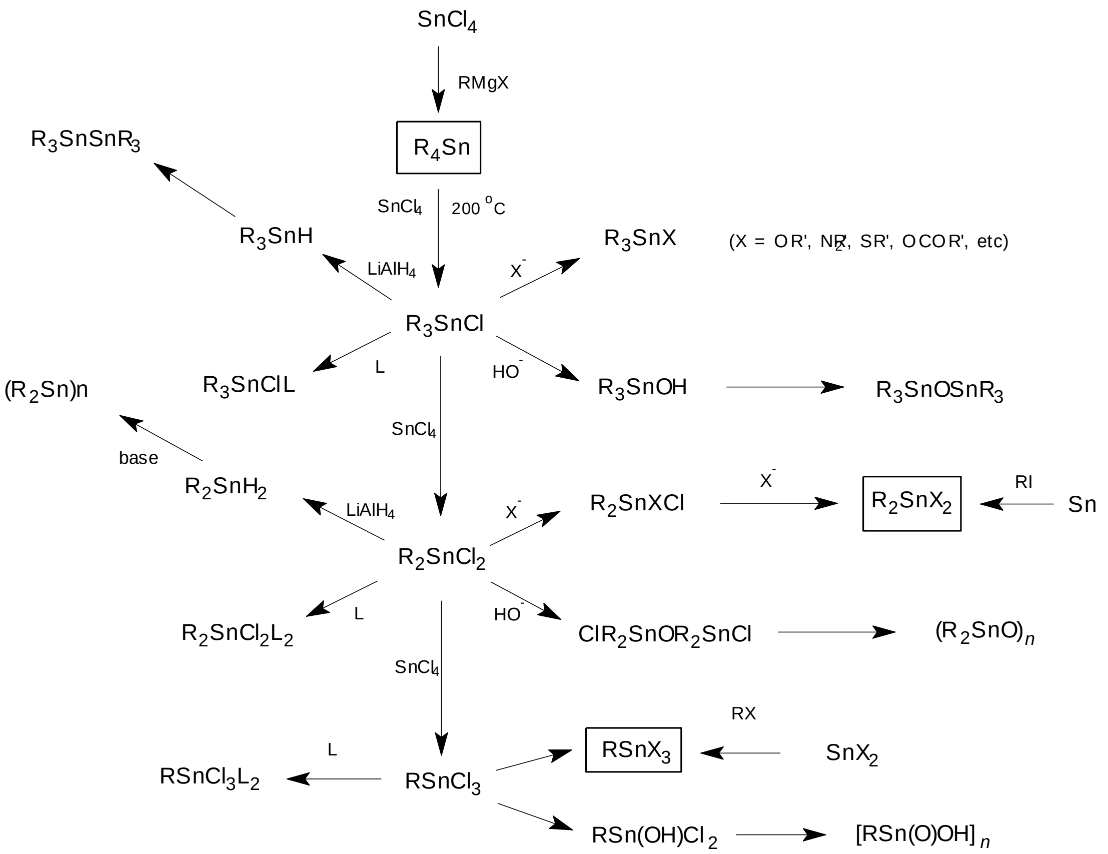

Scheme 1: Overview of possible reactions from Sn(IV) using Grignard and Kocheshkov routes[16]

The most popular method used is the reaction of a Grignard with tin tetrachloride. This usually goes to completion and results in a tetra-alkyltin compound. When heating at 200°C in the presence of tin tetrachloride, rearrangement of the R and Cl groups results in an organotin chloride, R_nSnCl_{4-n} (with $n < 4$). This is known as the Kocheshkov redistribution reaction or comproportionation[17] and is carried out without solvent, but sometimes with a catalyst such as aluminium chloride. Commercial preparation of tributyltin chloride and triphenyltin chloride follows this process. Reactivity of the initial step for R follows: phenyl > benzyl > vinyl > methyl > ethyl > higher alkyl, and for X: Cl > Br > I.[16] These organotin halides are often used as starting materials from which most useful organostannane compounds can be derived. Many examples of this rearrangement can be found in the literature.[18,19,20,21]

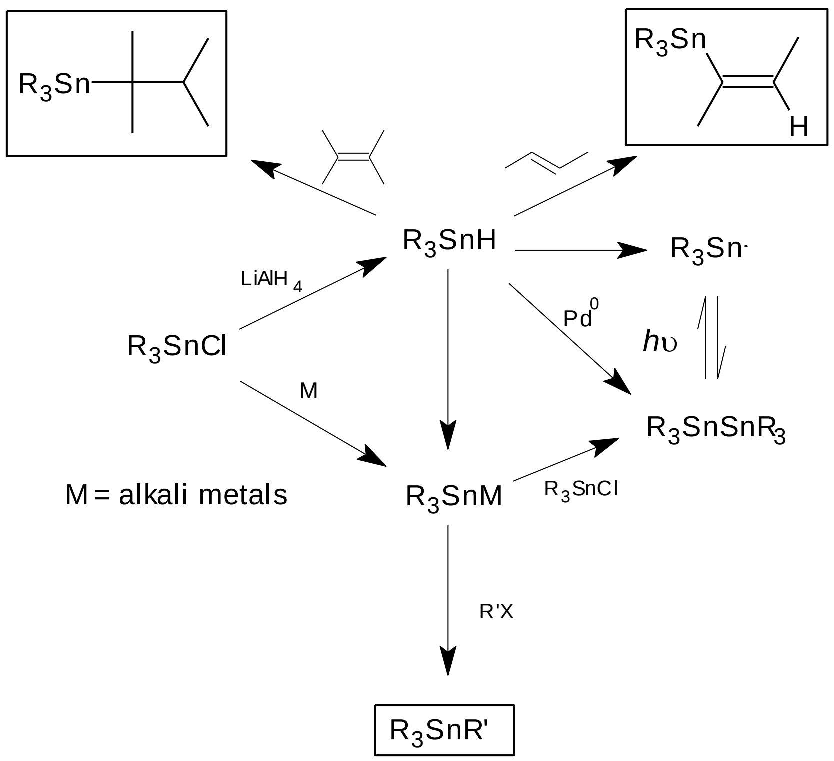

Scheme 2: Organostannane synthesis from SnH and SnM compounds[16]

When using a metal hydride as a nucleophile, the organotin hydrides R_nSnH_{4-n} are produced, which, when added to an alkene or alkyne, allow access to a second method of forming the tin-carbon bond (*via* stannyl radicals $R_3Sn\cdot$).

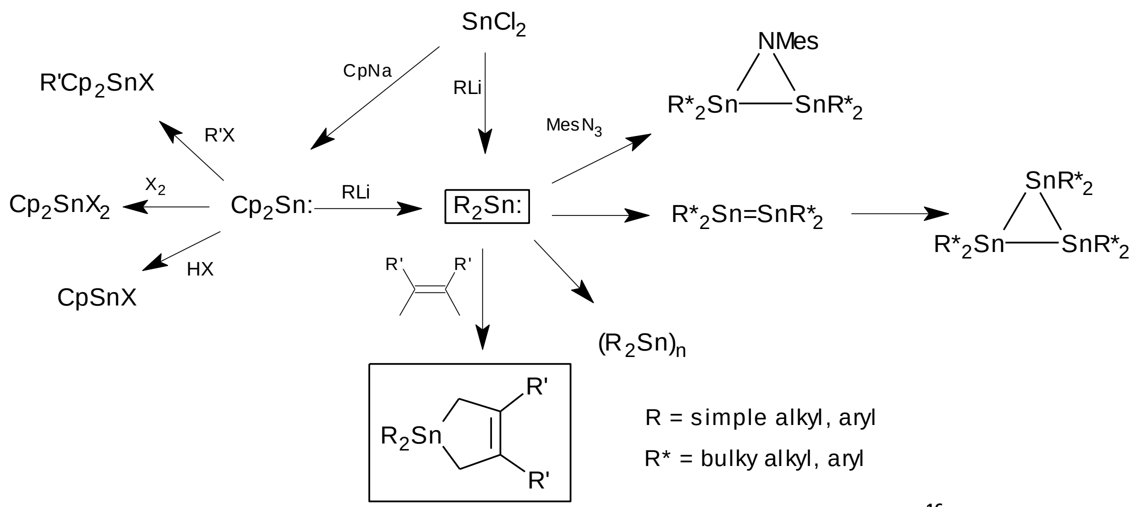

Scheme 3: Pathways to lower valence state organotin compounds[16]

Products within boxes represent the formation of a new tin-carbon bond. There are four main paths to do this: a reaction of a tin(II) compound with an organic halide; a reaction of an organolithium,

-magnesium or -aluminium with a tin(II) or tin(IV) halide; a reaction of a tri-alkyltin hydride with an alkene or alkyne; and a reaction of a tri-organostannyl lithium reagent with an alkyl halide.[16]

This study makes use of α-alkoxy organostannanes and α-amino organostannanes as precursors for Fischer carbenes, and so these will be expanded upon.

i) *α-Alkoxy Organostannanes*

The synthesis of α-alkoxy organostannanes for use as precursors to organolithiums was achieved by Still in 1979.[22,23] The general approach involves an initial nucleophilic addition of a tributylstannyl anion to a suitable aldehyde (**1**) or ketone in THF, a known coordinating solvent. The tributylstannyl anion is prepared *in situ* by reaction of tributyltin hydride (Bu_3SnH) and LDA in THF (Scheme 4). This tributylstannyl lithium solution was found to react well with aldehydes at -78°C to give high yields of α-hydroxystannanes (**2**).

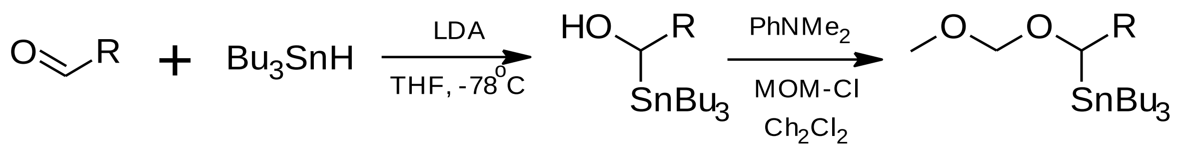

1 **2** **3**

Scheme 4: Synthetic route to α-alkoxy organostannanes[23]

These must be immediately protected because hydroxyl derivatives are acid sensitive and decompose on standing. Still found that simple alkoxyalkyl moieties were the most efficient protecting groups for these systems, and the protection was carried out by treating **2** with α-chloromethyl methyl ether in the presence of *N,N*-dimethylaniline in dichloromethane at 0°C for 10-60 minutes to give the desired α-alkoxy organostannanes (**3**) in good yields (up to 90%). This became a well-established reaction method for α-alkoxy organostannanes, and was used essentially unchanged in this study.

ii) *α-Amino Organostannanes*

α-Amino organostannanes have been extensively explored, for example, by Beak[24,25] and Gawley.[26,27] Beak *et al*. described the method for synthesis that was used in this project, with *sec*-BuLi/TMEDA as the lithiating base. These compounds can be synthesized by reaction of *sec*-BuLi/TMEDA and tributyltin chloride (Bu_3SnCl) with a suitable amide (**4**). The reaction is an electrophilic substitution that takes place at the α-position on the amide. The amines chosen for this project were pyrrolidine and piperidine. In order to direct the lithiation to the α position, the amides were initially treated with di-*tert*-butyl dicarbonate (**5**), in DCM at 0°C for up to 12 hours, to form the carbamate protected derivative (**6**). This *tert*-butoxycarbonyl (BOC) protecting group is an activating group that has a dipole stabilizing effect on the α-lithiation and subsequent substitution adjacent to the nitrogen to give the desired α-amino organostannane (**7**).[28,29]

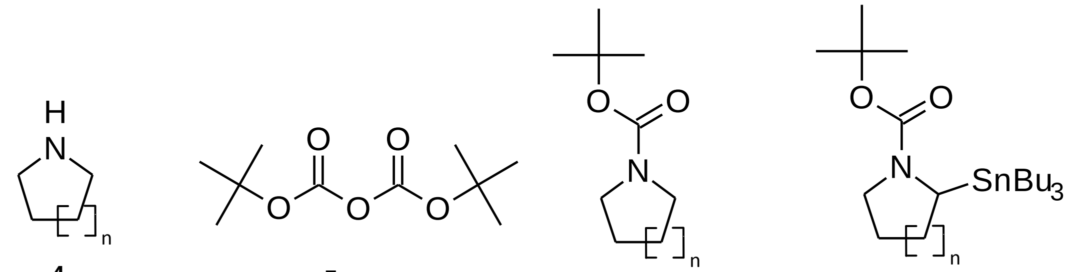

4 **5** **6** **7**

n = 1, 2

These α-amino organostannane compounds are formed in satisfactory yields (40-70%) and, once purified, are stable at cold temperatures and under argon.

1.2.2.2. Applications of Organostannanes in Tin-Lithium Exchange

Organolithiums were required for the synthesis of the novel Fischer chromium carbenes, which are of interest in this project. Non-trivial organolithium reagents, however, are not readily sourced. Still has demonstrated the use of organostannanes as intermediates in the preparation of substituted and non-trivial organolithium compounds.[22] Since most organostannanes can undergo rapid metal-exchange in the presence of a suitable alkyl lithium under favourable conditions, they allow for the *in situ* formation of the desired organolithium complex. This means organostannanes can find application in any field that could take advantage of novel organolithiums.

α-Alkoxyorganolithiums and some α-aminoorganolithiums cannot be formed *via* direct lithiation methods. These compounds contain oxygen or nitrogen attached to the carbon atom requiring metallation, and the hydrogen atom cannot always be removed by basic lithiating agents.[30] They can, however, be accessed *via* a rapid tin-lithium exchange process. The mechanism of this process is similar to that of an oxidative insertion of lithium metal into alkyl halides.[30] The tin atom is attacked by a strong lithiated nucleophile, such as *n*BuLi, forming a five-coordinate stannate anion intermediate.[30] This short lived species leads to the release of the most stable organolithium and a by-product, tetraalkyltin. It is found that vinyl, allyl, aryl and alkenyl, as well as α-alkoxy and α-amino lithiums, are more stable than alkyl lithiums.[30] Since the process is thermodynamically controlled, the reformation of the butyl lithium species is not favoured.[30]

Organolithium compounds have been found to be stabilized by suitable protecting groups,[31] as well as the effect of the heteroatom.[24,31,32] Of some interest is the stability of organolithiums formed from α-alkoxy organostannanes. McGarvey has investigated these compounds and found that there is a stabilizing effect from oxygen-lithium chelation.[23] Further, it was found that this effect is a function of the reaction conditions, solvent, temperature and the nature of the groups attached to the oxygen (since these would affect the electronic properties of the oxygen atom).[23]

Amino organolithiums are very important compounds in synthesis due to the prevalence of nitrogen-containing compounds in natural products and biologically active compounds. Peterson showed in the early 1970s that it is possible to form α-aminolithiums *via* tin-lithium exchange from α-amino organostannanes.[33,34,35] This process, though, does not seem to be general, and several important and interesting failures have been reported. For example, Chong *et al.* found that when Peterson's original example (**8a**) from 1970 was modified with a substituent on the metal-bearing carbon atom (**8b**), there was no metal-exchange activity.[36]

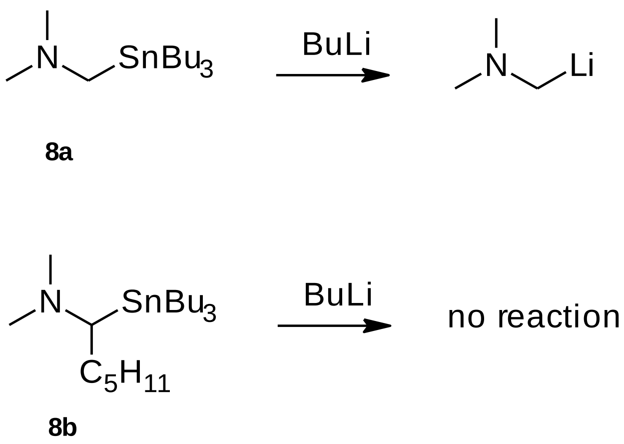

In 2000, Chambournier and Gawley reported the exchange failure of a conformationally rigid 2-(tributylstannyl)piperidine.[37] They found that when the 2-(tributylstannyl) moiety of a 4-*tert*-butylpiperidine is equatorial, tin-lithium exchange occurs, but when the 2-(tributylstannyl) is axial, the exchange fails. This suggests that there is a conformational requirement for transmetallation in these rigid piperidines. They suggested that perhaps the nitrogen atom lone pair has to be synclinal to the adjacent carbon-tin bond for exchange to occur.[37]

There are some variable trends noticed when attempting to transmetallate an amino organostannane. Peterson's original compound (**9a**) was transmetallated in hexane at 0°C in a few minutes. When the nitrogen atom had one or two aryl groups (**9b**), a small amount of THF was needed for successful transmetallation.[34] For 2-(tributylstannyl)pyrrolidines, the conditions also depend on the nitrogen substituent.[37] The *N*-methyl compounds readily exchange in a few seconds in THF at -78°C. This transmetallation is sluggish in ether at that temperature, but is accelerated by addition of TMEDA.[38] In hexane at room temperature, the same compounds transmetallate very slowly, and give an amorphous white powder. In the case of 5-(tributylstannyl)-2-pyrrolidinone (**9c**), metal exchange takes 30 minutes at -50°C.[39] *N*-Isobutyl-2-(tributylstannyl)-pyrrolidine (**9d**) takes an hour to transmetallate in 4:1 hexane/ether at room temperature;[40] however, the *N*-methoxyethyl analog (**9e**) takes just seconds at 0°C in the same solvent system. *N*-Allyl, *N*-butenyl and *N*-pentenyl compounds undergo metal exchange readily in THF at -78°C, but at similar rates as **9d**.[41,42] Tin-lithium exchange fails with **9f**,[43] but succeeds with **9g**.[25,44,45] Piperidines (**9h**) readily undergo exchange, whereas the axial stannane (**9i**) does not.[46] Reasons for these failures are varied. In the case of **9f**, the resulting α-amino organolithium is not eliminated from the intermediate stannate complex since it is less stable than BuLi.[26]

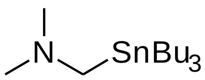

9a

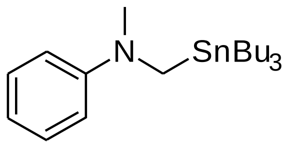

9b

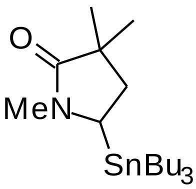

9c

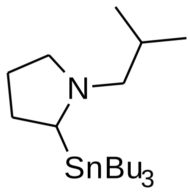

9d

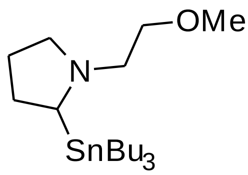

9e

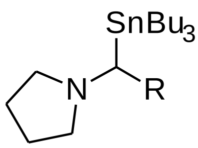

9f

R = Et, *i*-Pr

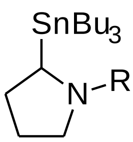

9g

R = Me, Et, *i*-Bu, allyl, Boc

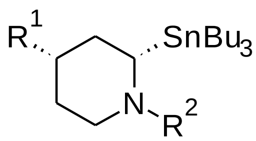

9h

R^1 = H, *t*-Bu

R^2 = Me, Boc

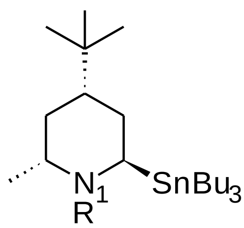

9i

R^1 = Me, Boc

Rapid-injection NMR kinetic studies have been performed by Klein and Gawley on **9g** (for R = Me, Boc), **9h** and **9i**.[47] It was confirmed that the solvent has a significant effect on transmetallation. THF increased metal exchange rates, with the reaction completing within 20 seconds. When carried out in Et_2O, however, the exchange took several hours to complete. They also found that the conformation of the ring influenced the rate of transmetallation. For *N*-BOC stannylpiperidines, **9h** and **9i**, when using the conformationally mobile piperidine ring (in the case of **9h** with R^1 = H), metal exchange was 2-3 orders of magnitude faster than either of the conformationally rigid piperidines (in the case of **9h** with R^1 = *t*-Bu).[47] In the corresponding lithium compounds, **10a-c**, the C-Li bond was in the nodal plane of the amide, and the lithium was coordinated to the carbonyl oxygen. In **10a** and **10b**, the rings adopt chair conformations, while **10c** adopts a twist-boat conformation.[47]

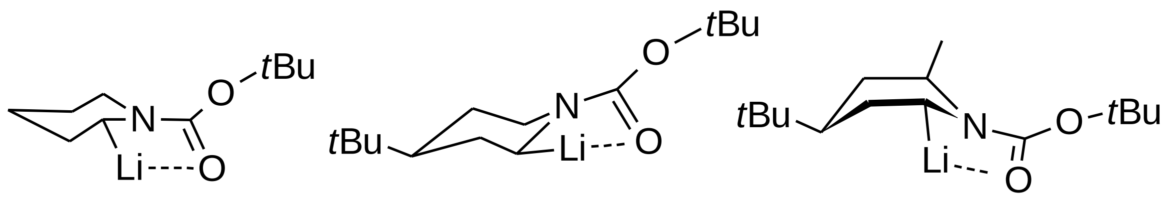

10a **10b** **10c**

This potential for metal-exchange makes many complex organolithiums accessible *via* the corresponding organostannane. While some challenges present themselves around the synthesis of these organostannanes, once synthesized and purified, they are a stable and useful class of organometallic compounds.

1.3. Organochromium Compounds

1.3.1. Introduction to Organochromium Compounds

Organochromium chemistry is a subclass of organometallic chemistry that deals with organic compounds containing a chromium bond to carbon, and the relevant chemistry. For chromium, oxidation states of importance can range from -2 to +6.[48]

The synthesis of the first organochromium compound was described by Franz Hein in 1919. It was synthesized by treating phenylmagnesium bromide with chromium(III) chloride.[49] Although Hein incorrectly identified the product, Zeiss *et al.* repeated the experiment in 1957 and correctly identified it as a cationic bisarene (Ar_2Cr^+).[50] Bis(benzene)chromium had been discovered a year earlier by Ernst Otto Fischer by reaction of chromium(III) chloride, benzene and aluminium chloride.[49] In 1963, Wilke *et al.* prepared tris-(n-allyl)chromium as an early but unsuccessful Zeigler-Natta catalyst.[51] Fischer later went on to describe the synthesis of the subclass of organochromium compounds bearing his name, the Fischer carbenes.

Carbenes are compounds that possess a neutral divalent carbon atom with 6 electrons in its valence shell, and have been part of a long history extending back almost 150 years.[52] Ongoing research into carbenes, ranging from physical to organic fields, nano-science and inorganic chemistry, have continued to expand our understanding of the nature of carbenes and how to apply them in a systematic manner.

1.3.2. Fischer Carbenes

The first unequivocal Fischer carbene synthesis was reported several decades ago, in 1964 by Fischer and Maasböl.[53] In 1967, the first crystallographically characterized Fischer carbene was reported, again by Fischer and Maasböl.[54] This is still an area of organometallic chemistry that holds many secrets. Many reviews can be found in the literature, which is added to on a regular basis.[55, 56]

1.3.2.1. Reactivity

Since carbenes are species containing a divalent carbon, their reactivity is unique. They can exist in either a triplet or singlet ground state.[57] Depending on the nature of interaction with the metal centre, the carbene carbon can be electrophilic or nucleophilic, or somewhere in between these two opposing states. In this sense, the bond order of the carbene carbon bond becomes a function of both the metal and carbene substituents.

Fischer carbenes (Figure 8) are typically electrophilic and have one π-donor (X) substituent (OR or NR_2 are common), which stabilizes the electron-deficient carbene carbon. The metals used are mainly middle- or late-transition metals in a low oxidation state with strong π-acceptor ligands (carbonyl or phosphine, for example).[53] The other substituent (R) on the carbene carbon can be any alkyl, aryl, saturated or unsaturated group. They tend to exist more readily in a singlet ground state and have a large difference in energy between their singlet and triplet states. They will readily undergo nucleophilic attack by an appropriate nucleophile.

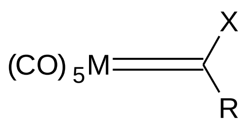

Figure 8: General structure of a Fischer carbene

Schrock carbenes,[58] first discovered just a few years after the first Fischer carbene, are nucleophilic, with an early transition metal in a high oxidation state, coordinated to strong π-donor ligands, such as O^- and Cl^-. These carbenes often have a small difference in energy between singlet and triplet states and are poorly stabilized as a result.

Bonding between the metal and carbene carbon is usually discussed and represented in terms of the Dewar-Chatt-Duncanson (DCD) donor-acceptor model (Figure 9).[59] Here, we determine a fundamental difference between Fischer and Schrock carbenes: in the Fischer carbene (Figure 9a), bonding interactions occur *via* a ligand → metal σ donation from the lone pair orbital of the carbene carbon into the empty d(σ) metal orbital, and a metal → ligand π-back donation from an occupied d(π) metal orbital into the formally empty p(π) orbital of the carbene carbon.[60,61] We can think of the complex as being the result of a singlet metal fragment coordinating to a singlet carbene fragment. It has been found from *ab-initio* computational work that the donation from the carbene fragment to the metal fragment is stronger than the back donation; however, the smaller the π-donor character of X, the larger the back donation.[61,62] In general, it was found that back donation is proportional to the $Cr\text{-}CO_{(trans)}$ distance, and inversely proportional to the $Cr{=}C_{(carbene)}$, and $C\text{-}O_{(trans)}$ distances (Figure 10).[61]

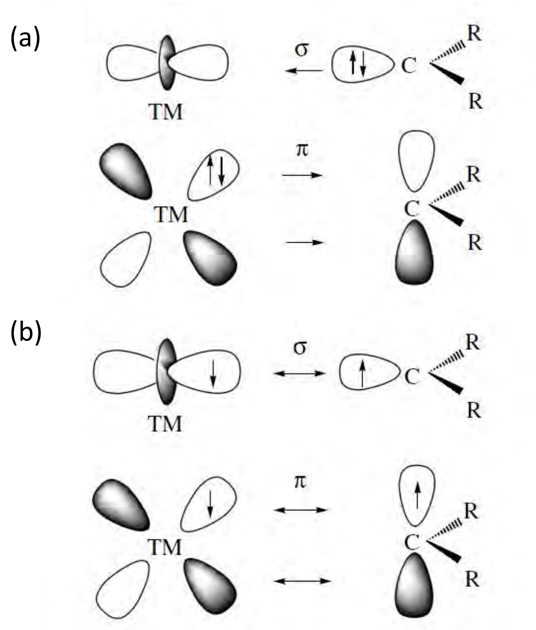

Figure 9: DCD representation of bonding within (a) Fischer carbenes and (b) Schrock carbenes, where TM = transition metal[60]

Reported analysis of this bonding behaviour shows that both σ donation and π back donation play significant roles in the reactivity and behaviour of this class of carbene.[63,64,65] It has also been proposed that a more accurate representation can be found by considering the bonding to be an M-C_1-X three-centre four-electron bond.[66,67] Of course, this would explain why the philicity of a Fischer carbene is so readily influenced by the π-donor substituent.[68,69,70] We expect from this observation that one could tune the electronic behaviour of the carbene by using specific X and R substituents. Indeed, the multiplicity of a carbene is greatly influenced by the electronegativity of both substituents on C_1; the singlet state is favoured by σ-electron-withdrawing groups, which stabilize the non-bonding orbital.[71,72]

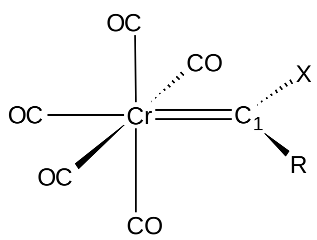

Figure 10: Schematic representation of a Fischer carbene

Bonding in Schrock carbenes (Figure 9b) is described as a covalent bond between a triplet carbene fragment and a triplet metal fragment.[61] This model does not make use of donor-acceptor arguments and therefore Schrock carbenes are sometimes referred to as alkylidenes.[60]

A third class of carbenes exists, as a subclass of Fischer carbenes.[60] These are known as *N,N'*-heterocyclic carbenes (NHC) and are as a result of the carbene ligand requiring very little π back donation from the metal fragment, and so are stable enough to be isolated and synthesized as free species. They were first discovered by Ofele[73] and Wanzlick.[74,75] It was only in 1991 when Arduengo *et al.* successfully isolated the free species that they could be used in transition metal chemistry.[76] These carbenes, when stable, have found a rich variety of applications due to their interesting coordination properties.[77] In 2006, Barluenga *et al.* successfully combined a Fischer carbene with an NHC ligand.[78] They did this by using a chromium(0)-rhodium(I) metal exchange,[79] previously seen by Göttker-Schnettmann *et al.* in 2001.[80]

Carbenes are traditionally classified into these three classes due to their reactivity. This linear approach leads to some anomalies, such as combining dichlorocarbene with methylene in the same electrophilic group, even though they each exhibit different chemistry. Sander has developed a two-dimensional scale taking into account electron affinities and ionization potentials.[81] Since the gap between singlet and triplet levels is a good correlation to the reactivity of carbenes,[82a] the philicity of the carbene complex should not be ignored. To this end, Brinker and Mieusset have also developed a two-dimensional classification of carbenes taking into account their philicity and reactivity (Figure 11).[57] Carbene free energy of activation was calculated at the B3LYP/6-31(G)d level of theory for an insertion in the C-H bonds of isobutene and acetonitrile While their classification was applied mainly towards nucleophilic carbenes, the methodology is an important step towards a fluid but accurate classification system for all carbenes.

Since this project is intended to explore the stability of electrophilic Fischer chromium carbenes, the Brinker and Mieusset scale is more relevant here. There is a general trend towards electrophilic carbenes being more reactive, and *vice versa* for nucleophilic carbene species. There are of course exceptions, with stable electrophilic carbenes and reactive nucleophilic carbenes both possible, although neither of these are as stable (or reactive) as the opposite philicity.

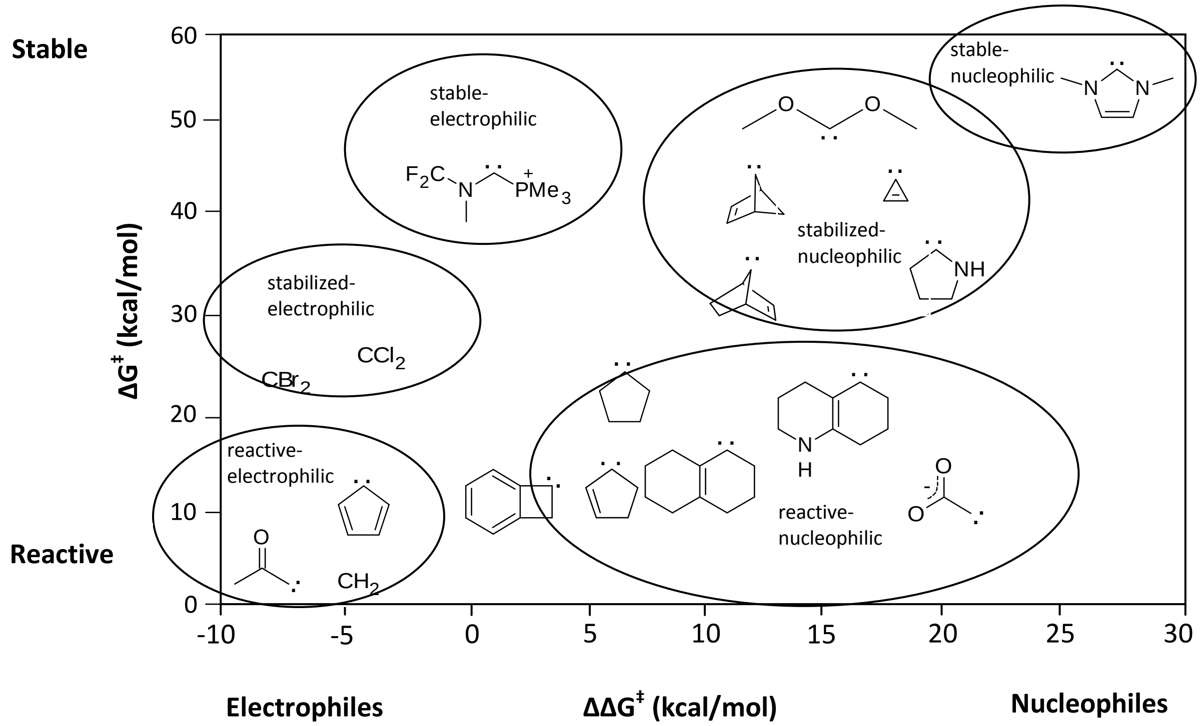

Figure 11: Brinker and Muiesset's two-dimensional classification of carbenes.[57]

Another complication is the classification of Grubbs catalysts.[82b] These are often referred to as ruthenium(II) carbenes, and so should fall into the Fischer class.[82c] However, a high M=C bond order and a large residual in the charge decomposition analysis (CDA) suggest that these should fall under the Schrock class.[83] This has recently been addressed by Occhipinti *et al.*, who have shown *via in silico* methods that the Grubbs catalyst should fall under the same class as Schrock carbenes.[83] This is due to the strong covalent character of the M=C bond. Fischer carbenes, in contrast, can be considered as having a large ionic character in the M=C bond, characterized by a high proportion of localized electron density.

1.3.2.2. Synthesis of Fischer Carbenes

There are two main synthetic pathways used to synthesize Fischer carbenes. The first is the one developed by Fischer himself (Scheme 4).[53] This involves the reaction of alkyl- or aryllithiums, **11**, with an appropriate metal carbonyl, such as $Cr(CO)_6$, **12**, giving an acyl metalate, **13.** This is followed by alkylation with a suitable alkylating agent, such as tetramethyloxonium tetrafluoroborate (Meerwein's salt), **14** (alkyl iodides have also been used for chromium carbenes, with the use of phase transfer catalysis),[84] to give the desired methoxy carbene, **15**. It was soon discovered that substituting the alkoxy group with nitrogen,[85] sulphur[86] and carbon[87] nucleophiles was relatively easy.

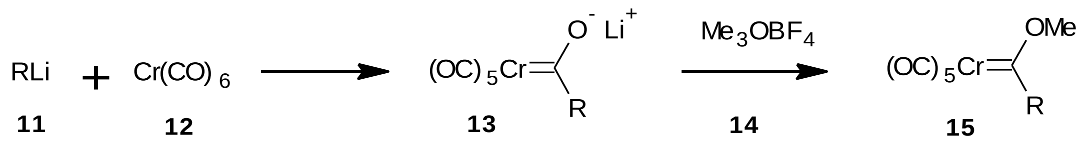

Scheme 4: Fischer method of carbene synthesis[53]

An important limitation of the Fischer method is the availability of various organolithium compounds. Semmelhack and Hegedus have provided an alternative method,[88] which involves the addition of a pentacarbonylchromate dianion, **16** (obtained from reduction of chromium hexacarbonyl, **12**, with sodium naphthalenide), to acyl chlorides or amides (Scheme 5). Addition to acyl chlorides gives the acyl chromate, **17**, which can be alkylated to give the alkoxycarbene, **18**. Addition of carboxylic amides gives the tetrahedral intermediate, **19**, which can be deoxygenated to give the aminocarbene, **20**.[89]

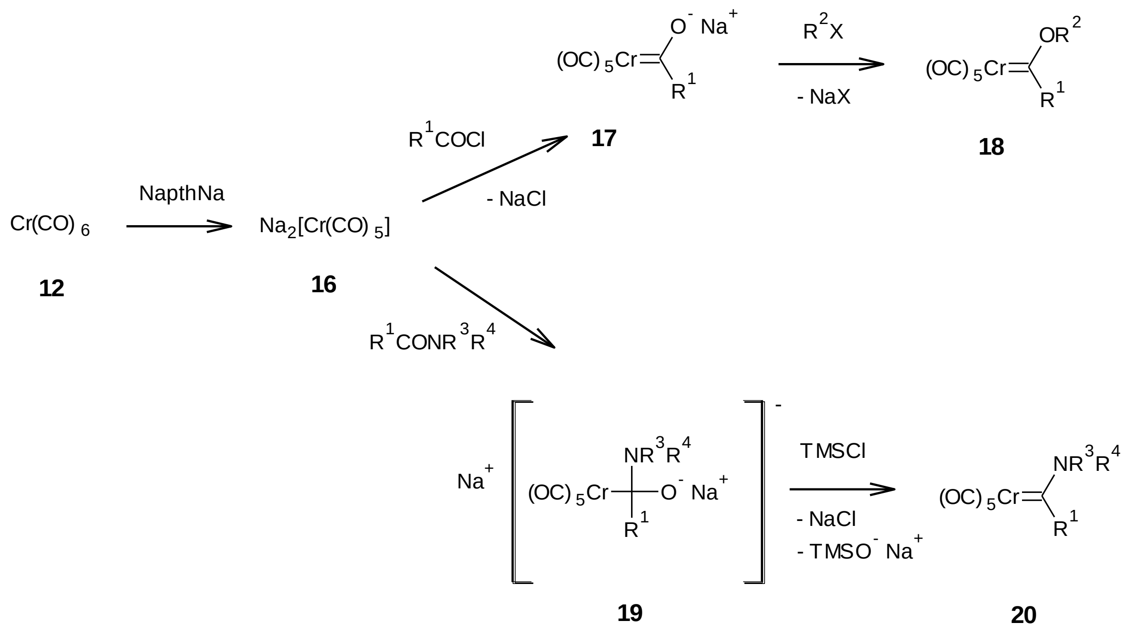

Scheme 5: Semmelhack-Hegedus method for synthesis of alkoxy- or aminocarbenes[88]

Fischer carbenes are not limited to group 6 metals, as Barluenga *et al.* have shown with the synthesis of late group metal-carbenes using rhodium(I) and nickel(0),[90] while Grubbs *et al.* have successfully synthesized and characterized an iridium(I) Fischer carbene complex.[91] These late-group metal-carbenes are generally synthesized through a transmetallation process.

Matsuyama *et al.* have developed another alternative method for Fischer alkoxycarbene synthesis.[92] Their method allows for greater variety and substitution on the alkoxy moiety than is allowed by the standard Fischer method and complements the acyl chloride route devised by Semmelhack and Hegedus. This was effected by alkylation of the acylate complex, **21**, with functionalized alkyldiphenylsulfonium salts, **22**, to give the Fischer carbene, **18** (Scheme 6).

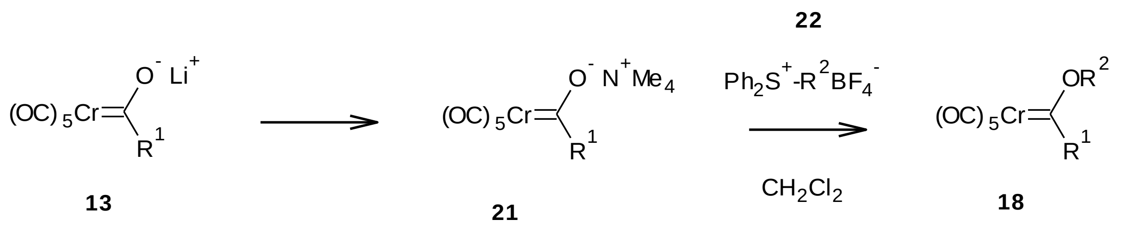

Scheme 6: Matsuyama *et al.* synthetic route for functionalized Fischer alkoxycarbenes[92]

1.3.2.3. Photochemistry of Fischer Carbenes

The seminal work reported by Hegedus[93] in 1982 on the photochemical behaviour of Fischer carbenes in the presence of an appropriate nucleophile paved the way for the synthesis of a vast array of compounds:[94] β-lactams, cyclobutanones, amino acids and peptides, and β-lactones, *via* what is known as a photocarbonylation reaction.[94] Hegedus later proposed a mechanism consisting of a crucial, reversible insertion of a *cis*-carbonyl ligand into the metal-carbon bond to form either a metallocycle, **23**, or a ketene-like intermediate, **24** (Figure 12).[95] This rationalization was due to the similarity of the products to those formed when using a free ketene.[96] However, efforts to confirm the presence of either of these intermediates gave no success.[95] Since it has proven difficult to explore this photochemically driven reaction experimentally, even today very little is known about this process. This is beginning to change with the use of modern quantum mechanical methods. Also of note is that no other photochemical processes have been reported for group 6 Fischer carbenes.[97]

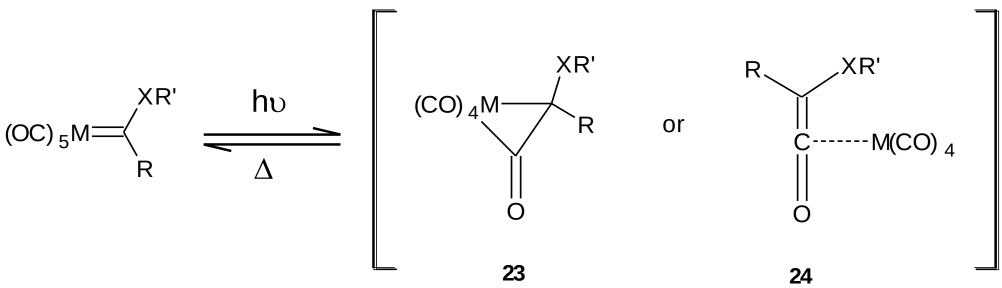

Figure 12: Initial mechanistic proposal by Hegedus[95]

The UV/Vis spectra of carbenes are well documented[94d] and show three dominant absorptions, classically assigned as: an intense ligand field (LF) transition in the region of 300-350 nm; a low-intensity ligand field transition between 350-450 nm; and a metal-ligand charge transfer (MLCT) absorption band around 500 nm.[94d] These bands can be manipulated by altering the substituents attached to the carbene carbon.

Early molecular orbital theory calculations assigned the MLCT band to the promotion of an electron from the non-bonding metal-centred HOMO to the carbene-carbon, p-orbital centred LUMO. The LF transition was assigned to the promotion into the metal-centred LUMO+1 orbital.

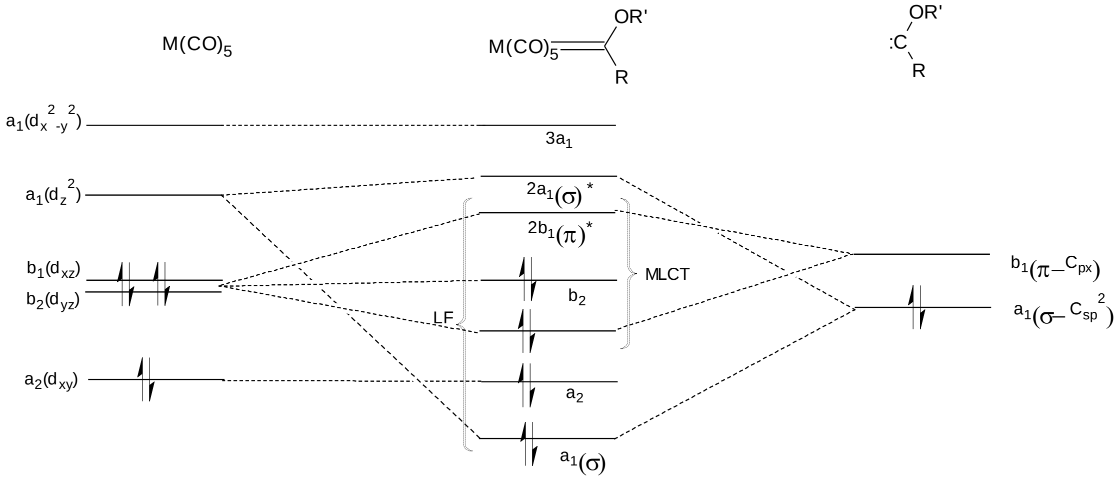

Figure 13: Simplified one-electron energy diagram for a Fischer carbene[97]

More recently, Fernández *et al.* have shown *via* time-dependant DFT (TD-DFT) calculations that the HOMO → LUMO transition is symmetry forbidden.[97] The MLCT band was reassigned to the promotion of an electron from the metal-centred HOMO-1 to the LUMO, a π-extended orbital involved with the p-atomic orbital of the carbene carbon atom. Also, the LF transition was reassigned to the excitation of an electron from the HOMO-3 to the LUMO (Figure 13).[97,98] While this HOMO-LUMO behaviour is important, it has been shown that a better indication of reactivity in carbenes is found in the singlet-triplet gaps.[82] A correlation has also been found between line-width in ^{53}Cr NMR and reactivity to photolysis with imines, although this relationship is not yet understood.

The LF and MLCT bands show a strong π-π* character, the implication of which means that the location of the band maximum is linked to the occupation of the p_z-atomic orbital of the carbene carbon. Fernández *et al.* have confirmed this relationship by using various *p*-substituted styrylchromium carbene complexes, showing that the positions of the respective absorption maxima correspond with the donor/acceptor behaviour of the substituent.[98] Alkyl and π-donor groups will cause a blue shift, while π-acceptor groups will cause a red shift.

Current experimental and computational insights suggest a photocarbonylation step that involves a transformation from a singlet ground state (S_0), which, when excited by irradiation into the LF or MLCT bands, results in a singlet excited state (S_1).[99] This S_1 species readily decays into a triplet state (T_1) *via* an intersystem crossing (ISC), which is allowed by spin-orbit coupling.[99,100] The T_1 species at this stage has a chromacyclopropanone structure, similar to the one proposed by Hegedus (Figure 10). This complex changes its multiplicity back to a singlet state by filling a vacant coordination site with a molecule of a coordinating solvent. At this stage, the chromacyclopropanone S_0 structure will, in the presence of an appropriate nucleophile, react further. If no nucleophile is present, it will revert back to the initial ground-state carbene complex in an exothermic process.[99]

This solvent coordination was explored by Fernández *et al.* by carrying out the same photolysis of an alkoxy carbene with an imine in several solvents, with increasing donor ability. It was found that the larger the donor number (that is, the more coordinating the solvent), the greater the conversion into the equivalent β-lactam.[101] Further exploration into this solvent-induced radiationless ISC was carried out *via* computational methods,[97] where it was found that as the solvent approached the metal from a distance, it allowed the system to follow an S_0 hypersurface at decreasing energy and increasing stability over the T_1 hypersurface until, eventually, a stable octahedral geometry was reached. This process is known as the "loose-bolt effect"[102] in organic chemistry; however, it is not known elsewhere in photochemical processes (Figure 14).

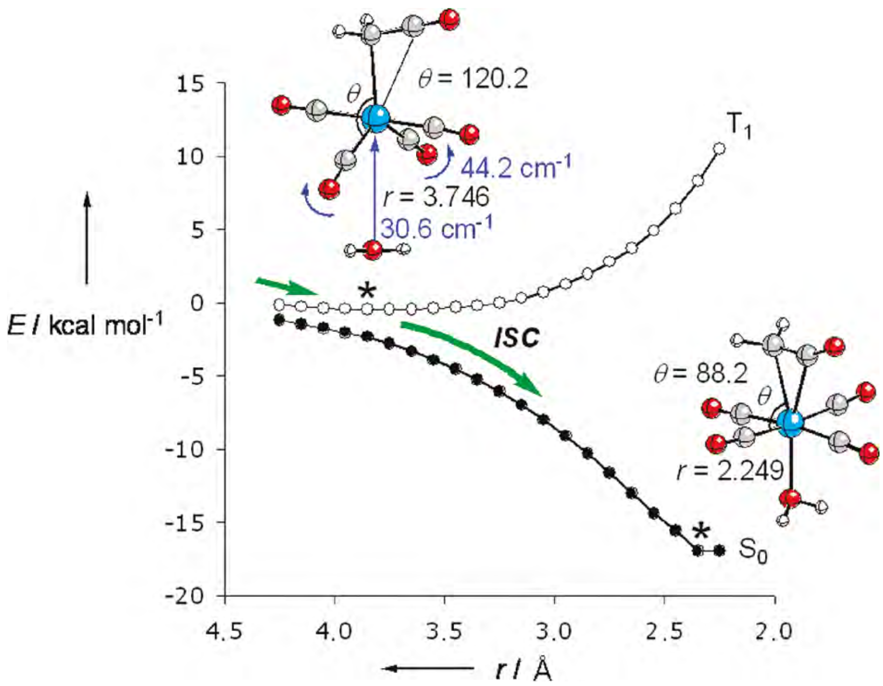

Figure 14: Fully relaxed scans of solvent-induced ISC[97]

1.3.2.4. *Applications in Organometallic Chemistry*

Carbenes have been used in many fields of chemistry, particularly but not exclusively, stoichiometric transition metal-mediated organic synthesis. Their unique reactivity and relative stability allow access to reaction pathways which had been previously unavailable.

Barluenga *et al.* have successfully demonstrated the use of *o*-aminophenyl alkynyl Fischer carbene complexes, **25**, in a [1,5]-hydride transfer/cyclization benzannulation cascade process to form 5,6-dihydrophenantridine complexes (Scheme 7).[103] The [1,5]-hydride transfer results in a 1,2-dihydroquinoline moiety, **26**, which can be manipulated to introduce various functional groups. This moiety allows access, through reaction with an electron poor alkyne, **27**, to the 5,6-dihydrophenantridine complexes, **28**.[103] More recently, the same group has shown that by using 1,3-dienes, various 1,2-dihydroquinoline derivatives can be accessed by this technique (Scheme 8).[104]

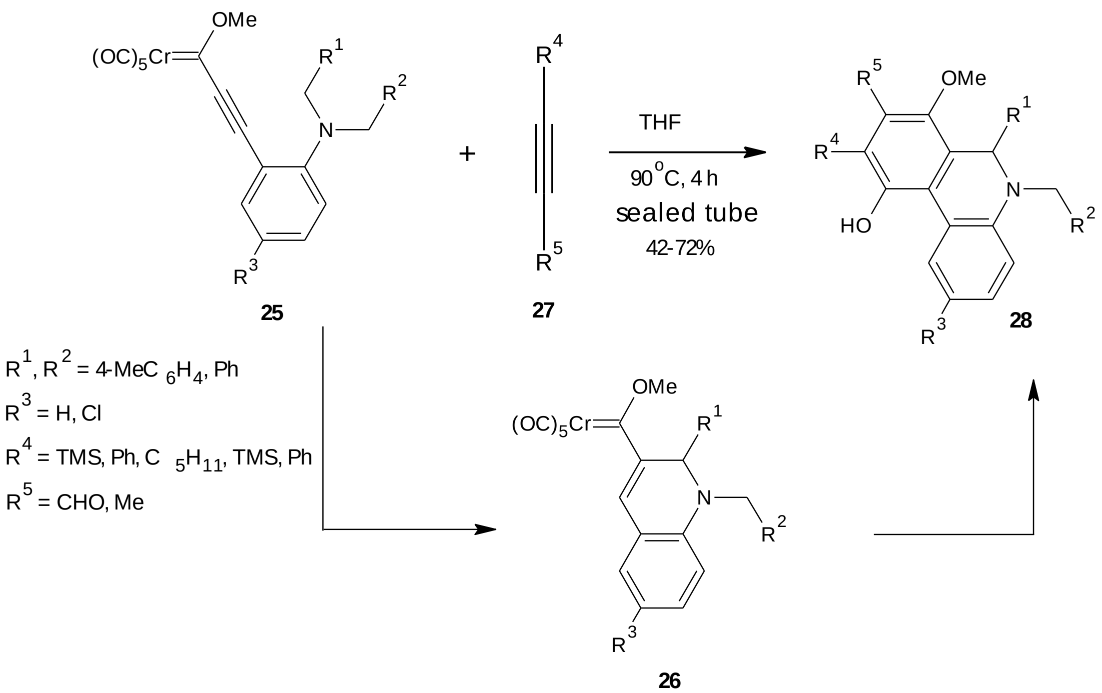

Scheme 7: Synthesis of 5,6-dihydrophenantridines[103]

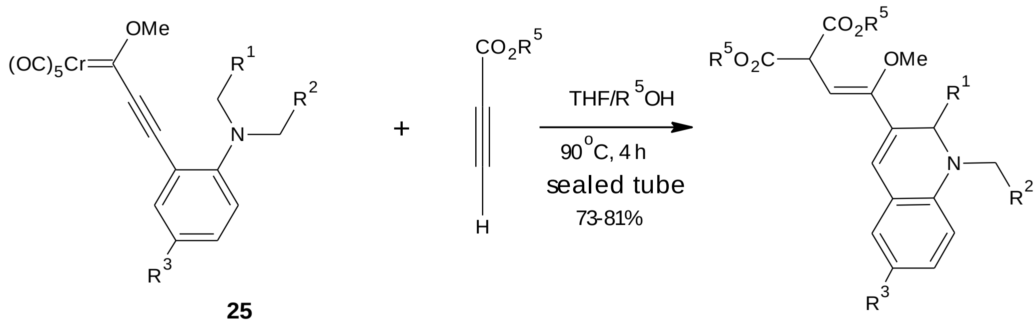

Scheme 8: Synthesis of 1,2-dihydroquinolines[104]

Application of Fischer carbenes has also been found in biomaterial fields. Srivastava *et al.* have demonstrated an application in antibody-antigen recognition, specifically the staphylococcal enterotoxin A (SEA) antibody.[105] This is done by immobilization of an amine *via* a copper-free “click” reaction between an azido self-assembled monolayer (SAM) and an alkynyl Fischer carbene complex. The formation of functional organic thin films is thought to be a key step in the development of “smart” materials, which can find use in various bio-fields. Initially, the same group reported the functionalization of gold nanoparticles and silica substrates with Fischer alkoxymetallocarbene complexes *via* cross-metathesis or Huisgen 1,3-dipolar cycloaddition reactions.[106,107] Scheme 9 shows the process of this immobilization.

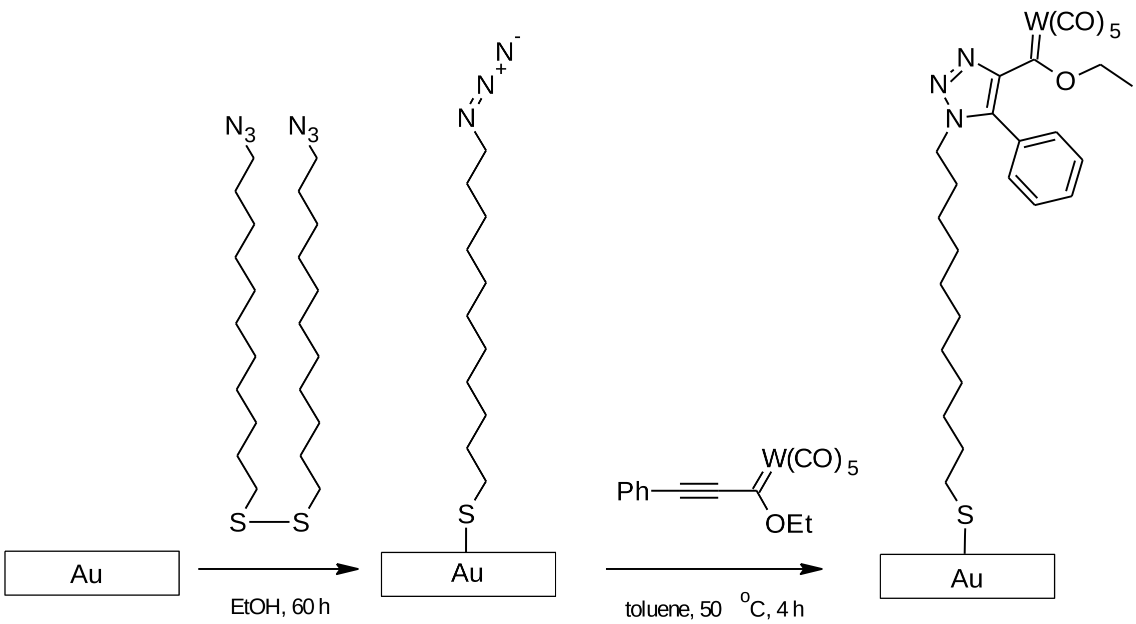

Scheme 9: Immobilization of a Fischer carbene on a gold slide[105]

A glass slide coated with a thin layer of gold was flame-annealed and treated with a 1 mM ethanolic solution of bis(11-azido-dodecyl)disulfide for 60 h at room temperature. This gold substrate was dipped into a solution of phenylacetylenylethoxycarbene pentacarbonyl tungsten in toluene at 50^oC

for 4 h. Interestingly, IR analysis revealed that the carbene complex had covalently bonded to the SAM *via* a 1,3-dipolar cycloaddition to the azidoalkylthiolate rather than simply being adsorbed onto the metal surface. These gold-coated chips showed the ability to recognize and capture SEA, as confirmed by *ex situ* PM-IRRAS analysis of the surface.[105] This research may allow access to immunosensors for detection of SEA in food samples.

Another example in bioorganometallic chemistry is from Maiorana *et al.*, who synthesized a chiral PNA monomer labelled with a Fischer carbene with the use of two Grubbs catalysts.[108] This labelling allowed detection of the complex in a solution until a concentration of 1 x 10^{-7} M was reached. Similarly, the same group has previously attached Fischer carbene complexes to amino acids and proteins in order to tag and detect them.[109]

Recent work with carbenes by Fernandes and Chavan took advantage of the Dötz benzannulation[110] of chiral and achiral alkynes with several Fischer carbenes as a key step in the enantio-selective synthesis of (-)- and (+)-juglomycin A (**28**).[110]

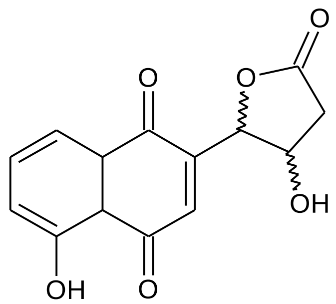

28

This step involves the Fischer carbene, **29**, undergoing a Dötz benzannulation with an alkyne, **30**, at 45°C in THF to afford the trisubstituted napthol, **31**, in good yield (Scheme 10). The remaining synthetic steps can be readily found in the reference.[110] These napthoquinones have found use as antibiotics and anti-tumour agents.[111]

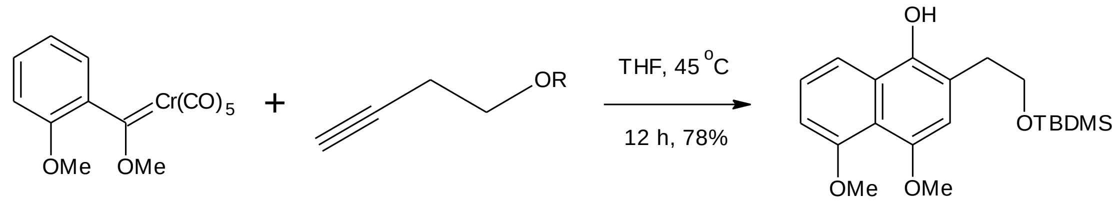

29 30 31

Scheme 10: Benzannulation step in the synthesis of napthoquinones[110]

Ghorai *et al.* have developed a one-pot synthesis of nitrogen-containing polycyclic heterocycles; quinoxaline, quinazoline and phenazine derivatives.[112] This was performed by coupling of a vicinal alkynylheteroaryl carbonyl complex, **32**, with a Fischer carbene, **33**, and a suitable dienophile, **34** (Scheme 11). Although yields were average (30-55%), the one-pot method is convenient when using sensitive reagents.

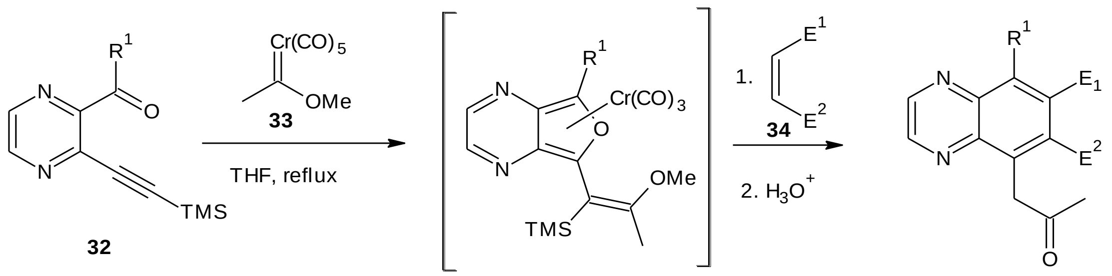

Scheme 11: One-pot, multicomponent synthesis of quinoxaline derivatives[112]

Chung *et al.* have established a method of using chromium Fischer carbenes in the synthesis of chromium *N*-heterocyclic carbene (NHC) complexes.[113] The chromium Fischer carbene was used as a source of pentacarbonylchromium, to which an appropriate imidazolium salt, **35**, was added. The product, a chromium NHC, **36**, was recovered in moderate to good yield (Scheme 12).

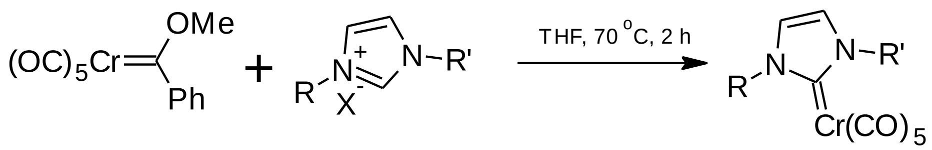

35 36

Scheme 12: Use of Fischer carbene in the synthesis of chromium *N*-heterocyclic carbenes[113]

The use of microwave heating in the application of Fischer carbenes was explored in the formation of uracil-derived Fischer carbene complexes by Ricart *et al.*[114] They reacted various alkynyl Fischer carbenes, **37**, in THF with mono- and disubstituted ureas, **38** (Scheme 13), in a microwave at 400 W for times ranging from 2.5 minutes to 4 minutes. Products **39** and **40** were obtained in similar yields as achieved with conventional heating at 60°C for times ranging from 60 min to 150 min. This result shows how much time can be saved with the use of microwave heating for synthesis.

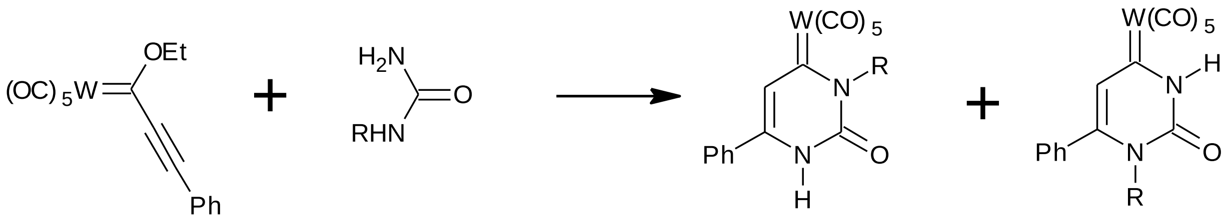

37 **38** **39** **40**

Scheme 13: Microwave synthesis of the formation of uracil-derived Fischer carbenes[114]

1.4. Computational Modelling in Chemistry

Experimental data and models provide invaluable information about a system, but sometimes a more theoretical insight is needed to unravel the deeper mysteries of how and why certain events happen the way they do. A greater understanding of a particular chemical reaction might allow researchers to design a more efficient experimental method, or predict the effects of changing various reaction conditions. These theoretical methods are almost impossible to apply to even simple systems with a manual "pen-and-paper" approach due to the great complexity in their calculations. However, with the advent of affordable and efficient computers, we are now discovering the power and usefulness of computational modelling in science. Two schools of thought are followed, both with complementary advantages and disadvantages.

1.4.1. Empirical Methods

The empirical method involves creating a model that has its roots in real-world experimental data. For example, empirical methods, such as the molecular mechanics (MM) and molecular dynamics (MD) theories, apply classical Newtonian physics to solve and describe the motion of atoms within a molecule by calculating the forces on each atom individually. This allows large molecules to be described very quickly, but accuracy is limited by the type of equations used (as the force field), as well as the fact that most reference values are found in libraries of reference structures (which may or may not contain the molecule of interest). MD calculates these energies at a finite temperature while MM does not.[115] In general, the mathematical form of the equations describing the model or force field is:

$$V(r^N) = \sum\nolimits_{bonds} \frac{1}{2} k_b (l - l_0)^2$$

$$+ \sum\nolimits_{angles} k_a (\theta - \theta_0)^2$$

$$+ \sum\nolimits_{torsions} \frac{1}{2} V_n [1 + \cos(n\omega - \gamma)]$$

$$+ \sum_{j=1}^{N-1} \sum_{i=j+1}^{N} \left\{ \epsilon_{i,j} \left[\left(\frac{\sigma_{ij}}{r_{ij}} \right)^{12} - 2 \left(\frac{\sigma_{ij}}{r_{ij}} \right)^{6} + \frac{q_i q_j}{4\pi\epsilon_0 r_{ij}} \right] \right\}$$

The first three terms are the contributions to energy caused by deviations from the ideal or reference bond parameters (length, angle, torsion). The last term is the non-bonded energy contribution between all atom pairs. It contains two summations: the first is the van der Waals contribution; and the second is the electrostatic contribution.[116] These terms are collectively called a force field. Molecular mechanics/dynamics methods fail to appropriately take into account electronic polarization effects, and so are not applicable to the study of electronic properties.

1.4.2. *Ab-initio* Methods

The second way of approaching the problem is by incorporating electrons explicitly, and not just the atom as a single unit. This is more of a bottom-up theoretical approach, almost by definition, and makes use of quantum mechanics. Accordingly, we refer to it as *ab-initio*, or "from the beginning". These methods have the advantage of providing detailed data regarding chemical reactivity and atomic interactions within the system in question, but require far more computational time to solve. As high-speed parallel computing has become more accessible, *ab-initio* methods have become increasingly prevalent in chemistry.[117]

In quantum mechanics, we describe a given system by using a wave-function, ψ, which contains all the information regarding that system. Describing the electronic structure of a molecular system is, at its root, a quantum mechanical problem. We can say this because each electron in a molecule has its own orbital or wave-function, and these orbitals strongly overlap. Added to this is the fact that most valence orbitals in a molecular system are distributed over many nuclei. Each nucleus is a massive entity with a strongly localized wave-function, and so can be considered in a more classical manner. The complexity does not end there, however, since each electron repels every other electron due to the negative Coulomb force, and interacts with every stationary nucleus via the attractive Coulomb force. Consequently, we have a many-body problem. In classical mechanics, a many-body problem is difficult to solve, but in quantum mechanics, this becomes effectively impossible. This is because for N_e electrons in a system, the many-body wave-function is then a function of $3N_e$ variables, $\psi\,(\mathbf{r}_1 \ldots \mathbf{r}_{Ne})$, where $\mathbf{r}_\mathrm{i}$ ($\mathrm{i}=1 \ldots N_\mathrm{e}$) is a three-dimensional position vector. Solving this problem accurately with numerical tools is essentially impossible for any system that contains more than one electron. Hence, methods incorporating various approximations are required to solve electronic structure problems.

One such simplification is the well-known Born-Oppenheimer approximation, which says that we can separate the motion of the electrons from the motion of the nuclei in a system. This follows from two assumptions:

i. The nuclei are moving considerably slower than the electrons; and

ii. The nuclear motion sees a "smeared" potential from the fast-moving electrons.

From these assumptions, we are allowed to separate the wave-function for the system into:

$$\psi_{\text{total}} = \psi_{\text{electronic}} \times \psi_{\text{nuclear}}$$

where $\psi_{\text{electronic}}$ is the wave-function describing only the electrons, and ψ_{nuclear} is the wave-function describing only the nuclei.

The struggle to accurately solve the quantum-derived many-body problem has led to more and more powerful computational methods. The problem, however, lies with the demand that these improved methods place on computational resources. Generally, the more accurate the method, the longer the time required to calculate the solution. This is also true as the size of the system increases. This makes it unfeasible to calculate, for example, the chemical properties of a 100-atom molecule with full configuration interaction (CI)*.[118] A balance must necessarily be found between available computational time and the required level of accuracy needed in the solution.

1.4.3. Density Functional Theory

The origins of density functional theory (DFT) come from the Thomas-Fermi model for the statistical treatment of the distribution of electrons in an atom (essentially the density of electrons as a function of position).[119,120] Two core elements of the theory are the Hohenberg-Kohn (HK)[121] theorems and the Kohn-Sham equations (KS).[122] The first HK theorem proves that the ground-state behaviour of a many-electron system is determined by an electron density depending on only three spatial coordinates.[121] That is, given a ground-state density $n_0(\mathbf{r})$, it is possible to calculate the corresponding ground-state wave-function $\psi_0(\mathbf{r}_1, \mathbf{r}_2\ldots, \mathbf{r}_N)$. We can see that ψ_0 is a *functional* of n_0. This facilitates the reduction of the many-body problem of *N* electrons each with 3N coordinates to just three spatial coordinates by the use of functionals of the electron density. By extending this theory to the time-dependent domain, time-dependent DFT models are constructed that can be

* CI is a matrix mechanics method for solving the time-independent non-relativistic Schrödinger equation, using the Born-Oppenheimer approximation. It is a general method applicable to excited states, open-shell systems and systems far from their equilibrium geometries. "Full" CI is a more exact solution of the Schrodinger equation, and is only computationally viable for small systems, due to the intractable nature of the matrix expansion required as the number of electrons in a system is increased.

used to describe excited states. The second HK theorem defines an energy functional for the system and proves that this is minimized by the correct ground-state electron density.[121]

As discussed earlier, real systems, whether they are atoms, molecules, clusters or solids, are both inhomogeneous (that is, the electrons are influenced by the nuclei) and interacting (the electrons interact with each other *via* the Coulomb force). The KS equations reduce the many-body problem of interacting electrons in a static external potential to one of non-interacting electrons moving in an effective potential, effectively decomposing the problem into two simpler interactions.[122] The solution of a spatially homogeneous interacting problem gives the uniform exchange correlation energy, and the solution of a spatially inhomogeneous non-interacting problem (the inhomogeneous electron gas described by the Kohn-Sham equations)[122] yields the particle density. These two problems are connected by the local-density approximation, a functional that shows how the exchange correlation energy of the uniform interacting system enters the equations for the inhomogeneous non-interacting system.

1.4.3.1. Local Density Approximation

The simplest approximation is to treat the electron density in a system as a uniform electron gas. This is called the *local density approximation* (LDA). The exchange correlation energy at each point in the system is approximated to be the same as that of a uniform electron gas of the same density. This approximation was first introduced by Kohn and Sham[122] and holds for a slow varying density. It has proven to be useful in determining such properties as structure, vibrational frequencies, elastic moduli and phase stability. Some important errors become apparent when computing energy differences (exchange energy – E_x) between some systems, resulting in an overestimation of around 20-30%,[123] and an underestimation in energy barriers (correlation energy – E_c) in diffusion or chemical reactions. When combined, these two errors tend to balance each other out in some systems, which may be one reason for the relative success of the LDA (this cancellation is not entirely accidental, but more systematic to the approximation).[124] This is well illustrated in Figure 15.[125] While LDA provides accurate and useful data in solid-state research, it is less popular in computational chemistry because it fails to provide quantitative data on chemical bonding in molecules. A useful concept is that of *chemical accuracy*; as a rule of thumb, we can assume that calculations with errors larger than around 4 kJ/mol (or about 1 kcal/mol) are not chemically accurate.

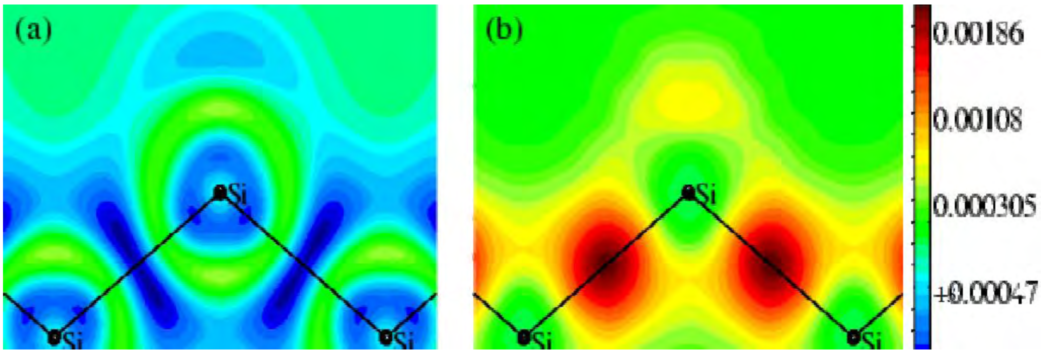

Figure 15: The difference between (a) the exchange E_x energy density and (b) the correlation E_c energy density computed using variational-quantum Monte Carlo (V-QMC) and the LDA in bulk silicon[125]

1.4.3.2. Generalized Gradient Approximation

Understanding the shortcomings of the LDA has been important in developing improved theories. The first attempted improvement was the *generalized expansion approximation* (GEA). This involved including low-order expansion terms in a power-series approach to the calculation of the LDA. However, in practice, this technique seldom improves on the LDA, and can actually result in greater inaccuracy. By experimenting with more general functions of $n(\mathbf{r})$ and the gradient, $\nabla n(\mathbf{r})$, an improvement was found. Here, $n(\mathbf{r})$ denotes some dependence of n on $\mathbf{r}$, for example, electron density (n) as a function of position ($\mathbf{r}$). The gradient[*] function $\nabla n(\mathbf{r})$ will give information relating to the rate of variation of $n(\mathbf{r})$; in this example, the change of electron density with changing position $\mathbf{r}$ will be calculated. This is known as the *generalized gradient approximation* (GGA). Depending on the exact form of $f(n, \nabla n)$, vastly different GGAs can be developed. This ability to vary the GGA means that there is potentially more difference between various GGAs than there is between LDA and GGA.[124]

Perdew *et al.* have demonstrated the improvements of GGA against LDA,[126] but it is worth noting again that LDA provides accurate results in solid-state research, for example, obtaining an accuracy of about 1% when determining lattice constants in simple crystals.[127] Further examples of the significant improvement and variation of LDA and GGA can be found in the literature.[128,129] The two most popular GGA functionals nowadays are PBE,[130] proposed by Perdew, Burke and Ernzerhof, and BLYP, denoting the combination of Becke's exchange functional[131] with the correlation functional of Lee, Yang and Parr.[132] Although GGA improves on LDA, *chemical accuracy* is generally not achieved.

[*] The **del** operator, ∇, is used to denote the standard derivative of a function, vector or matrix.

1.4.3.3. Meta-GGA and Hybrid Functionals

Improvements on GGA are ongoing, resulting in various hybrid and "meta"-GGA functionals. An example of a hybrid is the popular B3LYP functional. This is a hybrid of the LYP GGA for correlation, mixed with Becke's three-parameter hybrid functional B3 from Hartree-Fock for exchange.[133] A useful hybrid for metallic systems is the HSE (Heyd, Scuseria and Ernzerhof) exchange-correlation functional.[134] Meta-GGA functionals are relatively unexplored, but can give improved results over GGA functionals in certain systems.[135,136] They depend not only on density and its derivatives (as with the GGA), but also on the KS kinetic-energy density $\tau(\mathbf{r})$. This provides an additional degree of freedom, which is used to satisfy additional constraints on the exchange-correlation energy.[124]

1.4.3.4. Comparing Functionals

It is possible to roughly group functionals within families. There are, of course, several functionals that cross the boundary between the groups, but the classification is useful to predict the accuracy of a particular functional in an unknown system.

Table 1: Grouping of functionals within families

Family	Functional
LDA	PWC, VWN
GGA	BLYP, PBE, HCTH, PW91, BP, BOP, VWN-BP, RPBE
Meta-GGA	VS98, PKZB
Hybrid	B3LYP, HSE

The performance of these functionals has been evaluated by Kurth *et al*.[137] and Adamo *et al*.[138] Some selected results are given in Table 2. The over-estimation of the LDA by 20-30% for atomization energies is apparent in Table 2, as well as its relative accuracy in crystal structure determinations. As expected, significant improvements are seen for GGA methods. The highly parameterized (more empirical) HCTH functional performs better than the purer GGA methods. Meta-GGA functionals again improve on GGA with relative errors of 2-3%. For simple systems, it is clear that the meta-GGA and hybrid functionals are approaching the limit of accuracy; however, for complex systems, the errors still range from 50-160 kJ/mol.

Table 2: Mean relative errors (MRE)* for a collection of 20 molecules, and mean absolute errors (MAE)† for a collection of 148 molecules, with the maximum absolute error given in brackets

Functional	Atomization Energies[137]		Structures[138]	
	MRE %	MAE (max) kJ/mol	MRE %	MAE (max) Angstrom
LDA	22	-	5	-
BLYP	5	-	8	-
PBE	7	71.1 (213.4)	4	0.011 (0.064)
HCTH	3	-	6	-
VS98	2	12.6 (50.2)	8	0.008 (0.08)
PKZB	3	20.9 (159)	3	0.019 (0.111)
Hybrid	-	12.6 (50.2)	-	0.007 (0.062)

The two most widely used functionals in modern chemical applications of DFT are the Becke-Yang-Lee-Parr (B3LYP)[131,132] and Perdew-Burke-Ernzerhof (PBE).[130] As previously explained, B3LYP is a hybrid Hartree-Fock/DFT functional, while PBE is a pure DFT method and falls under the GGA family of functionals.

1.4.3.5. Bond Order and Atomic Charge Calculations

Calculation of supplementary data can be done efficiently with computational methods, and although these are generally not limited to DFT, some ideas will be introduced here.

Classically defined, the concept of *bond order* can be thought of as the number of chemical bonds between a pair of atoms. This simple definition is fundamental to much of our understanding of chemistry and chemical processes with such concepts as resonance, delocalization, valence and electron density all closely stemming from bond order.

A simple definition would be easiest, but in real terms, bond order is far more complicated. In practice, bond orders are generally not integers, although this depends on the method and level of theory used to perform the calculation. It should be noted, however, that there is yet to be a universally agreed quantum mechanical definition of bond order (such concepts as atomic charge and valence are similarly undefined from a quantum mechanical and electronic structure view). The bond order can give an indication of the length and strength of the bond.[139]

* Given as percentages

† Given in kJ/mol and angstrom for energies and structures, respectively

Pauling defined[140] an empirical relationship between bond order and bond length (where *a* is 0.3 for carbon):

$$n_{\mathrm{bond}} = exp^{\left(\frac{r_0 - r}{a}\right)}$$

This relationship suggests that the bond order decreases exponentially as bond length *r* increases (and *vice versa*) with respect to the single bond length r_0. For simple hydrocarbon chemistry, this relationship can be useful in providing insights, but there is no quantum chemical basis for it.

Molecular orbital theory is widely used in combination with computers to calculate bond orders. One method is that proposed by Wiberg.[141] This is used in many semi-empirical calculations and is closely matched to classical bond valences. Mayer[142,143] extended the Wiberg bond order index. This extension leads to classical integer values when minimal basis sets are used in the calculation, while non-integer values are given for larger basis sets and more complicated molecules. These variations illustrate the ionic character of the bonds, as well as distortions due to delocalization.

Mayer's extension is basis-set dependant, as is the Mulliken population analysis to which it is closely related. This means that comparisons between different systems can only be done if calculated with identical basis sets. It has been found that Mayer bond orders have an advantage when applied to large systems with little or no symmetry.[144] This is because the Mayer bond order calculation gives an efficient method of combining and summing all contributions to the bonds in a system and is not limited to the high- and low-lying orbitals. Bridgeman *et al.* has shown this in their analysis of bonding in the ground-state of tetragonally compressed copper(II) complexes.[145]

There are several different theories that can be applied to calculate bond orders, including but not limited to the Coulson bond order[146] and Bader's application of *atoms in molecules* (AIM) method. However, for the purposes of this project, Mayer bond orders were used where applicable.

Another useful concept is *atomic charge*. By knowing the charge on a certain atom or fragment and how it has changed in bonding, it is possible to estimate the ionic or covalent character of the bond. As with bond order, however, atomic charge is an arbitrary concept in quantum mechanical terms. Mulliken proposed a method of charge partitioning that has become well known.[147] This method sums the contributions from all the atomic orbitals located on the atom, and assumes that the contributions from orbitals involving basis functions on different atoms are equally divided. This is a similar method to the Mayer bond order calculations, and as mentioned, both of these techniques suffer from high sensitivity to the basis set being used.[148] Hirshfeld's method circumvents the basis-set dependence by estimating the charge as a weighted spatial integral of the self-consistent field charge density associated with the atom.[149] Either method can be used to compare atoms on similar systems, but the Mulliken method must use identical or analogous basis sets for each system in order for comparisons to remain quantitative.

1.4.3.6. Applications of DFT

The importance of DFT was recognized with the awarding of the 1998 Nobel Prize in Chemistry to Walter Kohn[150] and John Pople[151] for their work in developing and implementing the theory. It has great versatility and can be relatively easily implemented. Researchers have taken advantage of DFT in molecular physics, calculation of ionization potentials,[152] vibrational spectra, chemical reactions, structure elucidation in bio-fields,[153] atoms within laser pulses, relativistic effects in heavy elements, magnetic properties of alloys, active sites and catalysis,[154] as well as various fields within solid state physics.[155,156,157] DFT can sometimes provide a useful alternative to *ab-initio* methods, especially with larger molecules.[158] Conventional quantum chemical models increase in computational effort exponentially with increasing number of electrons, N, whereas DFT methods grow at an average of a third of N.[158] A further computational shortcut sometimes used is to incorporate pseudopotentials,[159] which replace the almost inert inner-core electron wave-functions with a single known wave-function. DFT provides a relatively efficient way to calculate the ground-state energy in realistic models of bulk materials and their surfaces. Applications are found in drug discovery and development, metal catalytic systems and solid state chemistry.

Chen *et al.*[160] have investigated the structure and chemical shifts of the carbene complex $(CO)_4FeCF_2$ at the DFT level. Making use of the BP86[*] and B3LYP functionals, they calculated that the CF_2 ligand is found to occupy an equatorial position in a trigonal bipyramidal iron complex (Figure 16b). The axial configuration (Figure 16a) was, however, only 4.2 kcal/mol higher in energy, which is close to the limit of chemical accuracy (around 1 kcal/mol). They also found that the carbene carbon is more deshielded (~40 ppm) with respect to the CO ligand in ^{13}C NMR.

[*] BP86 is a GGA functional that has the same exchange correlation as BLYP, but uses the older Perdew86 correlation functional. It has been reported in the literature that BP86 can give results slightly too large, in comparison to the more widely used B3LYP hybrid functional.[161]

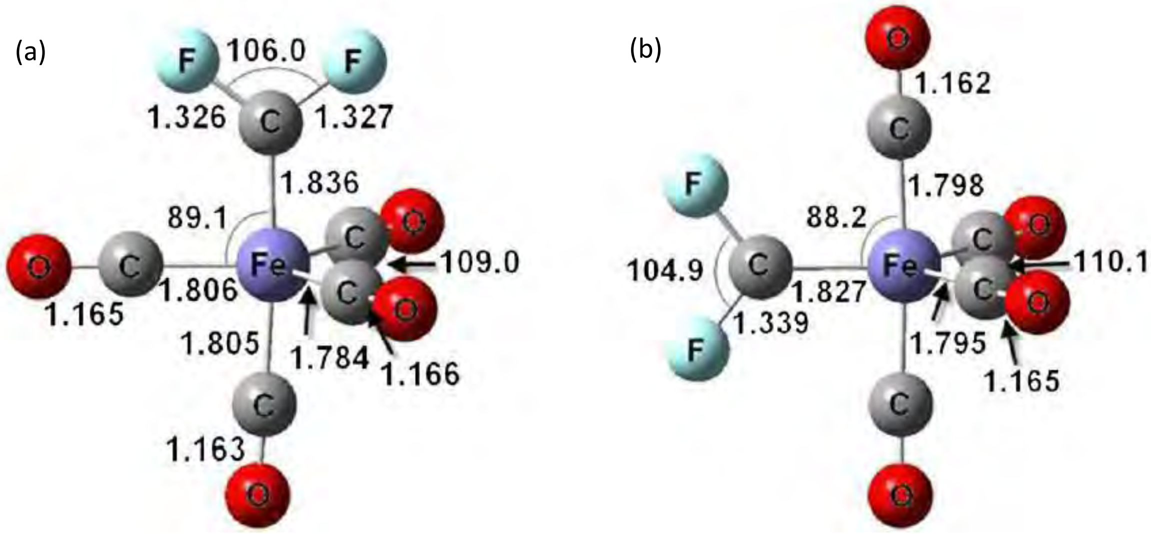

Figure 16: Possible isomers of $(CO)_4FeCF_2$, axial configuration (a) and equatorial configuration (b)[160]

Generally, computational studies are carried out to support or confirm explanations of experimental observations, or to provide insights and reasoning for certain anomalous experimental behaviour. In this sense, studies such as the one by Chen *et al.* are useful for shedding light on experimental data that may not seem clear at first.

1.5. Aims of the Current Study

(I) Prepare a range of simple and complex Fischer carbenes of varying stability, followed by application of the Fischer method for carbene synthesis.

This will be achieved *via* the use of α-alkoxy- and α-amino organostannanes as stable precursors to organolithiums.

(II) Calculate the optimal ground states of representative products.

This will utilize *in silico, ab initio* methods to determine the ground-state structures and energies of some Fischer carbenes.

(III) Compare calculated and experimental data as a means of validation.

The correlation between experimentally determined vibrational spectra (such as IR and Raman) and with theoretically calculated data will be explored to confirm the validity of computational methods used.

(IV) Apply computational methods to determine the source of chemical instability.

The complex and unpredictable chemical stability of these Fischer carbenes will be explored computationally in the hopes of providing insights into their reactivity and possible application.

Chapter 2: Results and Discussion

2.1. Synthesis of Organostannanes

Organostannanes are useful precursors to organolithium reagents, which in this study are themselves useful for the synthesis of novel Fischer carbenes. Several challenges were uncovered in early attempts to synthesize, isolate and characterize these organostannanes; however, most were overcome with careful attention to detail. Three α-alkoxy organostannanes and two α-amino organostannanes were successfully synthesized, isolated and characterized in this study.

2.1.1. α-Alkoxy Organostannanes

The synthesis of α-alkoxy organostannanes was carried out using the method developed by Still,[22] and involves the nucleophilic addition of a tributylstannyl anion to the carbonyl of an aldehyde (or ketone), **41a-e,** to give a substituted stannous alcohol, **42a-e**. The tributylstannyl anion was formed *in situ* by the deprotonation of tributyltin hydride with LDA, to give tributylstannyllithium. The reaction was performed using Schlenk techniques[162] and anhydrous solvents due to the sensitivity of LDA to facile quenching in water. The stannous alcohol, **42**, was immediately protected under mild conditions using dimethyl aniline (DMA) and α-chloromethyl methyl ether (MOM-Cl) as the protecting group to give the desired α-alkoxy organostannanes, **43a-e** (Scheme 14). A range of α-alkoxy organostannanes were synthesized, or attempted, with varying chain lengths (Table 3).

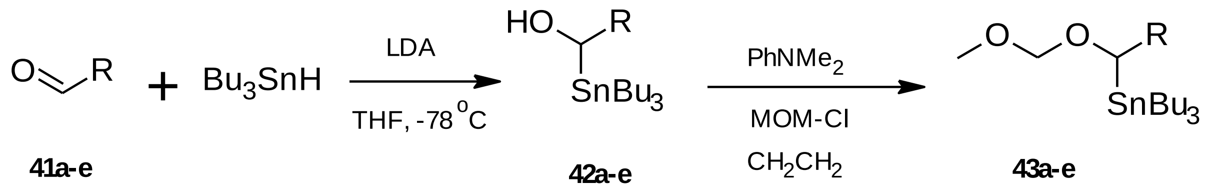

Scheme 14: Synthetic route to α-alkoxy organostannanes

Table 3: Yields of α-alkoxy organostannanes synthesized

43	R	% Yield
a	C_2H_5	61
b	C_3H_7	35
c	$CH(CH_3)_2$	32
d	H	-*
e	Benzaldehyde	-*

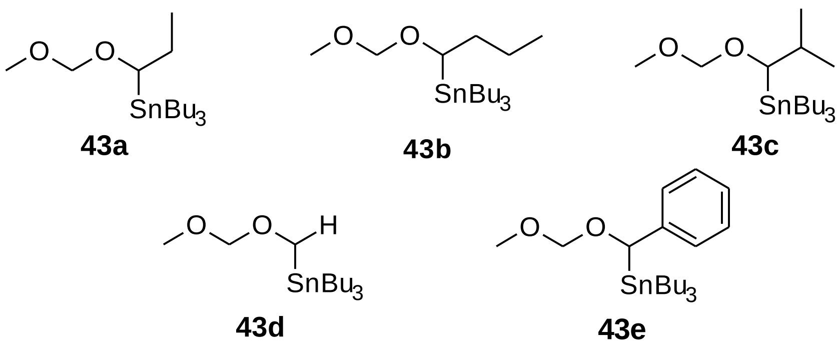

* Attempted but not successfully isolated

Although known to be relatively unstable,[163] it was possible to purify the unprotected α-hydroxy organostannane, **42a**, through column chromatography in the same manner as the protected stannane, **43a**. Interestingly, the Rf values of the protected stannane were thought to be as high as they are (0.73 in 10% ethyl acetate:hexane on silica TLC, for compound, **43a**, due to the non-polar protecting group.[164] However, the Rf value of **42a** was found to be 0.71 in the same solvent system. Similar behaviour was found when compared in a 10% DCM:hexane solvent system. This suggests that the protecting group is not entirely responsible for the non-polar character, and the nature of the tributylstannyl moiety dominates the behaviour of the free alcohol. ^{13}C DEPT 135 NMR (Figure 17) and ^{1}H NMR (Figure 18) confirmed the structure of the unprotected alkoxy organostannane.

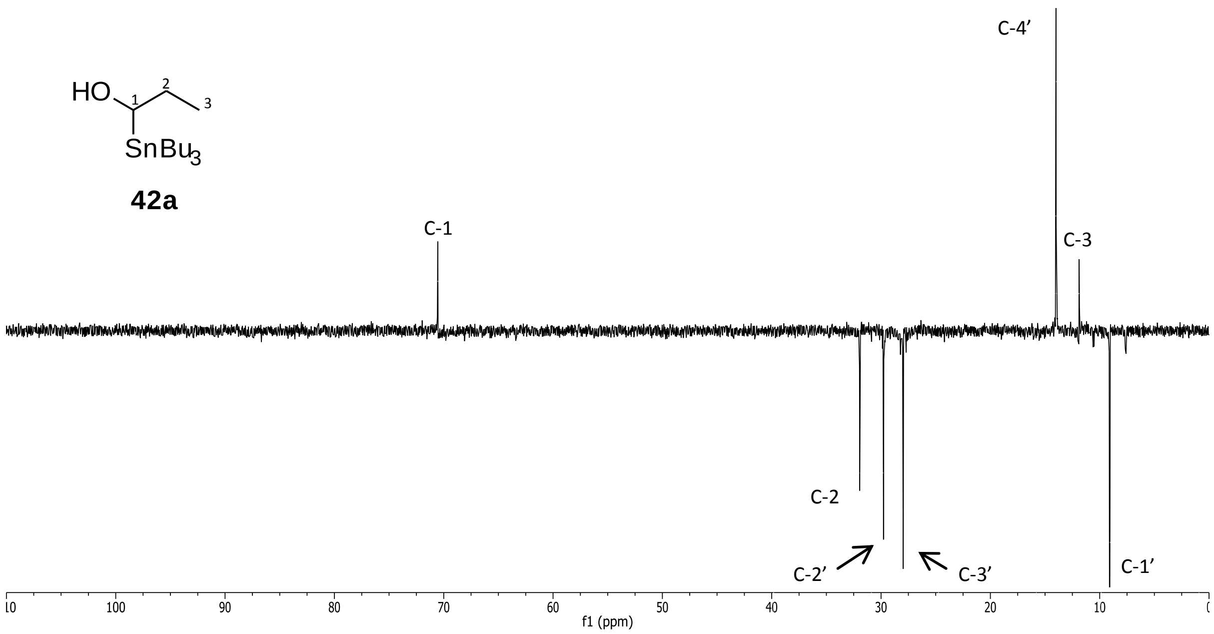

Figure 17: ^{13}C DEPT 135 NMR of unprotected stannane 42a in C_6D_6

Assignment of the spectrum was relatively simple. The methylene carbon (on the butyl chains) closest to the tin atom, C-1', is found at 9.1 ppm and exhibits two pairs of satellites. These satellites are due to two NMR-active isotopes of tin, ^{117}Sn and ^{119}Sn, coupling to ^{13}C, and the magnitude of the $^{1}J_{C\text{-}Sn}$ coupling is diagnostic.[16] The rest of the butyl chain, C-2', C-3' and C-4', are found at 29.8, 28.0 and 14.0 ppm, respectively. The signal at 70.5 ppm corresponds to C-1, while C-2 is seen at 32.0 ppm and C-3 at 11.9 ppm.

In the ^{1}H NMR spectrum (Figure 18), the signal at 3.99 ppm is due to the single proton at 1-CH. The broadening of this signal is mostly due to coupling to exchangeable OH groups, although splitting caused by the methylene protons at 2-CH_2 (with a small coupling constant) may also contribute to the observed broadness. These methylene protons, 2-CH_2, are seen as a multiplet at 1.85 ppm, and the 3-CH_3 methyl protons are located in the multiplet between 0.8 and 1.2 ppm. The remaining signals are due to the tributyl chains attached to the tin atom.

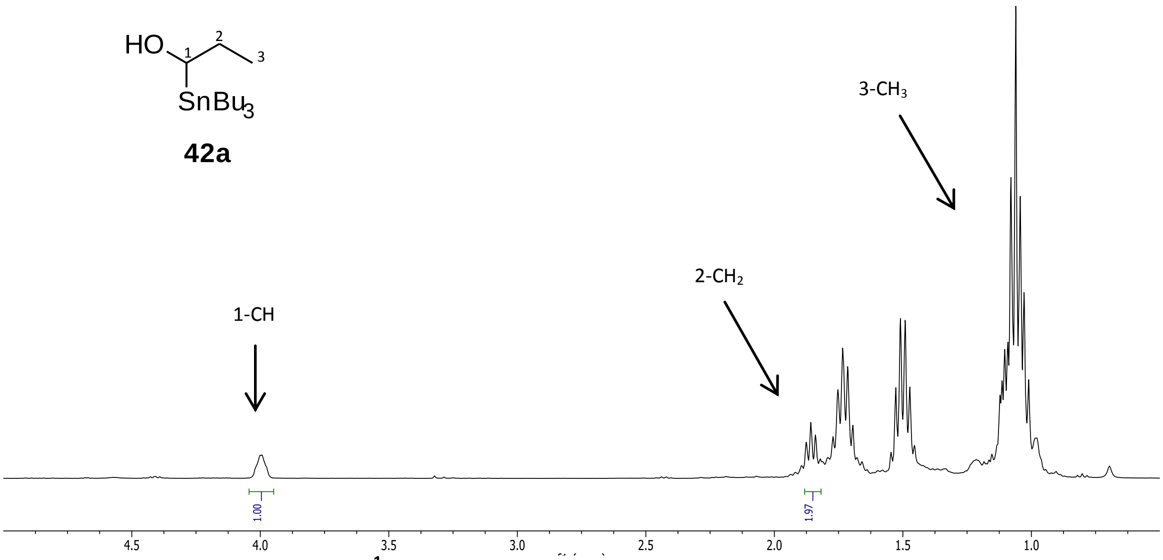

Figure 18: ^{1}H NMR of unprotected stannane 42a in C_6D_6

As mentioned, the stannous alcohol is relatively unstable and reacts readily, eliminating the tin moiety. The protection step was carried out in the presence of a mild base and α-chloromethyl methyl ether at -40°C in DCM. ^{13}C DEPT135 (Figure 19) and ^{1}H NMR (Figure 20) spectra confirmed the presence of the MOM-protected product, compound **43a**. The MOM protecting group can be readily hydrolyzed under mild acid conditions and improves the stability and shelf life of these α-alkoxy organostannanes.

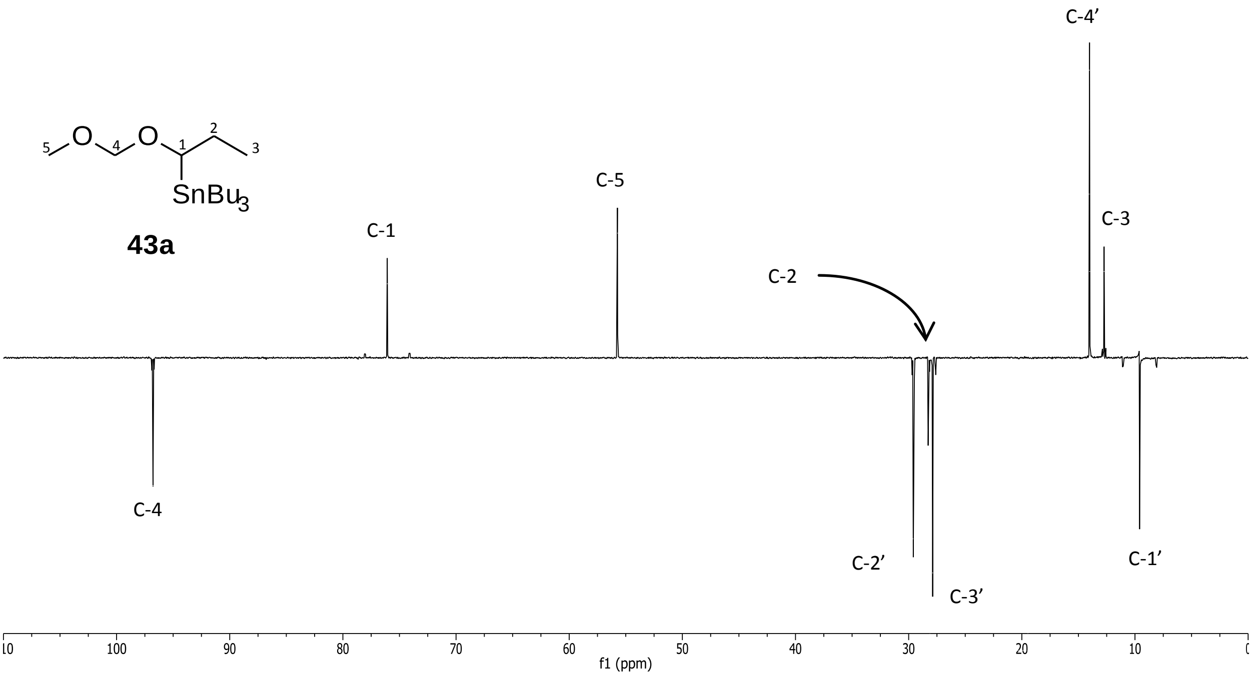

Figure 19: ^{13}C Dept135 NMR spectrum of MOM-protected stannane 43a in $CDCl_3$

The MOM group adds two additional signals to the ^{13}C spectrum. The methylene carbon, C-4, resonates at 96.4 ppm while the methoxy carbon, C-5, is observed at 55.2 ppm. The ^{1}H NMR (Figure 20) was also interesting, due to the splitting patterns observed. The triplet at 3.99 ppm is due to the methine proton at the chiral centre, which is split by the methylene protons on C-2. The doublets between 4.5 and 4.7 ppm are due to the diastereotopic methylene protons on the MOM group. These two protons are in different chemical environments, and so each resonates at a different frequency, and couple to each other with a geminal coupling constant of 6.6 Hz.

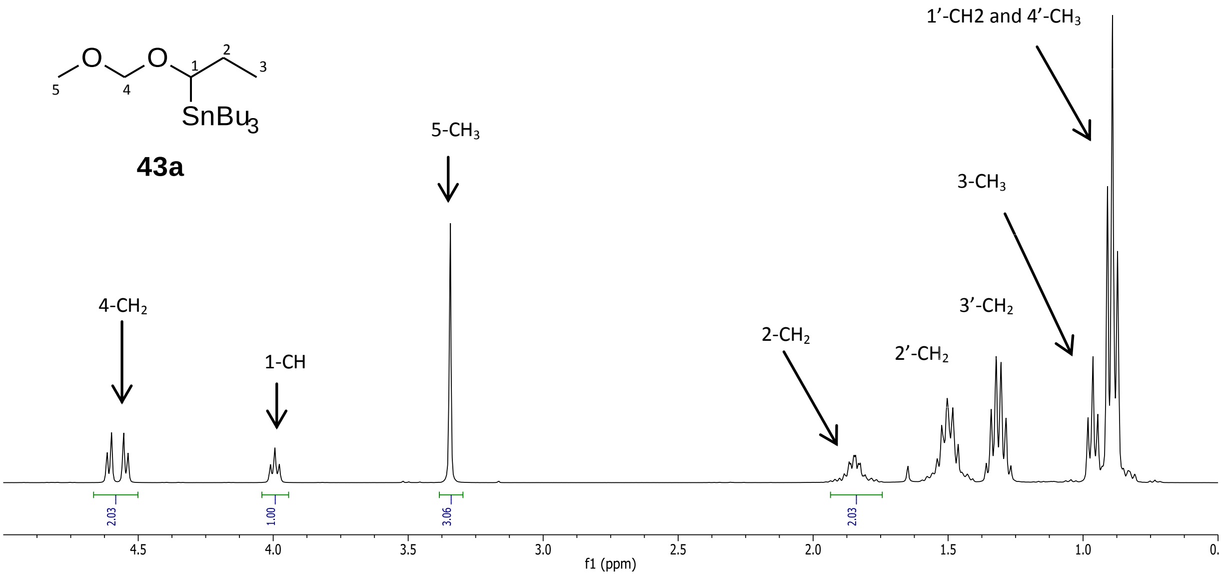

Figure 20: ^{1}H NMR of MOM-protected stannane 43a in $CDCl_3$

As with the unprotected compound, pairs of satellites are visible, most notably in Figure 19, on C-1 and C-1'. This is due to two NMR active isotopes of tin, ^{117}Sn and ^{119}Sn, coupling to the carbon atoms attached directly to the tin atom.[16] There is a third NMR active isotope, ^{115}Sn, but with a natural abundance of just 0.35% (compared to 7.61% and 8.58% for ^{117}Sn and ^{119}Sn, respectively), any coupling effects are not visible in these spectra. Figure 21 shows an expansion of C-1 from Figure 19, illustrating the satellites due to the coupling.

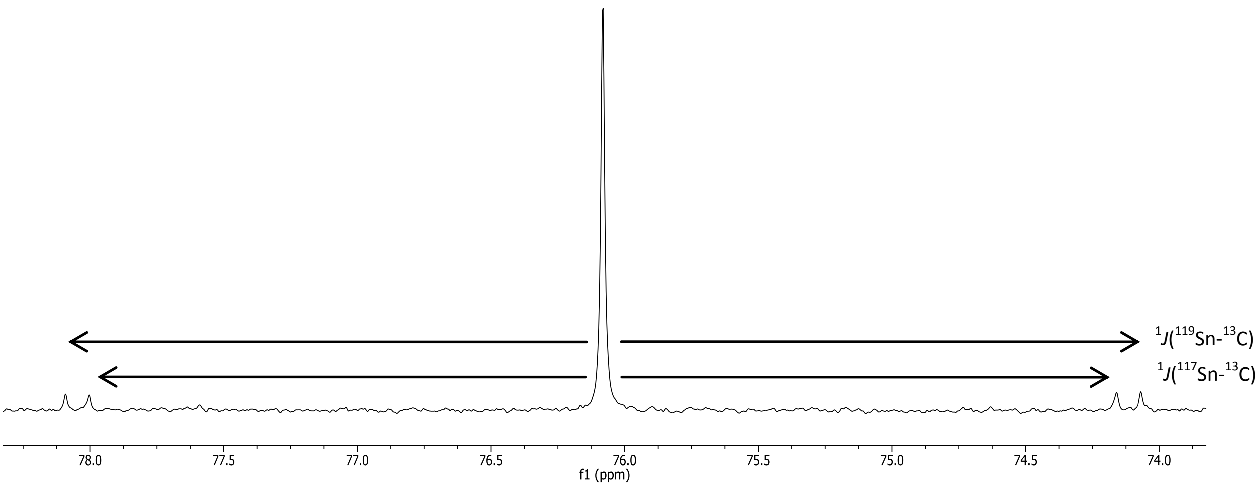

Figure 21: Expansion of DEPT135 spectrum of 43a showing satellites due to $^{117}Sn-^{13}C$ and $^{119}Sn-^{13}C$ coupling

Single satellites are visible on several carbons not adjacent to the tin atom (Figure 22). The overlapping satellites are due to these carbon atoms being progressively further away from the tin atom. The closer the carbon is to the tin, the larger the coupling constant observed. This is consistent with reports in the literature.[165,166,167]

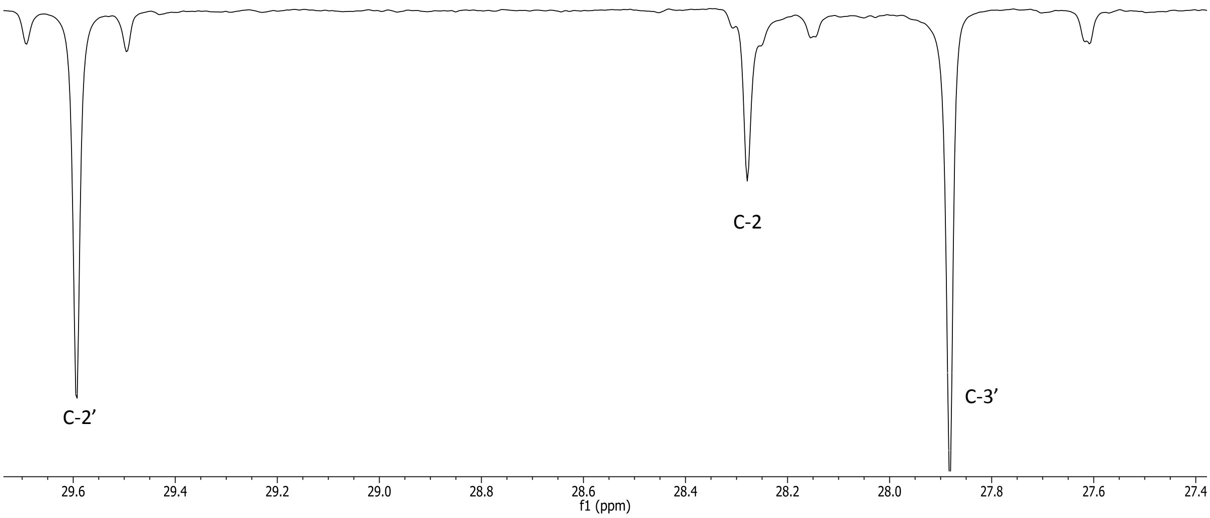

Figure 22: Overlapping satellites on carbons not directly attached to a tin atom for 43a

Table 4: Coupling constants for Sn-C coupling

Compound	C-1	C-3	C-5	C-1’	C-2’	C-3’
42a (C_6D_6)	-*	32.6 Hz	N/A	288.6, 301.7 Hz	20.1 Hz	52 Hz
43a ($CDCl_3$)	386.4, 404.7 Hz	30.6 Hz	20.3 Hz	290.6, 304.0 Hz	19.8 Hz	53.2, 54.9 Hz

* No value can be read due to poor signal to noise ratio in this spectrum.

Synthetic Challenges

Several challenges presented themselves in the synthesis and purification of α-alkoxy organostannanes.

It was found that solvents were needed to be freshly dried on the day of the reaction for optimum results. Also, THF is known to be decomposed by BuLi at room temperature, so care was taken to ensure that the temperature was kept below 0°C until transmetallation was complete.

Although most alkylithium reagents deteriorate over time once the container is opened, it was initially assumed that the manufacturer-specified concentration of the *n*BuLi would be sufficiently accurate. Hence reactions were calculated and carried out using that concentration. However, it quickly became apparent that the actual concentration of the reagent was lower than the labelled concentration. This deficiency is often detrimental to metallation reactions[168] and so a convenient method of analysis was found. Kofron *et al.* have described a method for estimation of alkyllithium concentrations using diphenylacetic acid.[169] This is a convenient reagent since it is stable on storage, and an easily weighed solid. A sample of diphenylacetic acid, **44**, was weighed (typically 1 mmol) into a small round-bottom flask and dissolved in dry THF at 0°C. Using a syringe, the alkyllithium was added dropwise to the clear solution until the yellow end point was reached. This is a 1:1 titration, so when the end point was reached, the volume of alkyllithium reagent added was equivalent to 1 mmol. The yellow colour indicates the formation of orange lithium α-lithiodiphenylacetate, **46**, once all the carboxyl proton is consumed, and hence that one equivalent of the alkyllithium has been added (Scheme 15). All reactions were preceded by a titration of the alkyllithium reagent to determine and confirm the concentration.

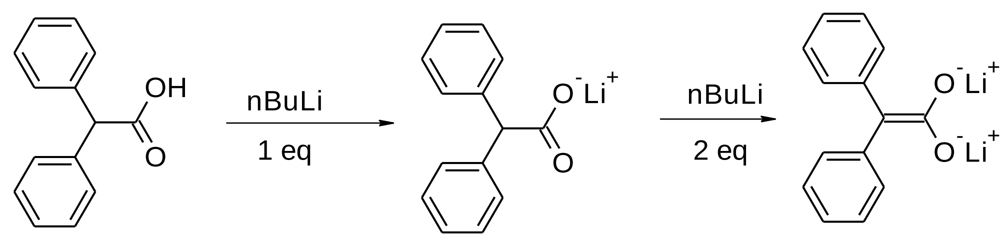

44 colourless **45** colourless **46** orange

Scheme 15: Reaction of diphenylacetic acid with *n*BuLi

Purification was carried out using column chromatography on silica gel. Organostannanes are known to elute rapidly on silica gel, even when using a non-polar solvent, such as hexane, unless they contain highly polar substituents.[164] This caused them to elute with a range of components; by-products, such as tetrabutyl tin, and unreacted reagents, such as the aldehyde used. To facilitate easier separation, it was found that when using a 10% dichloromethane:hexane solvent system, most of the components where held back on silica, allowing for easier removal of the major impurity, tetrabutyl tin, which still eluted with an Rf of 0.85. The solvent system was then changed to 10% ethyl acetate:hexane, which promoted elution of the α-alkoxy organostannane product. Low flow rates were found to help with resolution of the components, especially regarding the components that were held back by the DCM:hexane system, and thus the gravity elution method was favoured over flash chromatography.

This method allowed synthesis and separation of three α-alkoxy organostannanes: **43a**, **43b** and **43c**. The synthesis of an α-alkoxy stannane derived from paraformaldehyde (**43d**) has been reported by Sawyer *et al*,[170] although attempts to synthesize this compound proved unsuccessful in this study. ^{13}C and ^{1}H NMR analysis showed the presence of **43d** after synthesis, but attempts at purification and separation resulted in the complete decomposition of the product. Attempts to isolate α-alkoxy stannane, **43e**, synthesized from benzaldehyde, were similarly unsuccessful. Seven fractions were collected from silica chromatography, and ^{13}C and ^{1}H NMR proved inconclusive in determining which fraction was the desired product, or even if it had been synthesized.

2.1.2. α-Amino Organostannanes

α-Amino organostannanes derived from pyrrolidine, **47a**, and piperidine, **47b**, were synthesized, according to the method laid out by Beak *et al.*[25] As the synthesis involves a deprotonation/lithiation sequence before the electrophilic substitution, it was important to protect the NH group of the amines. To this end, **47a** and **47b** were reacted with di-*tert*-butyl dicarbonate, **48,** (tBoc$_2$O) to produce the carbamate-protected amines, **49a** and **49b**, respectively. This protection was easily carried out by combining the amine with tBoc$_2$O in CH_2Cl_2 at 0°C for 1 h (Scheme 16). Fractional distillation afforded the products in good yields (70%).

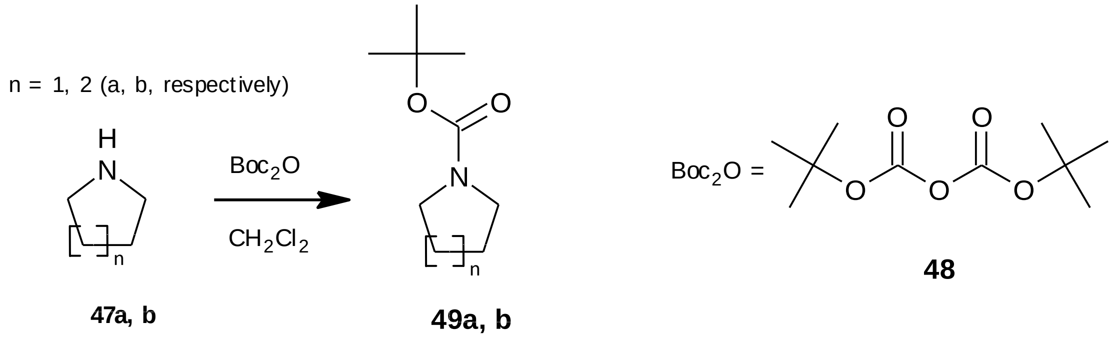

Scheme 16: Addition of the BOC protecting group

NMR analysis of **49a** confirmed the presence of the product, and illustrates some interesting structural behaviour. The ^1H NMR spectrum (Figure 23) shows a singlet due to the three equivalent methyl groups of the *t*-butyl at 1.49 ppm. A broadened singlet at 1.87 ppm is due to the chemically similar methylene protons furthest from the nitrogen in the ring, 3-CH_2 and 4-CH_2. A broad multiplet between 3.30 and 3.35 ppm is due to the methylene protons on either side of the nitrogen, 2-CH_2 and 5-CH_2. The broadening is due to restricted rotation around the amide bond of the carbamate group, which reduces the symmetry of the system. At higher temperatures, we would expect faster rotation and hence narrowing of the signal.

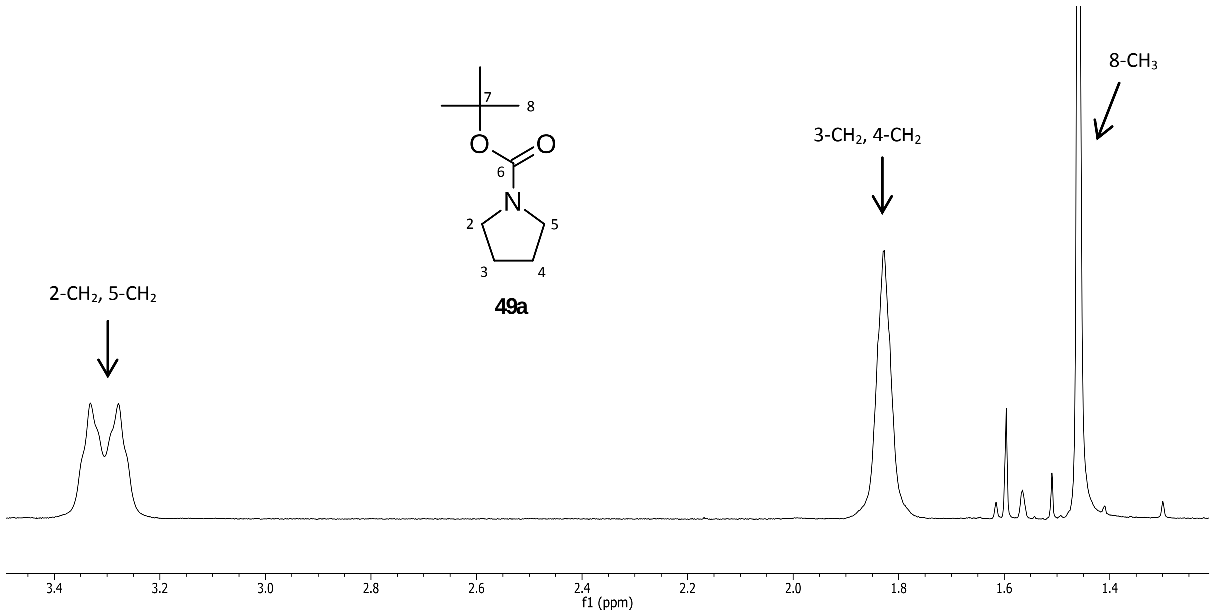

Figure 23: ^1H NMR spectrum of 49a in $CDCl_3$

The ^{13}C spectrum (Figure 24) shows two signals at 25.6 and 24.8 ppm, which are due to the two methylene carbons, C-3 and C-4, furthest from the nitrogen. The methyl carbons of the *t*-butyl group resonate at 28.6 ppm as a singlet, as expected. Signals corresponding to the methylene carbons adjacent to the nitrogen are found at 45.6 and 45.3 ppm. The quaternary carbon signals of the BOC group are found at 78.5 and 154.3 ppm. These are due to the *t*-butyl and carbonyl groups, respectively. As before, the carbamate group causes a slight distortion of the symmetry on the ring due to restricted rotation around the amide bond as a result of the lone pair of electrons present on the nitrogen. This results in pairs of carbon signals where we would see only one for the unprotected pyrrolidine ring.

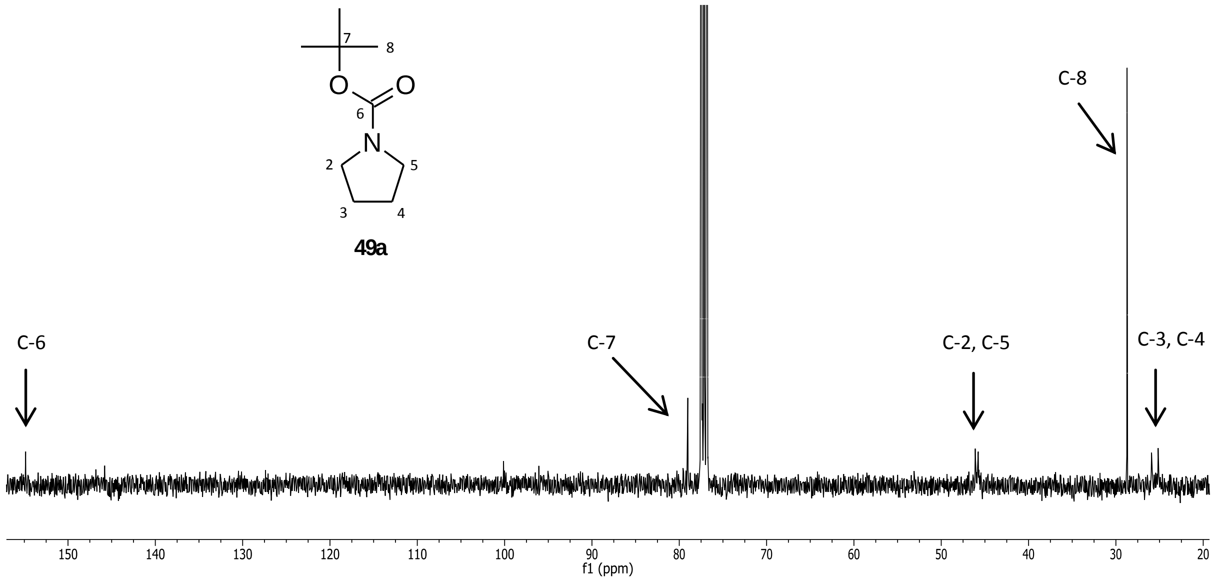

Figure 24: ^{13}C NMR spectrum of 49a in $CDCl_3$

α-Lithiation with *sec*-BuLi in the presence of TMEDA is carried out in freshly dried Et_2O. TMEDA is added to reduce aggregation of the lithium species in solution. It has an affinity for lithium ions and converts the hexameric *sec*-BuLi into a more reactive/basic dimer 2:2-adduct (*sec*-BuLi)$_2$TMEDA$_2$.[171] Addition of tributyltin chloride gives the *N*-BOC α-amino organostannane, **50a**, with a yield above 50% (Scheme 17). Although reasonably stable, purification and removal of side-products and excess starting materials was done quickly to increase the lifespan of the stored organostannane.

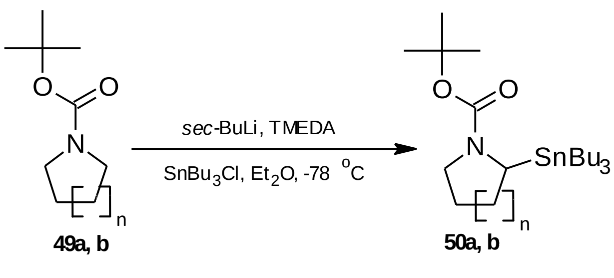

Scheme 17: Reaction of *N*-BOC protected amine 47a to give α-amino organostannane 50a

^{13}C and ^{1}H NMR spectra confirmed the presence of the α-amino organostannane, **50a**, as well as the effects of the tin atom in further reducing symmetry on the pyrrolidine ring. The ^{1}H NMR (Figure 25) was assigned with the assistance of an HSQC spectrum, allowing even the three multiplets between 3.0 and 3.5 ppm to be assigned. The two methylene protons on C-5 are split further than they were in **49a** (Figure 23), due to the loss of symmetry caused by the attachment of the tributyltin moiety, and appear at 3.34 ppm and 3.16 ppm. The multiplet at 3.24 ppm is due to the proton on the, now chiral, carbon at C-2. The multiplet at 1.92 ppm is due to the diastereotopic protons on C-3, each in a slightly altered chemical environment.

There are two mechanisms that increase the broadening in these multiplets. The first is the restricted rotation around the amide bond, as mentioned with **49a** (Figure 23). The second is a result of the loss of symmetry on the ring, which now places the protons in non-identical chemical environments. The nine *t*-butyl protons on C-8, stemming from C-7, are within the large multiplet at 1.5 ppm. The butyl chains on the tin atom are somewhat more complicated to assign, due to the splitting patterns associated with butyl chains, and are seen as the remaining four multiplets at 1.0-1.1 ppm, 1.1-1.2 ppm, 1.4-1.6 ppm and 1.7-1.8ppm. The protons on C-4 are masked by the large tributyl signals but, as corroborated by the HSQC, it can be found in the region between 1.5 and 1.7 ppm.

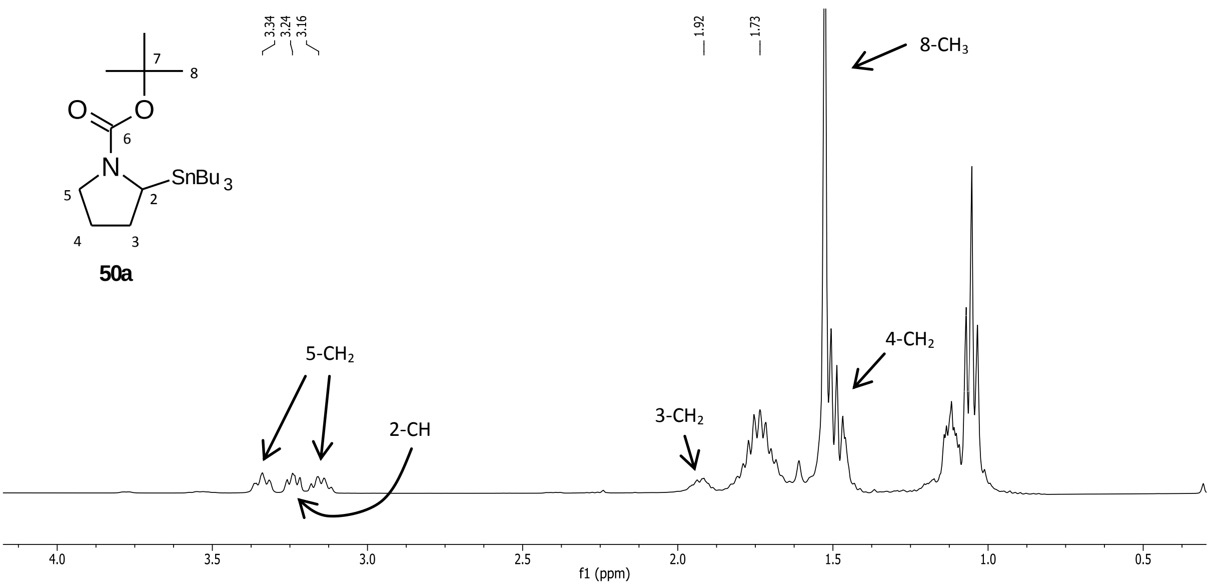

Figure 25: ^{1}H NMR of 50a, in C_6D_6

The ^{13}C NMR of **50a** is shown in Figure 26. The carbonyl, C-6, is at 154.5 ppm. The quaternary *t*-butyl carbon C-7 is at 78.4 ppm. Two close signals at 46.7 and 46.5 ppm are assigned to C-2 and C-5, respectively. Since C-2 is close to C-5, we can see that the $SnBu_3$ moiety does not electronically interact with the C-2, and that most changes are likely to be caused by the steric bulk of $SnBu_3$. The similar electronegativity between tin and hydrogen (1.96 and 2.2 respectively, while the electronegativity of nitrogen is larger at 3.04) implies that each would affect carbon in a similar manner. In other words, the deshielding of C-2 and C-5 is almost entirely due to the carbamate, and not due to the presence of the tin atom.

C-3 is found at 30.9 ppm, while C-4 is at 27.8 ppm. The three *t*-butyl methyl carbons, C-8, are assigned to the signal at 28.7 ppm. The butyl chain on the tin is assigned on Figure 26, where C-1′ is closest to the tin atom, and C-4′ represents the terminal methyl carbon. Since the three butyl chains are equivalent, we see only four signals (one for each carbon on the chain), as expected.

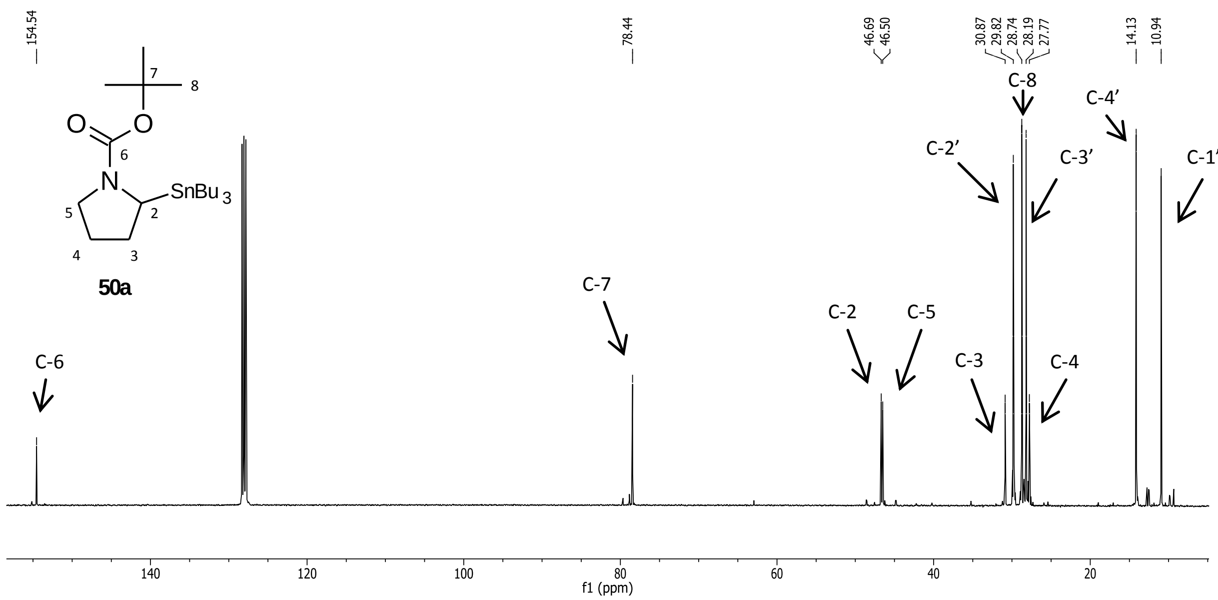

Figure 26: ^{13}C NMR of 50a, in C_6D_6

The nature of the ring inversion has been well explored and discussed by Santigao *et al.*[26] and applied in this group by Meyer,[172] with the six-membered piperidine ring α-amino organostannane, **50b**, and some derivatives. Satellites due to coupling between $^{117}Sn/^{119}Sn$ and ^{13}C are also visible in the spectra of these α-amino organostannanes (Figure 26). By using a Karplus-type relationship between the Sn-C-C-C torsion angle and the ^{119}Sn-^{13}C coupling constants, modified by Kitching *et al.*,[30a] a general chair configuration of the ring (Figure 27) has been suggested. The Karplus-Kitching relationship can be described as:

$$^{3}J_{Sn\text{-}C} = 30.4 - 7.6\cos + 25.2\cos 2\theta\ (\pm 3.75\text{Hz or } 5°)$$

The relationship has been well established for proton-coupling constants and the corresponding dihedral angles.[30b] The coupling is the largest at 180° when the orbitals of the two C-H bonds are parallel; at 90°, there is no coupling; and at 0°, the coupling is very large again as the orbitals are in the same plane but not parallel. This relationship is useful to establish the conformation in rigid or constrained systems.[30b]

Computational investigations performed on the *N*-BOC piperidine compound, **50b**, suggest a predominantly equatorial substitution of the $SnBu_3$ moiety onto the ring (in a chair confirmation), with the carbamate preferring to be configured with the carbonyl oxygen inside the "cavity" between the nitrogen-carbamate bond and the tin group (Figure 27). These DFT calculations were performed using the BLYP functional within the DMol3 package, hosted within Materials Studio 4.4.

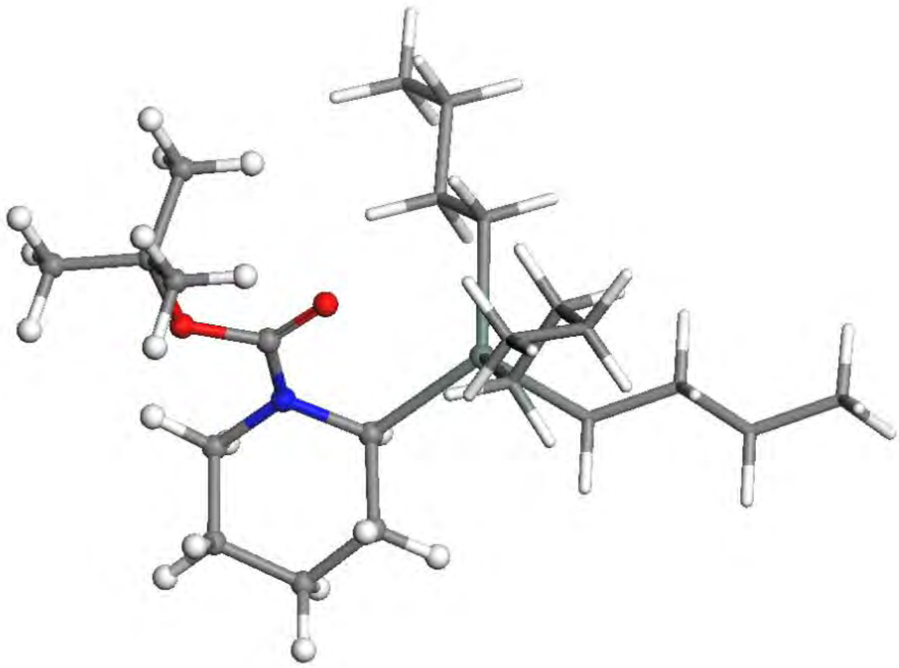

Figure 27: *N*-BOC piperidine-derived stannane 50b, showing the lowest energy ground-state configuration, as determined by DFT calculations.

2.1.3. Attempted BOC Protection of an α-Alkoxy Organostannane

The BOC protecting group was thought to exhibit some interesting effects on the experimental and synthetic behaviour of Fischer carbenes (discussed in detail in Section 2.2), and so an attempt was made to protect the stannous alcohol, **42a**, with the BOC group, rather than the typically used MOM ether protecting group (Scheme 18).

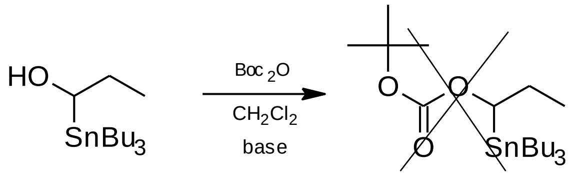

42a **43a-BOC**

Scheme 18: Attempted BOC protection of an α-alkoxy organostannane

The reaction, however, was unsuccessful. It was first attempted with *N,N*-dimethylaniline (DMA) as the base, and again with DMAP. The reaction was carried out at various temperatures, from -40°C to 0°C to 20°C. TLC and NMR analysis showed no traces of the desired product.

2.1.4. Attempted Grignard Reaction with Tributyltin Chloride

Due to high costs and low availability of tributyltin hydride (required for alkoxy organostannane synthesis), an alternative method was explored involving the synthesis of a Grignard reagent utilizing the cheaper and readily available tributyltin chloride (required for amino organostannane synthesis). It is worth noting that Grignard reagents have been used extensively with tributyltin chloride in organostannane synthesis,[22] but to the best of our knowledge, not in the manner attempted here.

As shown in Scheme 19, it was hoped that the magnesium would insert between the tin and chloride atoms to give a species that could be thought of as $Bu_3Sn^-[MgCl]^+$ and might act as a replacement reagent for the tributyltin lithium used in alkoxy organostannane synthesis.

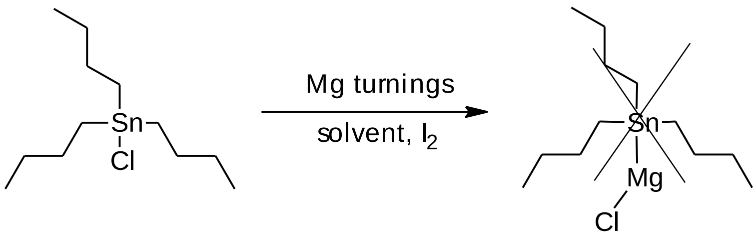

Scheme 19: Attempted Grignard Reaction with tributyltin chloride

The method followed was one adapted from Vogel.[162] A two-necked flask was filled with argon, and a stirrer and a condenser was attached. Magnesium turnings, which had been rinsed with dry THF and dried in the oven, were added, along with a single crystal of iodine (used in Grignard synthesis as an activator of the metal turnings). Once iodine vapours were visible in the flask, dry Et_2O (10 ml) and about 10% of the total tributyltin chloride was added to the flask.

Here, the reaction was expected to require a little warming to initiate the exothermic Grignard synthesis, and after a slow addition of the remaining Et_2O and Bu_3SnCl, it was left to reflux. This, however, did not occur, even on deliberate heating at reflux, in THF or Et_2O, as well as a combination of the two ether solvents. Low boiling points of these ethers forced us to consider using TMEDA, due to its higher reflux temperature of 120-122°C. TLC showed no change in starting products; titration of the reaction mixture in diphenylacetic acid showed no colour change even when great excesses of reaction mixture were added. Weighing the magnesium strips after the reaction showed no loss of mass, inferring that no reaction had taken place.

From these results, it was concluded that the reaction did not take place under the conditions applied to it. Since this was a tangential aspect of the project, no further exploration was carried out.

2.2. Synthesis and Stability of Fischer Carbenes

Fischer carbenes can have wide-ranging stabilities and reactivities, depending on the metal centre and substituents.

2.2.1. Methyl Carbene

The simple methyl carbene, **52**, was readily synthesized, as shown in Scheme 20, from methyllithium and provided a useful reference compound before using the organostannanes previously synthesized. Since carbenes are sensitive to oxidation in air, all reactions were performed using Schlenk techniques. Methyllithium was added dropwise to a solution of chromium hexacarbonyl, **12**, in freshly dried Et_2O. A nucleophilic addition mechanism attaches the methyl carbanion to a carbonyl carbon to form an acylpentacarbonyl-chromate salt, **51**, with the lithium ion serving as the cation. A Meerwein salt was added to alkylate the salt; in this case, trimethyloxonium tetrafluoroborate was used. This alkylation must be carried out in degassed water, so the Et_2O was removed *in vacuo*, leaving a brown residue, which was then taken up in degassed H_2O. Extraction with dry Et_2O, followed by removal of the solvent, resulted in **52** as bright yellow crystals in a yield of 56%.

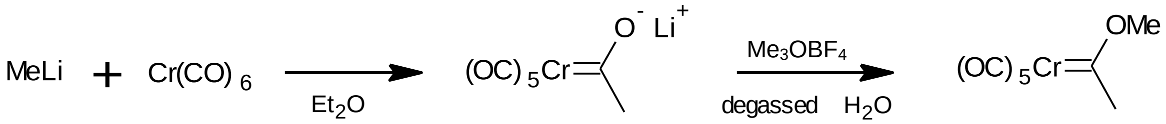

12 **51** **52** (56%)

Scheme 20: Synthesis of methyl carbene 52

Figure 28 shows the ^{13}C NMR spectrum of the methyl carbene, **52**, after column purification. The electrophilic carbene carbon is strongly deshielded at 360.5 ppm due to the electron-withdrawing nature of the pentacarbonyl chromium moiety.[89] The carbonyls are observed at 223.3 ppm for the single *trans* carbonyl, and 216.4 for the remaining four *cis* carbonyls. The methoxy and methyl groups are found at 67.5 ppm and 49.9 ppm, respectively. These signals are broad and of very weak intensity. The methyl is a little further downfield than might be expected for a methyl carbon, but again, this is due to the carbene carbon being strongly electrophilic. The broadness observed on the methoxy signal is likely due to the stabilizing effect of the methoxy group, since it is involved in π-back donation with the strongly electrophilic nature of the carbene carbon.

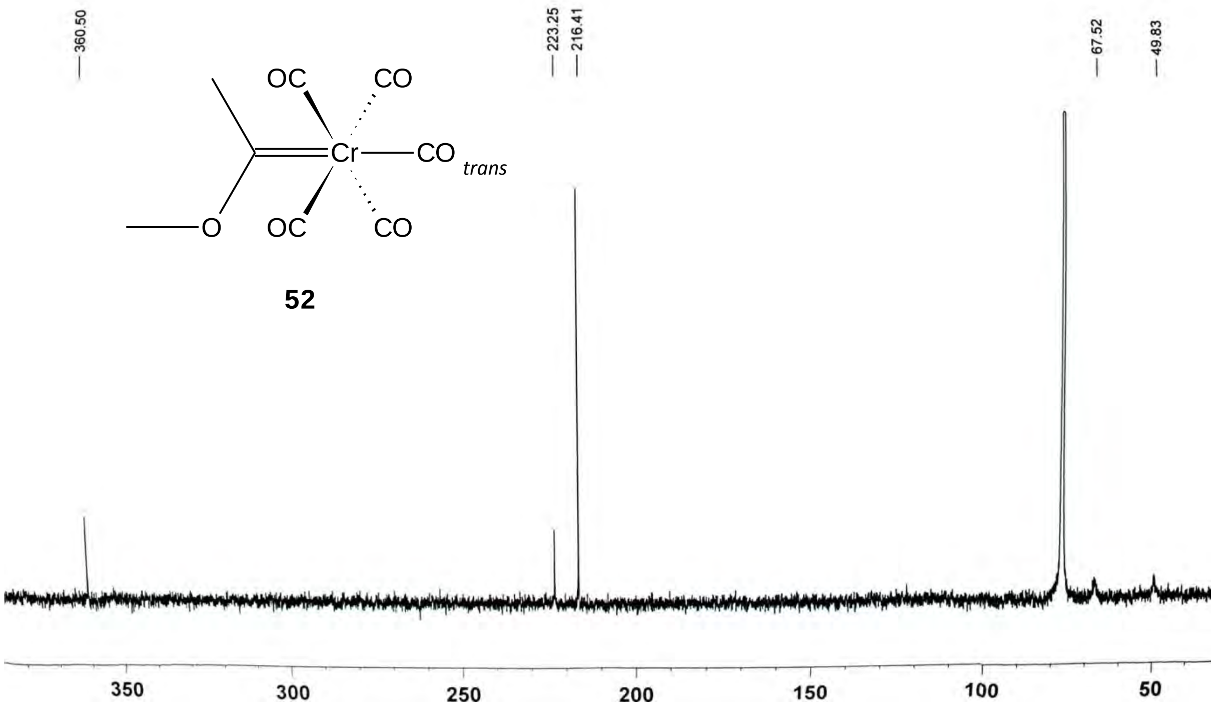

Figure 28: ^{13}C NMR of a methyl carbene in $CDCl_3$

By using *n*BuLi, it was possible to synthesize a simple butyl carbene, **53**. This was done using the same method as shown in Scheme 18. Figure 29 shows an expansion of the ^{13}C NMR spectrum of this unpurified butyl carbene acquired two hours after synthesis. The carbene carbon signal is seen at 360.1 ppm and three carbonyl peaks around 200-225 ppm. The inverted signal at 225.0 ppm is due to the carbonyl in the *trans* position on the chromium moiety. The signal at 217.0 ppm is due to the four *cis* carbonyls on the pentacarbonyl chromium moiety. The large signal at 211.6 is from unreacted chromium hexacarbonyl.

Such a signal inversion is often due to the T_1 relaxation delay being set incorrectly for that carbon signal. T_1 is defined as the decay constant for the recovery of the *z* component of the nuclear spin magnetization ($\mathbf{M}_z$) until reaching its equilibrium position parallel to the magnetic field ($\mathbf{B}_0$). A T_1 inversion recovery experiment can be done to determine the ideal delay time for the inverted carbonyl and has been attempted in our group for a simple carbene.

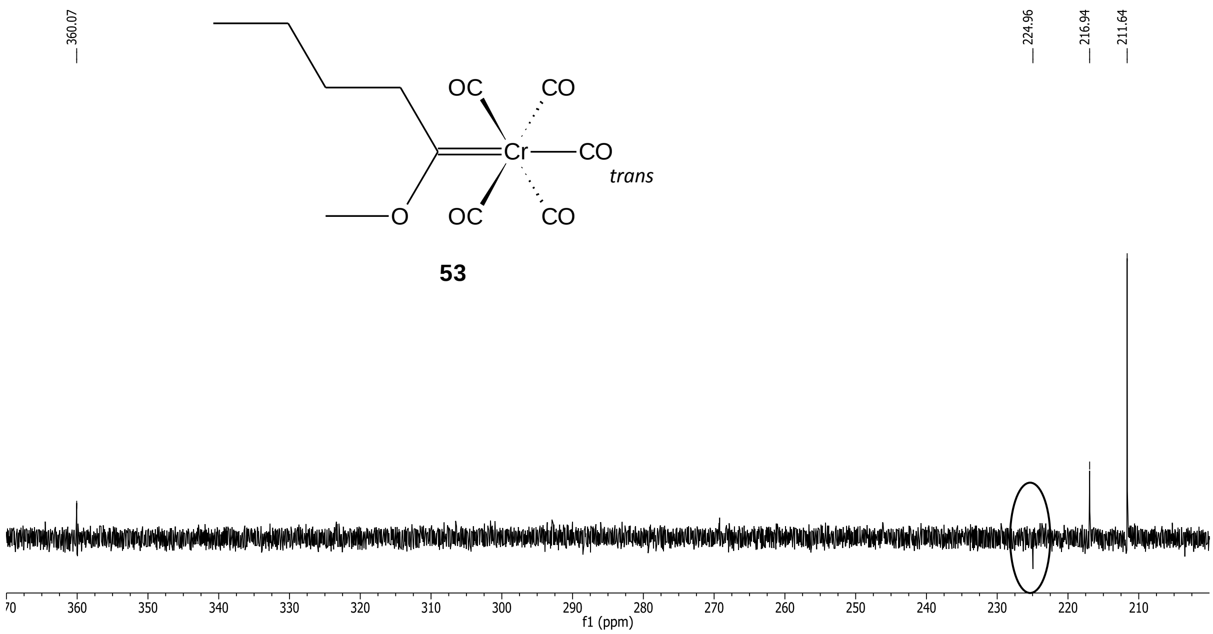

Figure 29: Expansion of ^{13}C NMR of butyl carbene 53 in $CDCl_3$, showing carbene carbon and carbonyl groups.

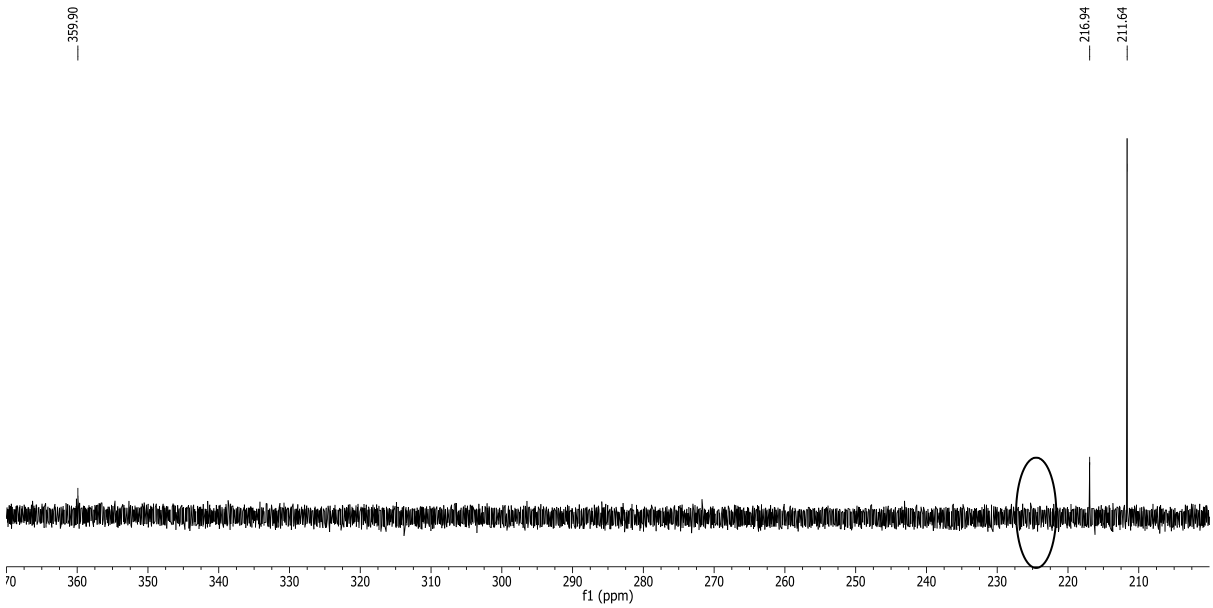

Figure 30: Expansion of ^{13}C NMR of butyl carbene 53 in CDCl3, 8hr after synthesis, showing absence of the *trans* carbonyl.

Figure 30 shows the results of a ^{13}C NMR experiment run six hours after the start of the one just described. The instability of even these simple carbenes at room temperature can be seen by the loss of the *trans* carbonyl signal at 225.0 ppm. This is consistent with fragmentation patterns observed by Lötz *et al.*,[173] who found that the carbene moiety disintegrates through two pathways, one of which is *via* the loss of carbonyls first, followed by fragmentation of the metal from the carbene carbon atom. Visual inspection of the NMR tube showed a green precipitate, illustrating the decomposition, *via* oxidation, of chromium(0) to green chromium(III). A decomposition product of this oxidization process is thought to be an ester compound, **54**.

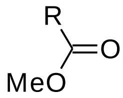

54

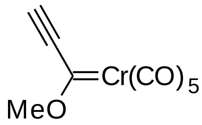

55

This has been shown by Meyer[172] through the addition of a suitable oxidizing agent followed by product identification by NMR. The carbonyl ester signal is seen around 167 ppm in most cases. The decomposition was slowed somewhat by storing the carbene products in a cold room under argon and shielded from light.

A lithium acetylide, ethylenediamine complex was used to synthesize a simple carbene, **55**. This carbene was found to be significantly more stable than many of the carbenes synthesized, remaining intact for more than six months while stored under argon at low temperatures.

2.2.2. α-Alkoxy-Derived Carbenes

Three α-alkoxy organostannanes, **43a-c**, were used to synthesize novel Fischer chromium carbenes. These were carried out as per Scheme 21, using the Fischer method.[174]

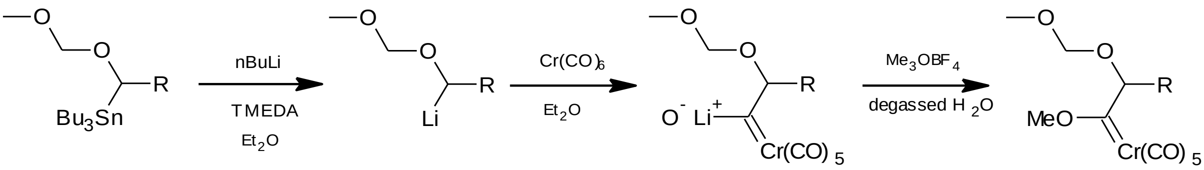

43a-c **55a-c** **56a-c** **57a-c**

Scheme 21: Fischer method of carbene synthesis, for α-alkoxy-derived carbenes[174]

The organostannane, **43a-c**, must first undergo a tin-lithium exchange, with *n*BuLi, in the presence of TMEDA and freshly dried Et_2O, under argon. This was done at 0°C and was accompanied by a colour change to pale yellow. The acyl-pentacarbonyl lithium salt, **56a-c**, was formed by reaction of the organolithium, **55a-c**, with finely crushed chromium hexacarbonyl at -78°C. A colour change from pale yellow to dark brown was observed while this was left to stir for four hours and allowed to warm to 0°C. Alkylation with Meerwein's salt (Me_3OBF_4) was carried out in water degassed *via* a freeze-pump-thaw method. The yellow carbene product, **57a-c**, was extracted with portions of Et_2O, which was then removed *in vacuo*. In all cases, the carbene was not isolated due to the presence of a side-product, tetrabutyl tin ($SnBu_4$). The side-product has proven difficult to remove without causing decomposition of the carbene.[172]

2.2.3. α-Amino-Derived Carbenes

Utilizing α-amino organostannanes as precursors, themselves derived from *N*-BOC-protected and later ethyl-substituted piperidine and pyrrolidine, these carbenes exhibited interesting but frustrating behaviour. Scheme 22 shows the method of synthesis for these α-amino-derived Fischer carbenes.

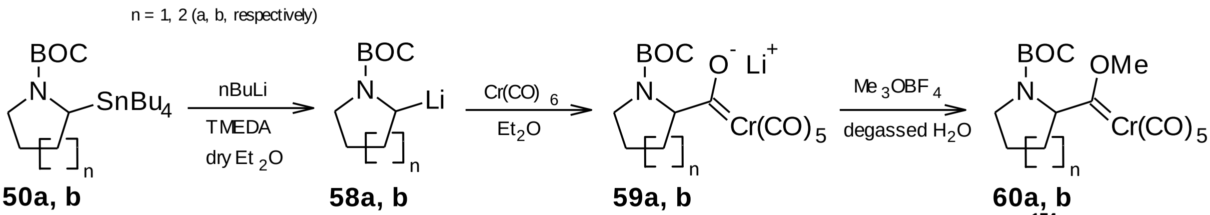

Scheme 22: Fischer method of carbene synthesis, for α-amino-derived carbenes[174]

This was essentially unchanged from the method used for α-alkoxy-derived carbenes. As with the α-alkoxy-derived carbenes, the $SnBu_4$ side-product was present in all cases and rendered isolation of the desired product impossible. It was found that for α-amino organostannanes protected with a *N*-BOC protecting group, **61**, signals corresponding to this *N*-BOC protecting group were not present in ^{13}C and ^{1}H NMR spectra of the respective carbenes. However, the distinctive carbene carbon signal was still present, although of very weak intensity. This is in contrast to carbenes derived from α-alkoxy organostannanes protected with a MOM group, **62**, where the protecting group was intact throughout the synthesis.

These two groups differ in the presence of an acyl group for **61** versus an ether for **62**, and the terminal *t*-butyl group on **61** versus the terminal methyl group on **62**. Interestingly, the carbenes derived from *N*-methyl- and *N*-ethyl-substituted α-amino organostannanes were found to be synthesized intact. This lead us to believe that the BOC group either negatively affects the stability of the carbene, or inhibits formation of the desired carbene.

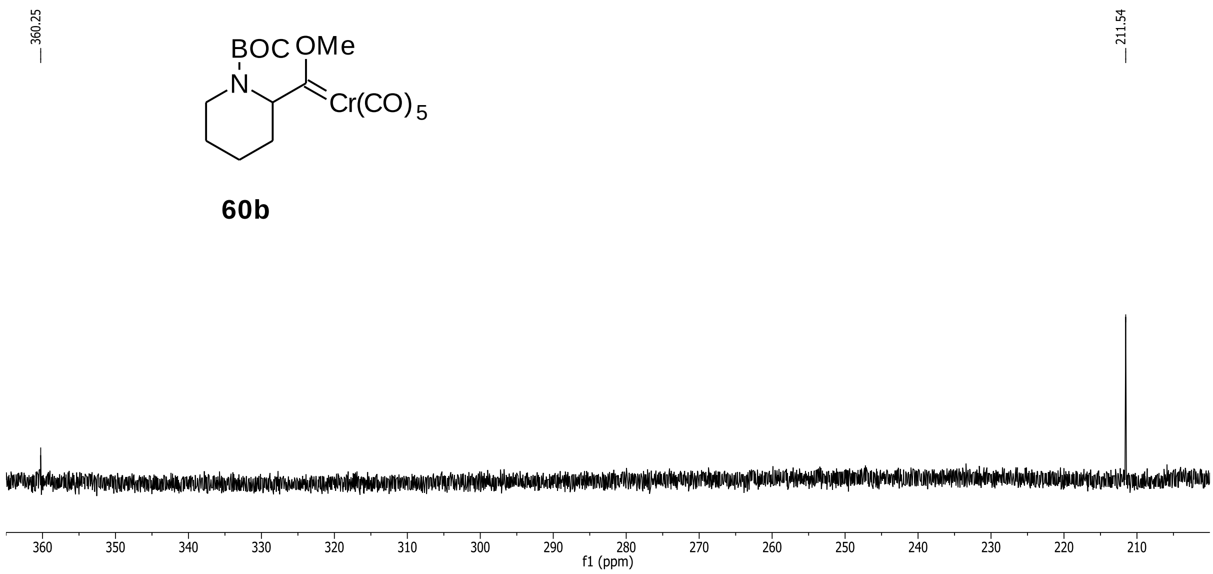

Figure 31: ^{13}C NMR (in C_6D_6) of Fischer carbene 60b showing a characteristic carbene signal and lack of *cis/trans* CO signals

Figure 31 shows the ^{13}C NMR spectrum of **60b**. The signal at 211.5 ppm is due to unreacted chromium hexacarbonyl, which is expected to show just the single carbonyl resonance due to its symmetry. At 360.3 ppm, the carbene carbon signal can be seen. From this signal, we infered that the carbon-chromium bond was indeed intact. The lack of *cis* and *trans* carbonyl ligand signals, however, could be a result of fragmentation around the chromium atom, facilitated by the presence of the BOC protecting group. Again, this was in contrast to the carbenes derived from MOM-protected alkoxy organostannanes, which showed an intact pentacarbonyl moiety and protecting group. The alkoxy organostannane-derived carbenes (**57a-c**) were found to be relatively stable, in comparison to the unstable amino organostannane-derived carbenes (**60a-b**), which either decayed within 30 minutes under argon (this is about the time it took to prepare and begin a ^{13}C NMR experiment) or were inhibited from forming in the reaction altogether.

Synthetic Challenges

Challenges to the synthesis of carbenes come from several areas. These difficulties could have been caused by poorly prepared organostannanes, which add impurities to the reaction, as well as reducing the actual amount of organolithium available in the reaction. Lower than expected concentrations of butyllithium used for tin-lithium exchange have the same effect of reducing the actual amount of novel organolithium in the reaction. Poorly prepared solvents and glassware can contain trace amounts of moisture, which may react with the organolithium reagents, further reducing the quantity available for reaction. Trace amounts of oxygen in solvents can oxidize the carbene product to give the ester. This is apparent from the ester signal observed around 167 ppm in the ^{13}C NMR spectra of these compounds. Maintaining cold baths at correct temperatures is also important to ensure a rapid and successful tin-lithium exchange, and to ensure that stability of intermediates is not compromised. All of these potential problems were compensated for, but it was impossible to eliminate both water and oxygen completely.

Purification of these carbenes is difficult, mostly due to the presence of the $SnBu_4$ side-product when using organostannanes as precursors to organolithiums. Several methods were attempted to remove this contaminant, including column chromatography and cold-finger sublimation. Flash chromatography was carried out on simple carbenes, with success, using hexane as the solvent and under argon pressure. These complexes were most often the first to elute and could be identified visually, based on their colour. Those with sp^3 carbons are usually yellow, while those with sp^2 carbons are red, and those with sp hybridized carbon substituents are generally dark brown or purple.[173] As expected, all the carbenes prepared in this study were yellow (except the sp hybridized **55)**

When chromatography was attempted on organostannane-derived carbenes, however, only limited success was found. In all cases, each fraction was contaminated with tetrabutyl tin, which is known to streak on silica. For α-alkoxy-derived carbenes, the fraction containing the carbene exhibited the four signals due to the $SnBu_4$ side-product, but did not contain signals from the MOM protecting group. This acetyl group is sensitive to acid hydrolysis and may have interacted with the acidic silica.[175] Even when pushed rapidly through the column in 10 minutes using argon pressure, ^{13}C NMR indicated the likely loss of the MOM protecting group. In the case of α-amino-derived carbenes, the carbene product moved slowly through the silica and decomposed prior to complete elution from the column. Altering the solvent system by the addition of a polar component did not increase the elution rate significantly, with the carbene continuing to rapidly decompose while on the column. This behaviour is further evidence to support the loss of the BOC group, since the free amine would be more strongly retained on silica.

Cold-finger sublimation was carried out on some of these carbenes, with mixed results. Although cold-finger sublimation is recommended for solid products, the impure carbene (if it existed at all) was a solid dissolved in the oily tetrabutyl tin contaminant. Sublimation of the alkoxy-derived carbene, **57b**, reduced the amount of contaminant in the product, while appearing to retain the carbene moiety. Sublimation of the amino-derived carbenes, **60a** and **60b,** was unsuccessful, however, and only served to oxidize the carbene resulting in a green oily mixture. Although not attempted, it is thought that washing the acyl-pentacarbonyl salt with a suitable organic solvent may remove the majority of the tin contaminant while not affecting the polar carbene salt.

Table 5 summarizes the results of simple and novel Fischer carbenes synthesized or attempted. Three simple carbenes were successfully synthesized in order to confirm the suitability of the Fischer method for synthesis. Three alkoxy-derived Fischer carbenes were also successfully synthesized, but not isolated. Neither of the BOC-protected amino-derived Fischer carbenes attempted were successful.

Table 5: Summary of Fischer chromium carbenes synthesized and attempted

Compound	Yield[*]/Crude Mass	Appearance	Shelf life[†]
52	56.4% / 1.61g	Bright yellow crystals	3-6 months
53	25.0% / 0.83g	Pale yellow crystals	2-5 months
55	31.3% / 0.93g	Dark purple/black solid	6 months
57a	-/0.26g	Yellow oil	2-4 days
57b	-/0.45	Yellow oil	2-4 days
57c	-/0.31g	Pale yellow oil	2-4 days
60a	-[‡]	Yellow oil	Possibly less than 30 min
60b	-[‡]	Yellow oil	Possibly less than 30 min

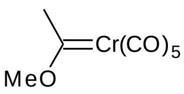
52

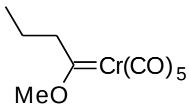
53

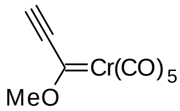
55

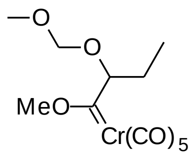
57a

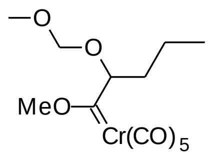
57b

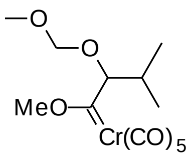
57c

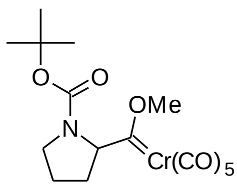
60a

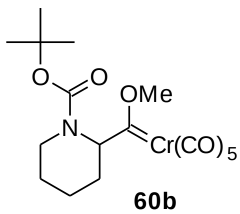
60b

[*] Some yields could not be determined due to $SnBu_4$ contamination.
[†] Shelf life is while stored under argon at low temperatures (~4°C).
[‡] Unable to confirm reaction success

2.3. Imine Synthesis

This project was initially intended to probe the use of carbenes **54** and **60** in a [2+2] cycloaddition reaction towards the formation of β-lactams. Since lactam formation required an imine, some focus was extended towards the synthesis of a suitable imine from aniline, **61**, and benzaldehyde, **62**.

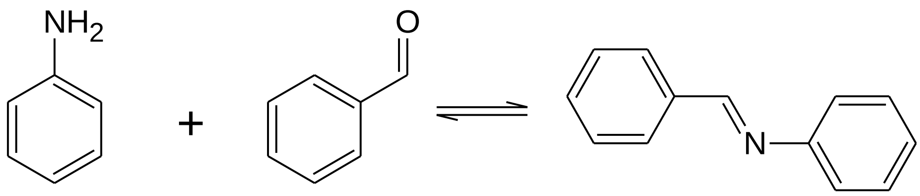

61 **62** **63**

Several methods were attempted: simple stirring with and without solvent, ultrasound sonication with silica,[176a] and microwave-assisted heating;[176b] neat, with solvent, and finally with an acid catalyst. Microwave-assisted heating with catalytic quantities of acetic acid without solvent was found to be most effective for synthesis of imine **63**.

Since the reaction is an equilibrium between reagents and product (with water as a by-product), it was found that over a 24-hour period, approximately half of the product would revert back to the original starting material. Nevertheless, IR and NMR analysis confirmed the presence and initial purity of the imine.

Figure 32 shows an IR analysis, performed using neat compounds, demonstrating the disappearance of the carbonyl stretching band at 1710 cm^{-1} and the simultaneous appearance of the C=N band at 1590 cm^{-1}.

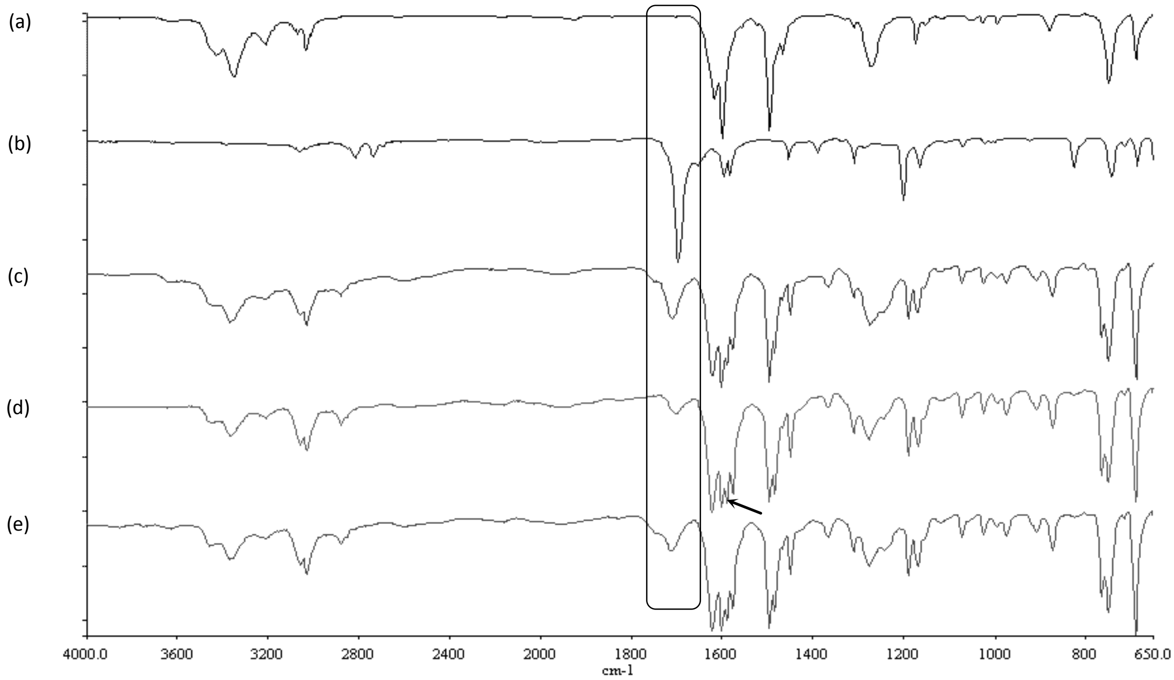

Figure 32: IR results of the reaction of benzaldehyde and aniline to form imine 63

The traces are as follows: (a) Aniline, 61. (b) Benzaldehyde, 62. (c) Unreacted combination of a + b. (d) After 20 minutes of microwave heating with catalytic amount of acetic acid (arrow indicates the IR weak band of the N=C bond). (e) The sample 24 hours after heating.

The combination of **61** (a) and **62** (b) is shown as trace (c) before heating, trace (d) after heating, and 24 hours later, as the final trace (e). Of note is the slight suppression of the carbonyl vibration in (c), which was further reduced after heating, demonstrating the consumption of the aldehyde reagent. After 24 hours, this carbonyl vibration was seen to increase, showing the decay of the imine product, **63**, back to the initial starting reagents in the equilibrium. The characteristic C=N imine band is found between 1690 and 1600 cm^{-1} but is IR weak.[176c] There is a weak band (indicated with arrow), however, which becomes more apparent in (d) after heating. Figure 33 shows the ^{13}C NMR for benzaldehyde.

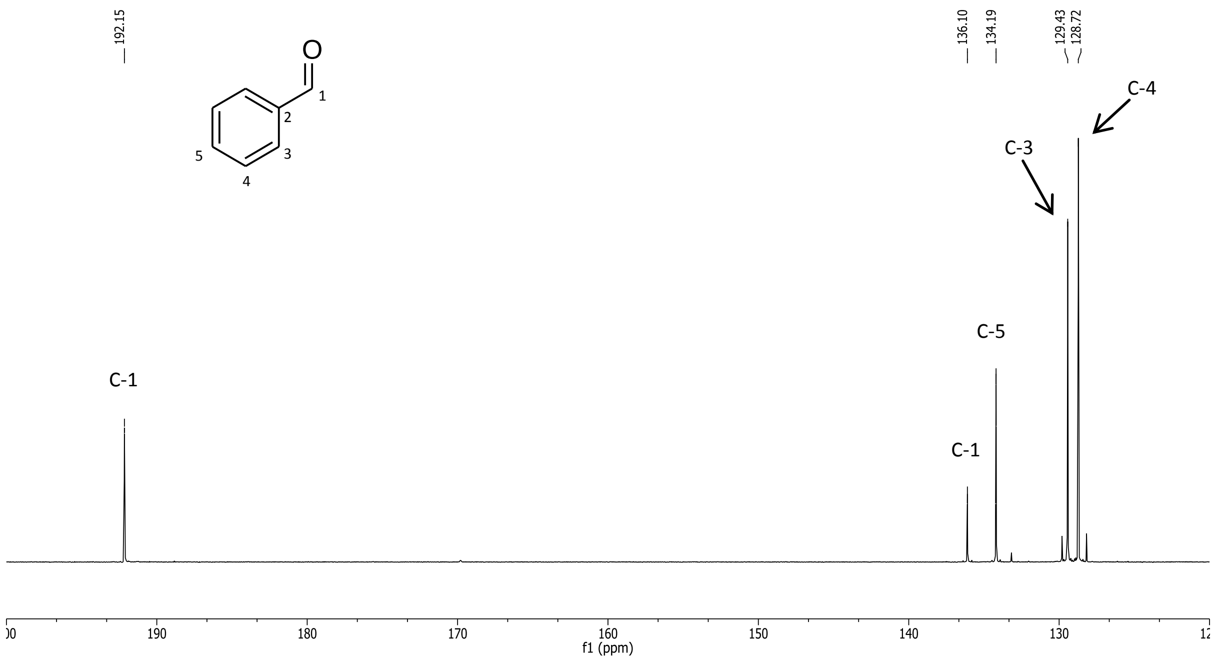

Figure 33: ^{13}C NMR spectrum of benzaldehyde, in $CDCl_3$

Of most interest to us is the carbonyl signal at 192.2 ppm because this can be used as a diagnostic signal for completion of the reaction. After the addition of aniline and microwave heating for 20 minutes, ^{13}C NMR (Figure 34) showed the complete consumption of the starting aldehyde, **62**. Assignment of the spectra was relatively simple and is shown on Figure 34. The characteristic imine RC=NR' carbon was found at 160.6 ppm and confirmed the presence of the product. The impurity at 146.4 ppm is due to the small excess of residual aniline.

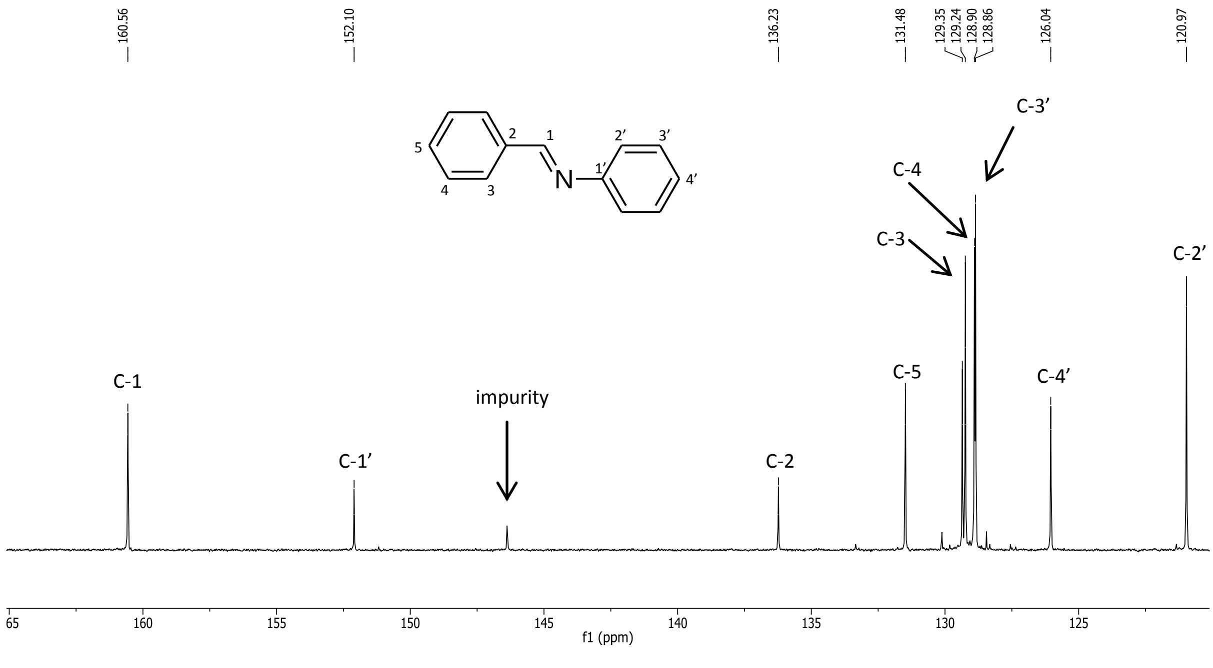

Figure 34: ^{13}C NMR spectrum of imine 63, 20 minutes after microwave synthesis, in $CDCl_3$

2.4. Computational Studies of Modified Fischer Carbenes

2.4.1. Significance of Computational Evaluation in this Study

Since the experimental isolation and characterization of certain carbenes proved generally difficult, a theoretical evaluation was considered useful in shedding light on the electronic behaviour of individual compounds. We hoped that the computed data would be useful in a diagnostic sense, helping determine why some carbenes were difficult (or impossible) to synthesize or isolate; or in a predicative sense, attempting to suggest how a particular reaction might proceed.

An *in silico* approach allowed us to manipulate compounds in terms of structure, geometry or charge, while providing feedback on this relationship in carbenes. Compounds that were not possible to synthesize were evaluated and compared against those which were synthesised.

2.4.2. Validation of Method

In order to evaluate the computational method chosen, a comparison was made with methods and results in the literature. Initial calculations were carried out using an LDA functional. A potential reaction pathway towards the formation of a β-lactam from the carbene was mapped out, with transition states. Comparison with literature, specifically results published by Fernández *et al.*, who performed similar calculations on a carbene to β-lactam reaction pathway using post Hartree-Fock methods,[99] suggests that the LDA method is not sufficiently accurate for these modified Fischer carbenes. Each compound and intermediate was re-optimized using the BLYP GGA method, giving results in line with literature. This GGA functional was therefore used for all remaining computations.

2.4.3. Theoretical Application to a [2+2] Cycloaddition Reaction

As the initial aim of this project was to evaluate the suitability of these novel carbenes for use in a [2+2] cycloaddition reaction with an imine, calculations were carried out to track the reaction coordinate towards the β-lactam.

Lactam formation begins with the excitation of the singlet ground-state carbene, S_0, to an excited singlet state, S_1, a photoactivation process. Due to spin-orbit coupling, intersystem crossing (ISC) allows the S_1 state to pass into an excited triplet state, T_1, and allows a crucial carbonyl insertion to take place. This results in a chromacyclopropanone moiety, and is the same configuration that exhibits interesting BOC-chromium interactions. Coordination of a suitable solvent allows the system to follow an S_0 hypersurface via the "loose-bolt" effect at increasing stability (versus the T_1 state) until a stable solvent-coordinated S_0 ground state is reached. Figure 35, for compound **60a**, illustrates this process.

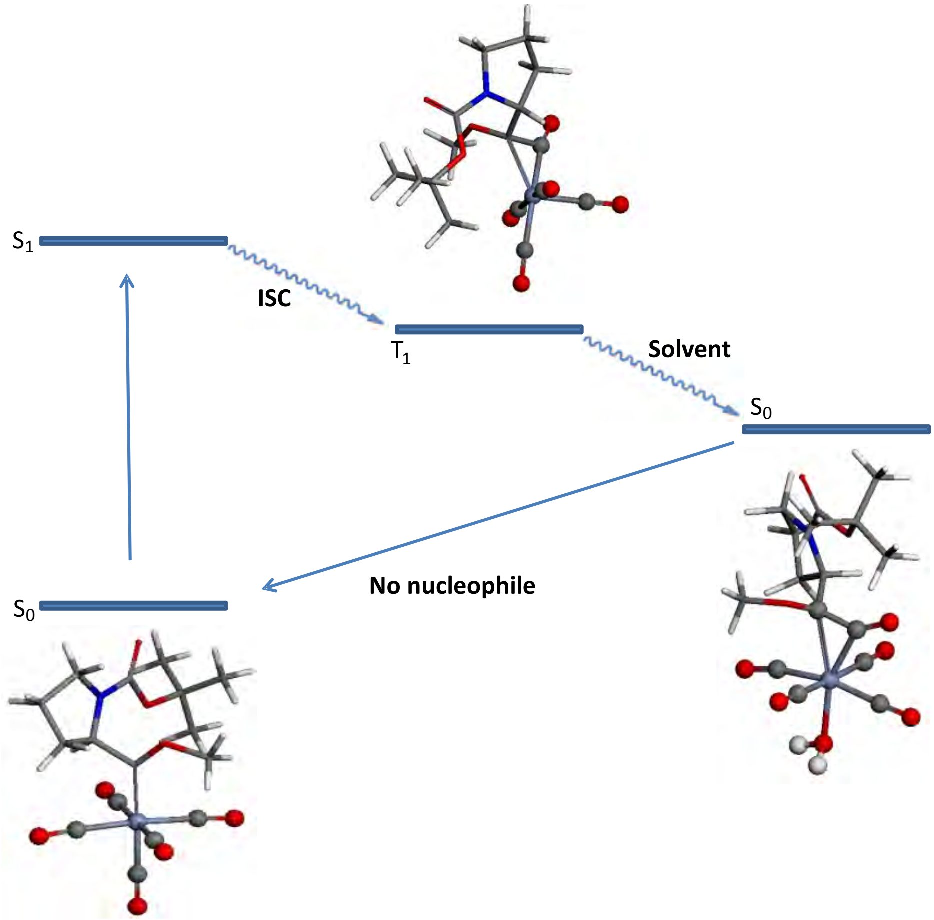

Figure 35: Photo-excitation cycle of Fischer carbenes

The second S_0 ground state, which has the solvent coordinated, as well as the carbonyl photo-insertion, allows access to the remaining steps in the cycloaddition process. These were mapped out first using the PWN functional, a local density approximation (LDA) method within DFT, but this was found to give results inconsistent with chemical expectations and the literature.[99] The calculations were repeated with the improved BLYP functional, a generalized gradient approximation (GGA) method, giving results that might correlate well with those found in the literature.[97,128,129,99] While geometries and structures of optimized structures looked similar when comparing the two approximations, the energies were quite different, especially when considering the transition states.

The actual [2+2] cycloaddition process (Figure 36) begins with the second S_0 ground-state chromacyclopropanone compound from above, which undergoes a 1,3-"chromatropy" of the inserted carbonyl to form an oxygen-coordinated ketene. This is attacked by an imine (acting as a nucleophile, of course) and is followed by ring closure to form the β-lactam. The effects on stereochemistry are unknown, so predicting whether the ring closure is conrotatory or disrotatory is still a difficult process, although empirical rules have been devised to help predict whether a *cis* or *trans* lactam is formed in the ring closure step.[177]

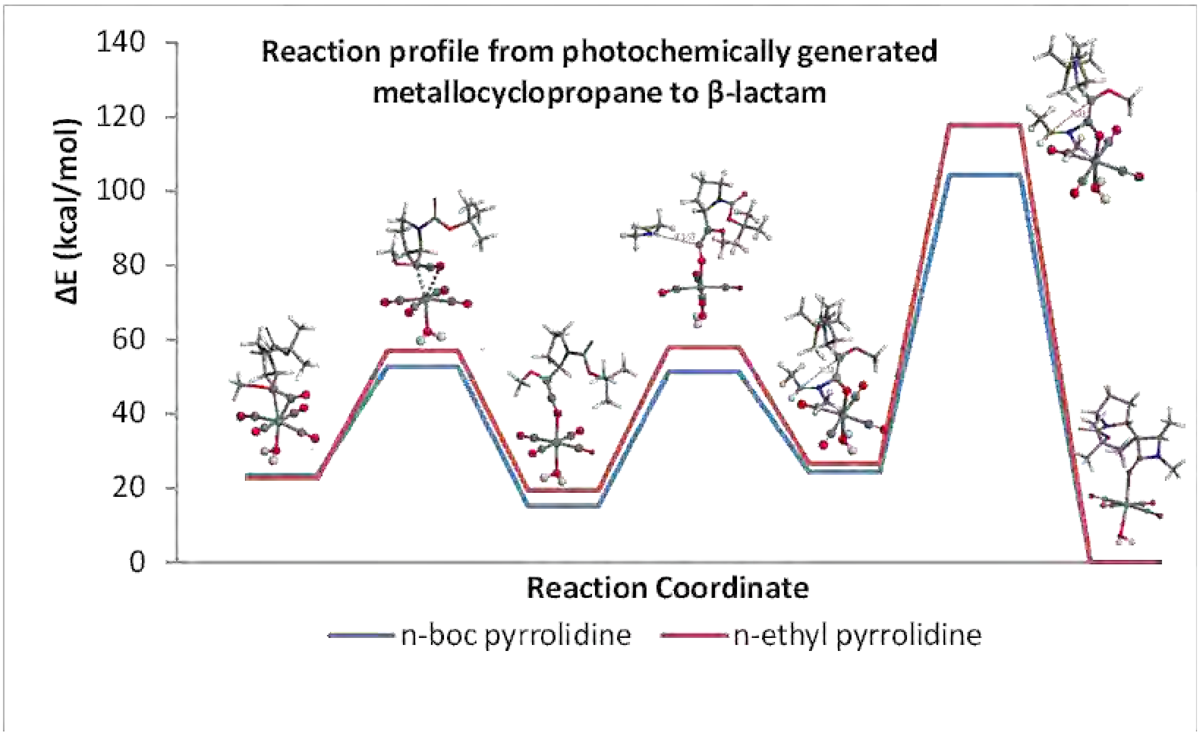

Figure 36: Possible mechanism of [2+2] cycloaddition of Fischer carbene, 60b, with an imine to form a β-lactam

Figure 36 shows this as a plot of reaction coordinate against energy for two carbenes derived from a pyrrolidine α-amino organostannane. For each step in the reaction, the *N*-ethyl substituted pyrrolidine-derived carbene was slightly higher in energy than the corresponding *N*-BOC-substituted pyrrolidine-derived carbene. The ring closure step involves a very large energy barrier, although this barrier is reduced by almost 20% for the unstable BOC-protected carbene over the ethyl-substituted carbene. This could be due to the interaction of the acyl oxygen on the BOC stabilizing the chromium during the ring closure, and therefore lowering the energy barrier slightly. It should be noted here too that the *N*-BOC carbene has so far been synthetically elusive, while the *N*-ethyl carbene has been successfully synthesized in this lab. Also of note is that the energy barrier for the ring-closure step (for these two compounds) is somewhat large, at just under 80 kcal/mol, or around 320 kJ/mol. Fernández *et al.* have calculated a similar profile for a simple methyl carbene, and found an energy barrier which, although lower in energy at 25-30 kcal/mol, is comparable.[97]

The photoactivation is required in both the formation of the metallocycle (Figure 35) and the cycloaddition reaction with the imine (Figure 36), and it is possible that the photoactivation effectively reduces this energy barrier.[97]

2.4.3. Effects of Oxygen on the Carbene Ligand

The experimental results suggest that oxygen plays a role in the stability of the carbene *via* an interaction with the attached ligand. Since we expect a solvent oxygen atom to coordinate to the metal during the photo-activation process of Fischer carbenes as an essential step to the formation of a nucleophilic chromacyclopropanone moiety, we can expect any nearby oxygen atoms to affect reactivity and stability. Indeed, we have seen that the BOC protecting group negatively influences the stability of the corresponding piperidine and pyrrolidine carbenes, while the Et-substituted variants are stable enough to synthesize and identify through NMR.

2.4.3.1. Effects of N-BOC Protecting Group

Some attempt was made to understand the role of the protecting group in the stability of the carbene complex formed from the α-amino organostannane. Computational studies conducted suggest that the *t*-butyl acyl oxygen on the BOC protecting group may attempt to coordinate to the chromium atom in the absence of a coordinating solvent, resulting in a distortion of the carbonyls around the metal (Figure 37a, see also Table 6). This was not observed with the MOM protecting group and may be due to the lesser nucleophilicity of the ether relative to the acyl oxygen (Figure 37b, see also Table 6). The relevant interatomic distances can be seen in Table 6. This distortion does not seem to affect the chromacyclopropanone moiety, with bond lengths remaining essentially unchanged (Table 6). However, it is possible that coordination of the *t*-butyl acyl oxygen to the chromium may mirror a similar elimination mechanism to the one proposed for deprotection of *t*-BOC-protected amines (Scheme 24).[178]

Table 6: Inter-atomic distances in Figure 38, for 60a, with and without a coordinated solvent (in Angstroms)

Atoms	Figure 38a	Figure 38b
O_{BOC} – Cr	3.666	4.744
$O_{solvent}$ – Cr	-	2.977
$C_{insertion}$ – Cr	1.545	1.561

(a) (b)

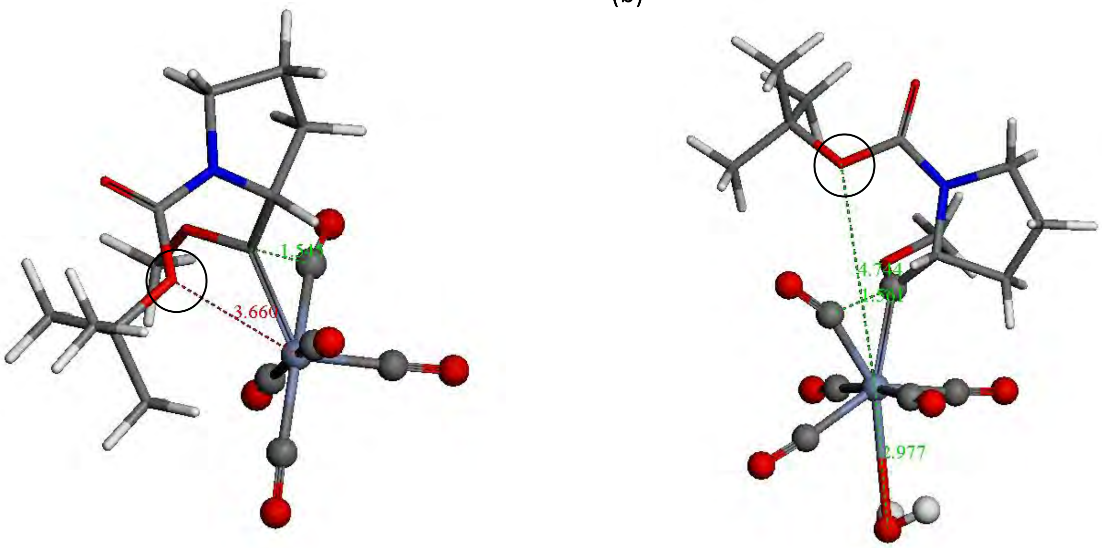

Figure 37: Carbonyl insertion into metal-carbene bond (a) in the absence of solvent and (b) in the presence of a coordinating solvent

By modifying the mechanism to the *N*-BOC-pyrrolidine Fischer carbene, as in Scheme 25, there is the suggestion that coordination of the *t*-butyl acyl group to the chromium may encourage a similar elimination of the BOC group to take place. This may result in the loss of the BOC group while keeping the carbene carbon bond to chromium intact, as seen in ^{1}H and ^{13}C NMR. It can also be seen from NMR that the pentacarbonyl moiety is altered. This is evident by the lack of the characteristic *cis/trans* signals, with the retention of the carbene carbon signal as seen in the ^{13}C spectrum in Figure 29. This could be due to the loss of a carbonyl along with the BOC group. It is also possible that the missing signals could be due to incorrectly configured T_1 delay times when running the NMR experiment.

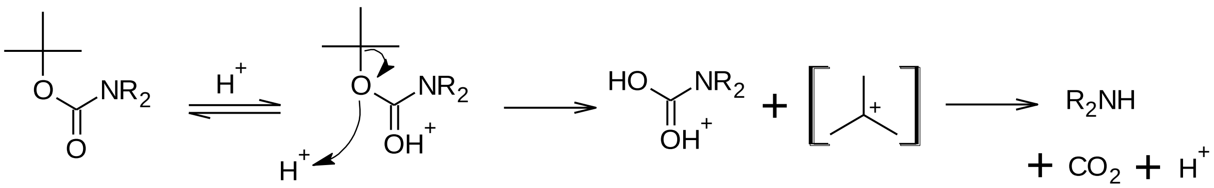

Scheme 24: Acid-catalyzed *N*-BOC cleavage *via* a bimolecular fragmentation of a protonated intermediate, as proposed by Ashworth *et al.*[178]

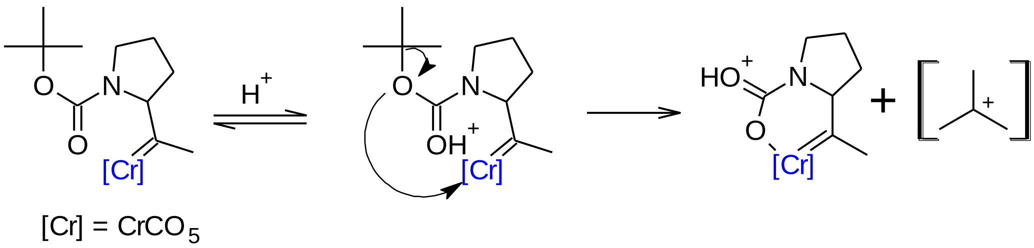

Scheme 25: Possible elimination mechanism for *N*-BOC from protected pyrrolidine Fischer carbene, 60a, adapted from Ashworth *et al.*[178]

2.4.3.2. *The Baylis-Hillman Carbene*

In general, the Baylis-Hillman reaction is a slow, carbon bond-forming reaction (it takes several days to complete), which requires an α,β-unsaturated electron-withdrawing group (such as methyl vinyl ketone, MVK) and an aldehyde (benzaldehyde, for example), and is carried out in the presence of stoichiometric amounts of a tertiary amine catalyst, such as DABCO (1,4-diazabicyclo[2.2.2]octane).[179] Since the pentacarbonyl chromium moiety is strongly electron-withdrawing, it has the potential to activate the alkene to a greater degree than a simple ketone might, in turn increasing the reaction rate of the Baylis-Hillman reaction. The Baylis-Hillman-derived carbene, **64**, was considered structurally interesting to this study due to the position of the oxygen and the potential for similar interference as seen in the *N*-BOC α-amino-derived carbenes. These carbenes have proven difficult to isolate, however, and so a theoretical investigation was undertaken.

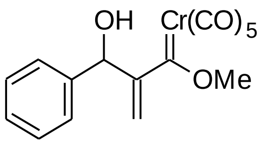

64

It was suspected that there may be some interaction between the hydroxyl oxygen and the chromium atom, perhaps leading to disintegration of the molecule, similar to what was observed in the *N*-BOC pyrrolidine-derived carbenes. In a triplet state, upon removal of the hydroxyl hydrogen, the oxygen atom was found to preferentially coordinate to one of the *cis* carbonyl ligands on the chromium atom. This results in a six-membered metallolactone (**65**, Figure 38a). When the hydroxyl was re-protonated, the system reverted back to the original configuration (Figure 38b). Thus, the involvement of the hydroxyl in the decomposition presupposes the presence of a base (such as DABCO, which we know is required in the Baylis-Hillman reaction).

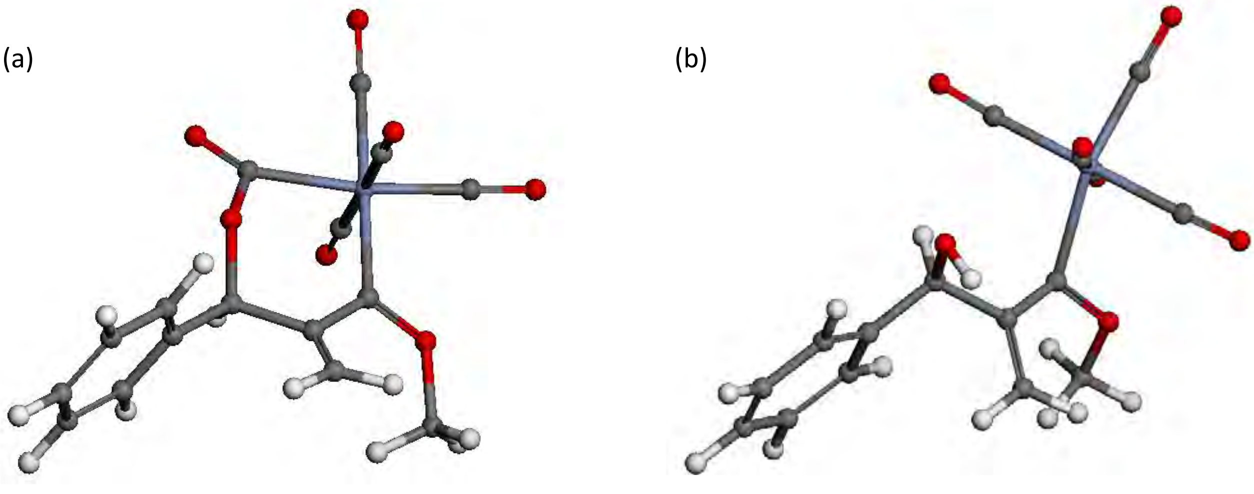

Figure 38: Six-membered cyclic ester (a) and original configuration (b)

The location and shape of the molecular bonding orbitals, namely the HOMO (highest occupied molecular orbital) and LUMO (lowest unoccupied molecular orbital) can be useful in understanding this intra-molecular interaction. Bonding occurs between these two orbitals with the HOMO donating electrons and the LUMO accepting these electrons.

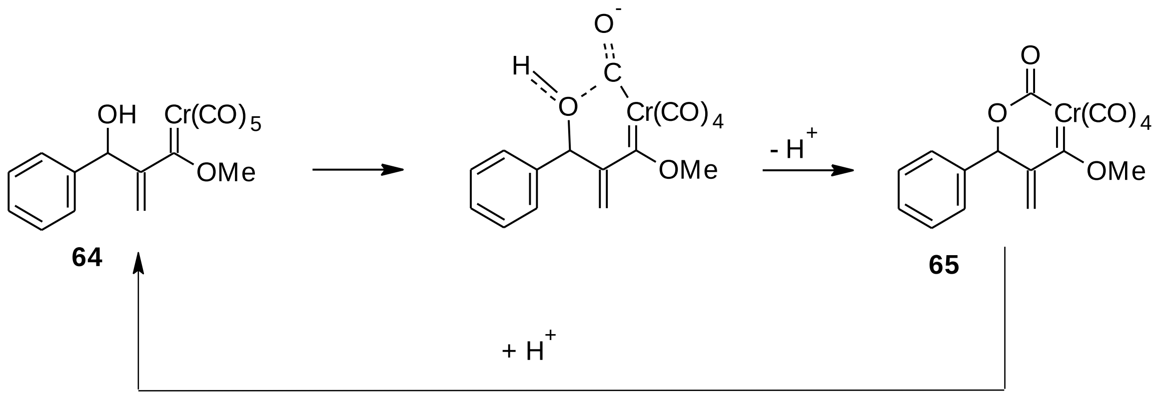

Scheme 23: Formation of cyclic six-membered ester on removal of a hydrogen

From Figure 39a, we can see that the carbonyl group closest to the hydroxyl group is capable of donating electrons to a suitable LUMO. In Figure 39b, which shows the LUMO configuration for the same compound with the hydroxyl proton in place, some electron-accepting potential around the hydroxyl group can be observed.

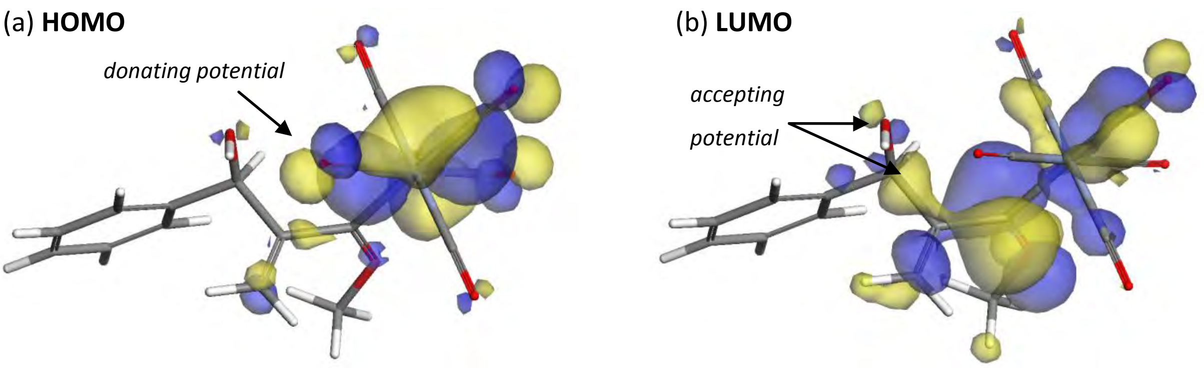

Figure 39: Molecular orbital maps of 64 showing (a) HOMO and (b) LUMO configurations

2.4.4. Bond Orders of Fischer Carbenes

By evaluating the bond orders and bond lengths of various Fischer carbenes, we hoped it would be possible to estimate the effect of substituents on the level of back donation. This relies on Pauling's empirical rule relating bond order to bond lengths.[140] Although quantitative results derived from this relationship would be highly empirical, a general qualitative trend of increasing bond order with decreasing length seemed reasonable to assume. Solà *et al.* have found that the back donation in carbenes is proportional to the $Cr\text{-}CO_{(trans)}$ distance, and inversely proportional to the $Cr{=}C_{(carbene)}$, and $C\text{-}O_{(trans)}$ distances.[61] Combining these two relationships, we can perhaps suggest that the level of back donation decreases with increasing bond order for the $Cr\text{-}CO_{(trans)}$ bond, while back donation increases with increasing bond order in Cr=C and $C\text{-}O_{(trans)}$. The back donation is a crucial (but not the only) factor implicated in stabilization of the electron-deficient carbene carbon.

Since the synthesis and stability of the simple methyl carbene is well documented, comparison of calculated bond orders or bond lengths of complex carbenes to the simple carbene may establish a trend of reactivity or stability. Figure 40 shows the bond lengths for two bonds of some selected carbenes (shown below), while Figure 41 shows the calculated bond orders for the same carbenes. The general trend we assumed was that an increase in bond length of $Cr{=}C_{(carbene)}$, along with a corresponding decrease in bond length of $Cr\text{-}CO_{(trans)}$, implies a reduction in back donation and hence a reduction in stability. Similarly, a decrease in bond order for $Cr{=}C_{(carbene)}$, together with an increase in bond order for $Cr\text{-}CO_{(trans)}$, implies less back donation and therefore reduced stability. Comparisons of stability are made against the simple methyl carbene, **52**.

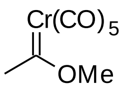

52

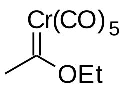

52-OEt

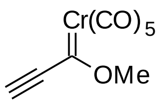

55

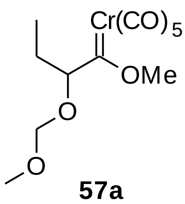

57a

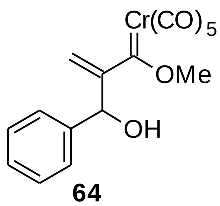

64

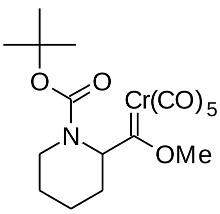

60b-BOC

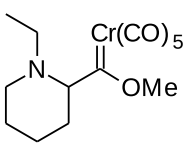

60b-Et

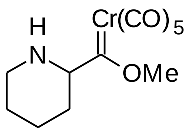

60b-H

Of interest in this context is the increased length of the $Cr{=}C_{(carbene)}$ bond in the *N*-BOC-protected piperidine-derived carbene, **60b**, versus the simple methyl carbene, **52**. Tied to this is the slightly contracted $Cr\text{-}CO_{(trans)}$ bond length. These two changes are most likely due to the *N*-BOC-protected piperidine substituent decreasing the back donation and hence also the stability. Looking at the bond orders of the same compound (Figure 41), we see a large drop in bond order for $Cr{=}C_{(carbene)}$, and a corresponding increase in the $Cr\text{-}CO_{(trans)}$ bond order. If the bond order is indeed linked to back donation, this suggests a drop in stability due to a decrease in back donation. Comparison of these values to the N-H piperidine-derived carbene, **60b-H**, as well as the *N*-Et piperidine-derived carbene, **60b-Et**, showed that the changes are most likely due to the presence of the BOC protecting group. This suggests an overall decrease in back donation, and a corresponding decrease in stability versus the simple methyl carbene. This decrease in stability may be a reason why the *N*-BOC-protected compounds have not been successfully synthesized in this study, while the methyl carbene and, more importantly, the *N*-Et compounds have been previously synthesized.[172]

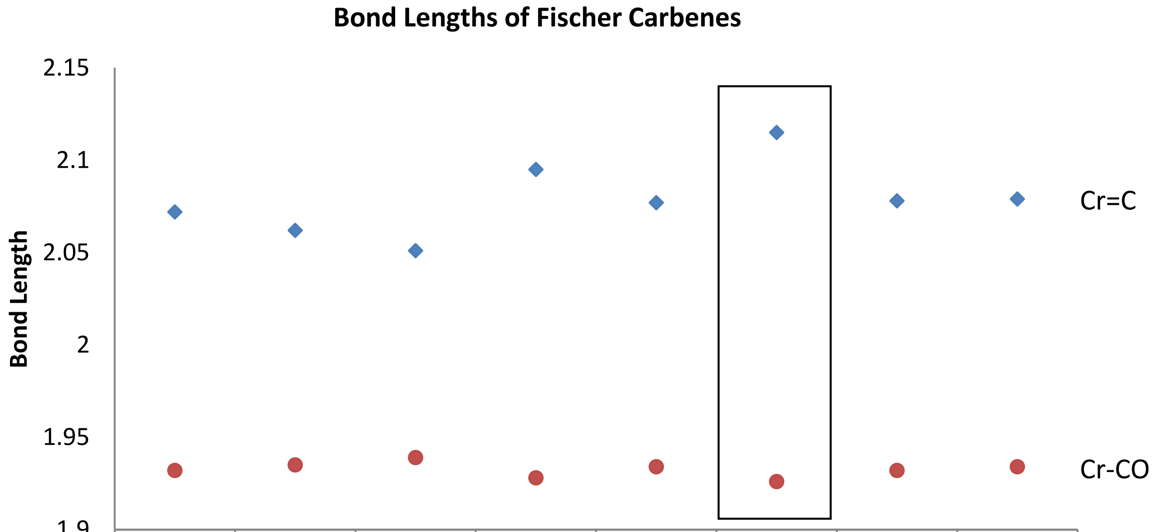

	52	52-OEt	55	57a	64	60b	60b-Et	60b-H
◆ Cr=C	2.072	2.062	2.051	2.095	2.077	2.115	2.078	2.079
● Cr-CO	1.932	1.935	1.939	1.928	1.934	1.926	1.932	1.934

Figure 40: Bond lengths for various Fischer Carbenes for the $Cr{=}C_{(carbene)}$ and $Cr\text{-}CO_{(trans)}$ bonds, in Angstroms, calculated at the DFT BLYP level of theory

In the case of the acetylide carbene, **55**, we saw that the $Cr{=}C_{(carbene)}$ bond length is noticeably decreased versus the simple methyl carbene, **52**. Correspondingly, the $Cr\text{-}CO_{(trans)}$ bond length is slightly extended, which is expected if these changes are from substituent-influenced effects on back donation. Figure 41 shows an increase in $Cr{=}C_{(carbene)}$ bond order, and a corresponding decrease in the $Cr\text{-}CO_{(trans)}$ bond order. This suggests an increase in back donation, and hence an increase in stability. We can also see that the MOM-protected alkoxy-derived carbene, **57a**, appears to be less stable than the simple methyl carbene, in terms of both bond order and bond length and hence back donation. We would expect electrostatic influences from the ligand to affect each bond in a similar way, such that the $Cr{=}C_{(carbene)}$ and $Cr\text{-}CO_{(trans)}$ bond orders would simultaneously change in the same sense (both increase, or both decrease). That each is moving in different directions lends support to the idea that bond order for these Fischer carbenes can be related to back donation.

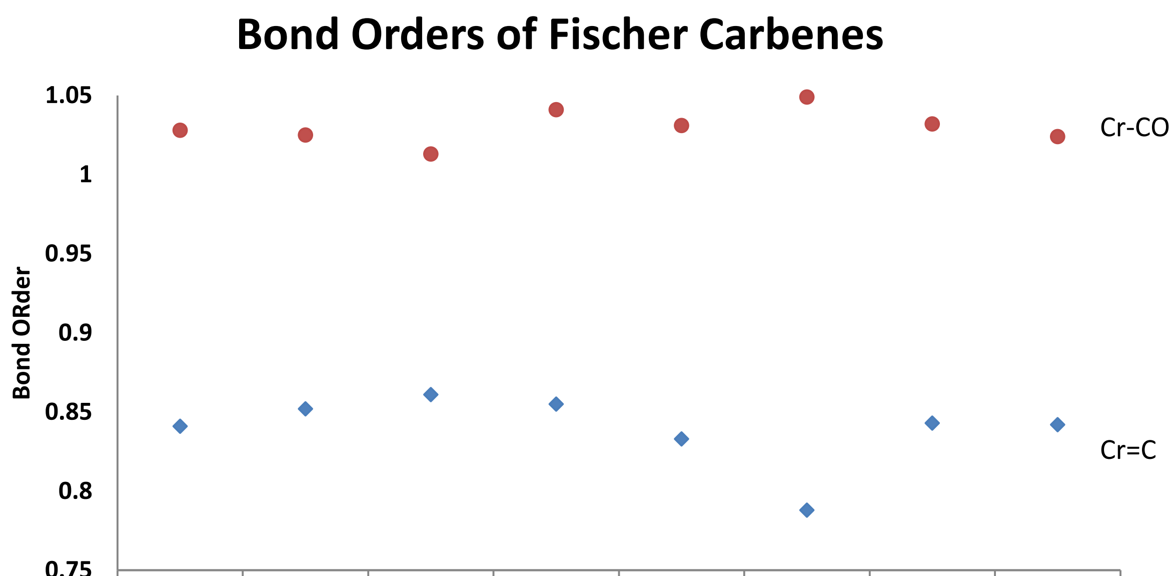

	52	52-OEt	55	57a	64	60b	60b-Et	60b-H
Cr=C	0.841	0.852	0.861	0.855	0.833	0.788	0.843	0.842
Cr-CO	1.028	1.025	1.013	1.041	1.031	1.049	1.032	1.024

Figure 41: Bond orders for various Fischer Carbenes for the $Cr{=}C_{(carbene)}$ and $Cr\text{-}CO_{(trans)}$ bonds, calculated at the DFT BLYP level of theory

It should be noted that the contribution from the π-bonding electrons is not the only indicator for stability in these compounds, as σ-bonds play a role in the reactivity and stability. It has also been found from *ab initio* computational work[61] that the donation from the carbene fragment to the metal fragment is stronger than the back donation; however, the smaller the π-donor character of the heteroatom substituent, the larger the back donation.[62] Looking at **52** and **52-OEt**, where the only change in structure is the replacement of the methoxy group with an ethoxy group, we see that the bond order for the Cr=C bond increases slightly, while the corresponding bond length decreases. This suggests an increase in back donation, to be expected from the reduced π-donor character of the ethoxy versus the methoxy group on the carbene. The Baylis-Hillman carbene, **55**, exhibits bond lengths and bond orders close to the methyl carbene, suggesting that the alkyl substituent does not play a large role in the back donation and relative stability of the complex. Any instability then can perhaps be attributed to the electrostatic and intra-molecular interactions discussed in Section 2.4.3.2.

2.5. Conclusion

Stable α-alkoxy- and α-amino organostannanes were synthesized, isolated and characterized for use as precursors to novel organolithiums for use in the synthesis of complex Fisher carbenes. α-Amino organostannanes were protected with a BOC protecting group, while α-alkoxy organostannanes were protected with a MOM protecting group. Several simple Fischer carbenes were successfully synthesized and purified, from readily available organolithium reagents, in order to confirm the suitability of the reaction conditions and apparatus. Novel organolithium compounds were accessed by making use of a tin-lithium metal exchange process, at low temperatures, with α-alkoxy- and α-amino organostannanes. The addition of chromium hexacarbonyl resulted in formation of the acylpentacarbonyl-chromate salt. Alkylation was carried out with Meerwein salt, resulting in novel complex Fischer carbenes. In the case of BOC-protected α-amino organostannanes however, the presence of the corresponding Fischer carbene was not confirmed. This lead to an attempt to synthesize a carbene derived from a BOC-protected α-alkoxy organostannane. Unfortunately attempts at the synthesis of the BOC-protected α-alkoxy organostannane were not successful. Difficulties in purification of Fischer carbenes made full characterization impossible, due to the presence of the tetrabutyltin by-product in all carbenes derived from organostannanes.

Some effort was put towards the synthesis of a Grignard reagent from tributyltin chloride, with the aim of creating a cheaper or more effective alternative to tributyltin hydride. This was unsuccessful however, and may require the use of a catalyst. A simple imine was synthesized *via* microwave heating.

A reaction mechanism was mapped out for the photoactivated [2+2] cycloaddition reaction of an imine with a Fischer carbene, including the photo-excitation cycle. This could be used to access novel biologically active heterocycles such as β-lactams.

Computational exploration revealed interesting behaviour influenced by the *t*-butyl acyl oxygen on the *N*-BOC protecting group in α-amino organostannane derived Fischer carbenes. These carbenes were synthetically elusive, while the *N*-Et α-amino organostannane derived carbenes have been synthesized in this group. It could be possible that coordination of the *t*-butyl acyl oxygen to the chromium atom may encourage the disintegration of the pentacarbonyl moiety to occur, along with the elimination of the BOC group, while keeping the C=Cr bond intact.

The Baylis-Hillman derived carbene exhibited an interesting interaction between the hydroxyl oxygen and the pentacarbonyl chromium moiety. A preferential coordination of the hydroxyl oxygen to a *cis* carbonyl ligand lead to the formation of a six-membered metallolactone, and although this was dependant on the presence of a base, the Baylis-Hillman reaction is often performed using a base such as DABCO.

The ligands surrounding the chromium moiety obviously influence reactivity and stability, hence a comparison of bond orders and lengths between several Fischer carbenes was carried out. It has been established that bond length is related to back donation in carbenes, which itself is related to the stability of carbenes. Since bond order is related to bond length, when compared to experimental results, some inference can be made between the stability of these Fischer carbenes and the bond orders of the $Cr{=}C_{(carbene)}$, $Cr\text{-}CO_{(trans)}$, and $Cr\text{-}CO_{(cis)}$ bonds. A higher bond order in $Cr\text{-}CO_{(trans)}$ coupled with a lower bond order in $Cr{=}C_{(carbene)}$ could indicate reduced stability (and *vice versa*), when compared to the simple methyl carbene.

Chapter 3: Experimental

3.1. General Experimental Details

Reagents used were purchased from Sigma Aldrich® and were used without further purification unless otherwise stated. Schlenk techniques were used for all organometallic reactions. All procedures requiring inert atmospheres were carried out using argon gas. Solvents were dried and purified using the methodology outlined by Vogel.[162] Ethers were distilled from sodium/benzophenone under nitrogen, and dichloromethane and hexane were distilled from calcium hydride. *N,N,N′,N′*-Tetramethylethylenediamine (TMEDA) was distilled from calcium hydride at atmospheric pressure. The concentration of *n*-BuLi was determined by titration into a 1,3-diphenylacetic acid solution before each use. All aldehydes were inspected *via* NMR and fractional distillation was used to isolate those found to be impure. A freeze-pump-thaw method was used to de-gas water where necessary. This was carried out by freezing a flask of water, and thawing it *in vacuo*. Once thawed, the process was repeated twice. Thin-layer chromatography was performed on Merck® TLC silica gel 60 PF_{254} plates and visualized either under ultraviolet light, or by staining with phosphomolybdic acid (20% in ethanol) and gentle warming with a heat gun. Chromatography was carried out with Merck silica gel 60 (particle size 0.063-0.200 mm), under argon where indicated. Radial thin-layer chromatography was carried out using silica gel 60 PF_{254} containing gypsum on a Harrison Research Chromatotron™. NMR spectroscopy was performed on a Bruker® 400MHz AVANCE spectrometer. Chemical shifts are reported in ppm and calibrated according to residual solvent resonance (δ_H 7.26 ppm for $CDCl_3$ and 7.15 ppm for C_6D_6; δ_C 77.0 ppm for $CDCl_3$ and 128.02 ppm for C_6D_6). IR spectra were performed neat on an ATR IR or recorded as thin films on a Perkin-Elmer® FT-IR Spectrum 2000 spectrometer using KBr and polyethylene discs.

All DFT calculations were carried out using the DMol3 package, hosted within Materials Studio 4.4. Geometry optimizations were initially performed using the PWN functional,[180] which falls under the LDA family of functionals, and later with the BLYP functional, a GGA method. Molecular dynamics was done on some compounds before geometry optimization to ensure that the correct configuration was used. Transition states were found by the Transition State Search function within DMol3, using the QST* method, and were further optimized and confirmed by vibrational analysis to have only one negative frequency (or eigenvalue). Energies were corrected by adding the free energy, G, calculated at 298.15 K.

* QST is a quadratic synchronous transit method used to search for transition states. It is an extension of the LST method, which uses a simpler linear synchronous transit method. They are “global” methods, which interpolate between the reactant and product. In general, they provide a good guess at the structure of the transition state, which must then be evaluated, optimized and confirmed.

3.2. Synthesis of Stannanes

3.2.1. Synthesis of α-alkoxy organostannanes

(a) Synthesis of tributyl[1-(methoxymethoxy)propyl]stannane[22]

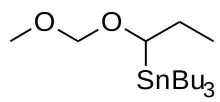

43a

Diisopropylamine (3.7 mL, 26.0 mmol) was dissolved in dry THF (50 mL) at 0°C. *n*BuLi in pentane (14.4 mL, 1.8 M, 26.0 mmol) was added dropwise over 30 min *via* cannula. After 30 min, tributyltin hydride in hexane (20.0 mL, 1.0 M, 20.0 mmol) was added. The solution turned dark orange during the addition. After 1 h, the mixture was cooled to -78°C, and a solution of propionaldehyde (1.08 mL, 15.0 mmol) in THF (2 mL) was added and left to stir for 5 h while maintaining the low temperature bath. The mixture was quenched with sat. NH_4Cl solution (3 x 20 mL), washed with water (3 x 20 mL) and extracted with petroleum ether (2 x 30 mL). The combined organic layers were dried over anhydrous $MgSO_4$, filtered and evaporated to afford 1-tributylstannyl-propan-1-ol, **42a**, as a colourless oil, which was used in the next step without further purification.

N,N-Dimethylaniline (3.80 mL, 30 mmol) was added to a solution of 1-tributylstannyl-propan-1-ol dissolved in CH_2Cl_2 (30 mL) at 0 °C. Chloromethyl methyl ether (2.28 mL, 30.0 mmol) was added slowly and left to stir for 1 h. The mixture was washed with ice-cold 0.5M HCl (3 x 30 mL), water (3 x 30 mL) and sat. $NaHCO_3$ (3 x 30 mL). The organic layer was dried over anhydrous $MgSO_4$, filtered and evaporated. The oil was purified by column chromatography. The by-product, tetrabutyltin, was eluted using 10% dichloromethane in hexane, followed by elution with 10% ethyl acetate in hexane to afford *tributyl[1-(methoxymethoxy)propyl]stannane* (**43a**, 3.61 g, 61.2%). IR (film) ν_{max}/cm^{-1} 2956, 2923, 1462, 1358, 1078 cm^{-1}; δ_H NMR (400 MHz, $CDCl_3$) 4.61 (1H, d, *J* = 6.7 Hz, O-CH^AH^B), 4.55 (1H, d, *J* = 6.7 Hz, O-CH^AH^B), 3.99 (1H, t, *J* = 6.5 Hz, 1-CH), 3.34 (3H, s, OCH_3), 1.95-1.75 (2H, m, 2-CH_2), 1.60-1.41 [6H, m, (2'-CH_2)$_3$], 1.36-1.27 [6H, m, (3'-CH_2)$_3$], 0.96 (2H, t, *J* = 7.2 Hz, 3-CH_2), 0.91-0.81 [15H, m, (1'-CH_2, 4'-CH_3)$_3$]; δ_C NMR (100 MHz, $CDCl_3$) 96.4 (OCH_2), 75.7 (C-1), 55.3 (OCH_3), 29.2 (C-2'), 27.9 (C-2), 27.5 (C-3'), 13.6 (C-4'), 12.3 (C-3), 9.2 (C-1').

(b) Synthesis of tributyl[1-(methoxymethoxy)butyl]stannane[22]

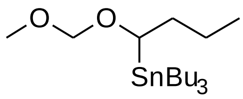

43b

Diisopropylamine (2.8 mL, 19.5 mmol) was dissolved in dry THF (50 mL) at 0°C. *n*BuLi in hexane (12.3 mL, 1.6 M, 19.5 mmol) was added dropwise over 30 min *via* cannula. After 30 min, tributyltin hydride (4.0 mL, 15.0 mmol) was added. The solution turned orange during the addition. After 1 h, the mixture was cooled to -78°C, and a solution of butanal (1.0 mL, 11.25 mmol) in THF (2 mL) was added and left to stir for 5 h, while maintaining the low temperature bath. The solution turned yellow. The mixture was quenched with sat. NH_4Cl solution (3 x 20 mL), washed with water (3 x 20 mL) and extracted with petroleum ether (2 x 30 mL). The combined organic layers were dried over anhydrous $MgSO_4$, filtered and evaporated to afford (tributylstannyl)butan-1-ol, **42b**, as a colourless oil, which was used in the next step without further purification.

N,N-Dimethylaniline (2.85 mL, 22.5 mmol) was added to a solution of 1-(tributylstannyl)butan-1-ol in CH_2Cl_2 (30 mL) at 0°C. Chloromethyl methyl ether (1.71 mL, 22.5 mmol) was added slowly and left to stir for 1 h. The mixture was washed with ice-cold 0.5M HCl (3 x 30 mL), water (3 x 30 mL) and sat. $NaHCO_3$ (3 x 30 mL). The organic layer was dried over anhydrous $MgSO_4$, filtered and evaporated. The colourless oil was purified by column chromatography. The by-product, tetrabutyltin, was eluted with 10% dichloromethane in hexane, followed by the elution with 10% ethyl acetate in hexane to afford *tributyl[1-(methoxymethoxy)butyl]stannane* (**43b**, 1.42 g, 34.8%). IR (film) ν_{max}/cm^{-1} 2957, 2925, 1463, 1378, 1147 cm^{-1}; δ_H NMR (400 MHz, C_6D_6) 4.59-4.57 (2H, m, OCH_2), 4.21 (1H, t, *J* = 6.4 Hz, 1-CH), 3.21 (3H, s, OCH_3), 1.99-1.82 (2H, m, 2-CH_2), 1.73-1.58 [6H, m, (2'-CH_2)$_3$], 1.54-1.47 (2H, m, 3-CH_2), 1.44-1.35 [6H, m, (3'-CH_2)$_3$], 1.10-1.00 [6H, m, (1'-CH_2)$_3$], 0.97-0.93 [12H, m, 4-CH_3 and (4'-CH_3)$_3$]; δ_C NMR (100 MHz, $CDCl_3$) 96.9 (OCH_2), 74.1 (C-1), 55.4 (OCH_3), 38.1 (C-2) 29.9 (C-2'), 28.1 (C-3'), 21.8 (C-3), 14.4 (C-4), 13.9 (C-4'), 9.7 (C-1').

(c) Synthesis of tributyl[1-(methoxymethoxy)-2-methylpropyl]stannane[22]

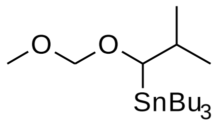

43c

Diisopropylamine (2.2 mL, 16 mmol) was dissolved in dry THF (50 mL) at 0°C. *n*BuLi in hexane (9.8 mL, 1.6 M, 16 mmol) was added dropwise over 30 min *via* cannula. After 30 min, tributyltin hydride (3.2 mL, 12 mmol) was added. The solution turned orange during the addition. After 1 h, the mixture was cooled to -78°C, and a solution of isobutanal (0.82 mL, 9.0 mmol) in THF (2 mL) was added and left to stir for 5 h while maintaining the low temperature bath. The solution turned yellow. The mixture was quenched with sat. NH_4Cl solution (3 x 20 mL), washed with water (3 x 20 mL) and extracted with petroleum ether (2 x 30 mL). The combined organic layers were dried over anhydrous $MgSO_4$, filtered and evaporated to afford a pale yellow oil, *2-methyl-1-(tributylstannyl)propan-1-ol*, **42c**, which was used in the next step without further purification.

N,N-Dimethylaniline (2.3 mL, 18 mmol) was added to a solution of 2-methyl-1-(tributylstannyl)propan-1-ol in CH_2Cl_2 (30 mL) at 0 °C. Chloromethyl methyl ether (1.4 mL, 18 mmol) was added slowly and left to stir for 1 h. The mixture was washed with ice-cold 0.5M HCl (3 x 30 mL), water (3 x 30 mL) and sat. $NaHCO_3$ (3 x 30 mL). The organic layer was dried over anhydrous $MgSO_4$, filtered and evaporated. The opaque oil was purified by column chromatography. The by-product, tetrabutyltin, was eluted with 10% dichloromethane in hexane, followed by the elution with 10% ethyl acetate in hexane to afford *tributyl[1-(methoxymethoxy)-2-methylpropyl] stannane* (**43c**, 1.19 g, 32.4%). IR (film) ν_{max}/cm^{-1} 2956, 2923, 1462, 1374, 1070 cm^{-1}; δ_H NMR (400 MHz, C_6D_6) 4.56-4.54 (1H, m, O-CH_2), 4.05 (1H, d, *J* = 4.5 Hz, 1-CH), 3.21 (3H, s, OCH_3), 2.28-2.13 (2H, m, 2-CH_2), 1.73-1.56 [6H, m, (2'-CH_2)$_3$], 1.43-1.37 [6H, m, (3'-CH_2)$_3$], 1.10-1.01 [9H, m, (3-CH_3 and (1'-CH_2)$_3$], 0.98-0.84 [12H, m, 4-CH_3 and (4'-CH_3)$_3$]; δ_C NMR (100 MHz, $CDCl_3$) 97.3 (OCH_2), 82.4 (C-1), 55.4 (OCH_3), 33.3 (C-2) 29.7 (C-2'), 28.0 (C-3'), 21.5 (C-3), 20.2 (C-4), 13.9 (C-4'), 10.4 (C-1').

(d) Attempted synthesis of tributyl[(methoxymethoxy)methyl]stannane[22]

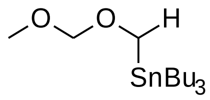

43d

Diisopropylamine (2.2 mL, 16 mmol) was dissolved in dry THF (50 mL) at 0°C. *n*BuLi in hexane (9.8 mL, 1.6 M, 16 mmol) was added dropwise over 30 min *via* cannula. After 30 min, tributyltin hydride (3.2 mL, 12 mmol) was added. The solution turned orange during the addition. After 1 h, the mixture was cooled to -78°C. In a separate flask, paraformaldehyde (0.27 g, 9 mmol) was crushed into a fine powder and suspended in dry THF (5 mL). The tributylstannyllithium was added to the paraformaldehyde solution *via* a syringe. The organolithium solution turned brown during the addition. The mixture was left to stir for 5 h, while maintaining the low temperature bath. The mixture was quenched with sat. NH_4Cl solution (3 x 20 mL), washed with water (3 x 20 mL) and extracted with petroleum ether. The organic layers were dried over anhydrous $MgSO_4$, filtered and solvent was removed to obtain a yellow oil, which was used in the next step without further purification.

N,N-Dimethylaniline (2.3 mL, 18 mmol) was added to a solution of the yellow oil in CH_2Cl_2 (30 mL) at 0 °C. Chloromethyl methyl ether (1.4 mL, 18 mmol) was added slowly and left to stir for 5 h. The mixture was washed with ice-cold 0.5M HCl (3 x 30 mL), water (3 x 30 mL) and sat. $NaHCO_3$ (aq) (3 x 30 mL). The organic layer was dried over anhydrous $MgSO_4$, filtered and the solvent was evaporated. TLC analysis of the crude material indicated the presence of the starting material paraformaldehyde and many side-products such as tetrabutyltin, but none of the desired product, *tributyl[(methoxymethoxy)methyl]stannane*, **43d**.

(e) Attempted synthesis of tributyl[(methoxymethoxy)benzyl]stannane[22]

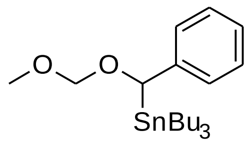

43e

Diisopropylamine (2.8 mL, 20 mmol) was dissolved in dry THF (50 mL) at 0°C. *n*BuLi in hexane (12.2 mL, 1.6 M, 20 mmol) was added dropwise over 30 min *via* cannula. After 30 min, tributyltin hydride (4.0 mL, 15 mmol) was added. The solution turned orange during the addition. After 1 h, the mixture was cooled to -78°C. Benzaldehyde (1.15 ml, 11.3 mmol) in dry THF (2 mL) was added to the tributylstannyllithium solution *via* a syringe. The organolithium solution turned yellow during the addition. The mixture was left to stir for 5 h, while maintaining the low temperature bath. The mixture was quenched with sat. NH_4Cl solution (3 x 20 mL), washed with water (3 x 20 mL) and extracted with petroleum ether. The organic layers were dried over anhydrous $MgSO_4$, filtered and solvent was removed to obtain a colourless oil, which was used in the next step without further purification.

N,N-Dimethylaniline (2.85 mL, 22.5 mmol) was added to a solution of the yellow oil in CH_2Cl_2 (30 mL) at 0°C. Chloromethyl methyl ether (1.71 mL, 22.5 mmol) was added slowly and left to stir for 5 h. The mixture was washed with ice-cold 0.5M HCl (3 x 30 mL), water (3 x 30 mL) and sat. $NaHCO_3$ (aq) (3 x 30 mL). The organic layer was dried over anhydrous $MgSO_4$ and filtered, and the solvent was evaporated. TLC analysis of the crude material indicated the presence of the starting material, as well as several by-products. The oil was purified by column chromatography. The by-product, tetrabutyltin, was eluted with 10% dichloromethane in hexane, after which the solvent system was changed to 10% ethyl acetate in hexane, and seven fractions were recovered. NMR analysis showed that none of the fractions contained the desired product, *tributyl[(methoxymethoxy)benzyl]stannane*, **43e**.

(f) Attempted synthesis of tert-butyl 2-(tributylstannyl)propyl -1-carboxylate

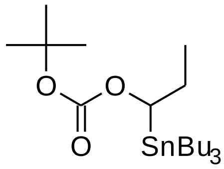

Diisopropylamine (2.39 mL, 16.9 mmol) was dissolved in dry THF (50 mL) at 0°C. *n*BuLi (1.8 M in hexan, 9.4 mL, 24.0 mmol) was added dropwise over 30 min *via* cannula. After 30 min, tributyltin hydride (6.4 mL, 24.0 mmol) was added and the solution turned dark orange. After 1 h, the mixture was cooled to -78°C, and a solution of propanal (0.70 mL, 9.8 mmol) in THF (2 mL) was added and left to stir for 5 h while maintaining the low temperature bath. The mixture was quenched with sat. NH_4Cl solution (3 x 20 mL), washed with water (3 x 20 mL) and extracted with petroleum ether (2 x 30 mL). The combined organic layers were dried over anhydrous $MgSO_4$, filtered and evaporated to afford *1-tributylstannyl-propan-1-ol*, **42a**, as a colourless oil.

The protection step was attempted on **42a** on the crude mixture, and on the pure compound [isolated *via* column chromatography in the same method as described in Section 3.2.1 (a)]. *N,N*-Dimethylaniline (2.47 ml, 19.5 mmol) was added to a solution of **42a** in CH_2Cl_2 (30 ml) at 0°C. Di-*tert*-butyl dicarbonate (4.26 g, 19.5 mmol) was added slowly over 10 minutes. The reaction mixture was allowed to warm to room temperature, and stirred for 5 hours. The mixture was quenched with sat. NH_4Cl solution (2 x 40 mL). The organic layers were dried over anhydrous $MgSO_4$ and filtered, and the solvent was evaporated. TLC analysis of the crude mixture revealed the presence of several compounds. NMR analysis confirmed that none of the desired product was present in the mixture.

This synthesis was also attempted with DMAP as the base, in the same molar ratio, again with no result.

(g) Attempted synthesis of tributyltin magnesium chloride ($Bu_3SnMgCl$)[162]

Dry THF was used to wash and clean magnesium turnings (0.358 g, 14.7 mmol), which were then dried in the oven and added to a flask along with dry THF (20 ml). A single crystal of iodine was added as an activator. Once iodine vapours were visible in the flask, dry Et_2O (10 ml) and about 10% of the total tributyltin chloride (4.0 ml, 14.7 mmol) was added to the flask. After a slow addition of the remaining Et_2O and Bu_3SnCl, the solution was heated at reflux. TLC showed no change in starting products, and titration of the reaction mixture in diphenylacetic acid showed no colour change even when great excesses of stannane were added. Weighing the magnesium strips after the reaction showed no loss of mass, inferring that no reaction had taken place. From these results, it was concluded that the reaction did not take place under the conditions described. The reaction was repeated with THF in place of Et_2O, and with TMEDA as solvent, with identical results.

3.2.2. Synthesis of α-amino organostannanes

(a) Synthesis of tert-butyl pyrrolidine-1-carboxylate[25]

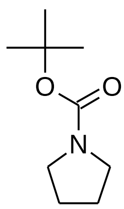

49a

Pyrrolidine (5.0 mL, 60.9 mmol) was dissolved in CH_2Cl_2 (50 mL) at 0°C. Di-*tert*-butyl dicarbonate (10.0 g, 45.7 mmol) was added slowly over 10 minutes. The reaction mixture was allowed to warm to room temperature, and stirred for 12 hours. The mixture was quenched with sat. NH_4Cl solution (2 x 40 mL). The organic layers were dried over anhydrous $MgSO_4$ and filtered, and the solvent evaporated. The oil was purified by vacuum distillation to afford *tert-butyl pyrrolidine-1-carboxylate*, **49a**, as a colourless oil (5.54 g, 70.9%). IR (film) ν_{max}/cm^{-1} 2978, 2890, 1695(C=0), 1391 (C-N), 1253 (C-O) cm^{-1}; δ_H NMR (400 MHz, $CDCl_3$) 3.33-3.28 (4H, m, 5-CH_2 and 2-CH_2), 1.83 (4H, br s, 3-CH_2 and 4-CH_2), 1.46 [9H, s, $(CH_3)_3$]; δ_C NMR (100 MHz, $CDCl_3$) 154.7 (C=O), 78.9 (C-8), 45.9 (C-2), 45.6 (C-5), 28.6 (3 x CH_3), 25.8 (C-3), 25.0 (C-4).

(b) Synthesis of tert-butyl 2-(tributylstannyl)pyrrolidine-1-carboxylate[25]

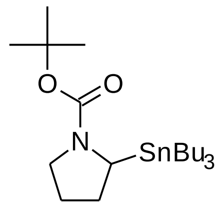

50a

sec-Butyllithium (1.1 M in cyclohexane, 25.5 ml, 28.0 mmol) was added dropwise over 45 min *via* syringe to a solution of TMEDA (4.20 mL, 28.0 mmol) in dry Et_2O (50 mL) at -78°C. After 20 min, *tert*-butyl pyrrolidine-1-carboxylate (**49a**, 4.0 g, 23 mmol) was added. The mixture turned milky yellow during the addition and was stirred for 4 h. Tributyltin chloride (12.7 mL, 46.7 mmol) was added and the mixture warmed to room temperature while being stirred for 12 h. The mixture was washed with water (2 x 50 mL) and then with 50 mL of 2% H_3PO_4(aq). The aqueous layer was extracted with petroleum ether (2 x 10 mL). The combined organic layers were dried over anhydrous $MgSO_4$, filtered, evaporated and purified by column chromatography, eluting with 10% ethyl acetate in hexane, to give *tert-butyl 2-(tributylstannyl)pyrrolidine-1-carboxylate*, **50a**, as a colourless oil (5.77 g, 53.7%). IR (film) ν_{max}/cm^{-1} 2923, 2875, 1675 (C=0), 1427 (C-N), 1270 (C-O) cm^{-1}; δ_H NMR (400 MHz, C_6D_6) 3.27-3.21 (1H, m, 5-C$H_A$$H_B$), 3.15-3.11 (1H, m, 2-CH), 3.07-3.01 (1H, m, 5-C$H_A$$\mathit{H}_B$), 1.89-1.78 (2H, m, 3-$CH_2$), 1.74-1.56 [12H, m, (2'-CH_2)$_3$ and (3'-CH_2)$_3$], 1.42 (9H, s, 3CH_3), 1.40-1.35 (2H, m, 4-CH_2), 1.03-0.98 [6H, m, (1'-CH_2)$_3$], 0.94 [9H, t, *J* = 7.3 Hz, (4'-CH_3)$_3$]; δ_C NMR (100 MHz, C_6D_6) 154.5 (C=O), 78.4 (C-8), 46.7 (C-2), 46.5 (C-5), 30.8 (C-3), 29.8 (C-2'), 28.7 (3 x CH_3), 28.1 (C-3'), 27.7 (C-4), 14.1 (C-4'), 10.9 (C-1').

(c) Synthesis of tert-butyl piperidine-1-carboxylate[25]

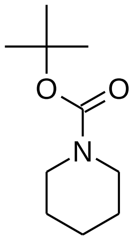

49b

Di-*tert*-butyl dicarbonate (7.03 g, 38.0 mmol) was dissolved in CH_2Cl_2 (50 mL) at 0°C. Piperidine (5.0 mL, 50.6 mmol) was added slowly over 30 min. The ice bath was removed and the mixture was allowed to warm to room temperature, and stirred for 12 h. The mixture was quenched with sat. NH_4Cl solution (2 x 40 mL). The organic layers were dried over anhydrous $MgSO_4$ and filtered, and the solvent evaporated. The oil was purified by vacuum distillation, to afford *tert-butyl piperidine-1-carboxylate*, **49b**, as a colourless oil (5.23 g, 74.4%). IR (film) ν_{max}/cm^{-1} 2934, 2857, 1692(C=0), 1421 (C-N), 1268 (C-O) cm^{-1}; δ_H NMR (400 MHz, C_6D_6) 3.29 (4H, br s, 2-CH_2 and 6-CH_2), 1.46 (9H, s, 3CH_3), 1.20-1.18 (6H, m, 3-CH_2, 4-CH_2 and 5-CH_2); δ_C NMR (100 MHz, C_6D_6) 154.7 (C=O), 78.7 (C-9), 44.7 (C-2 and C-6), 28.6 (3 x CH_3), 26.0 (C-4), 24.7 (C-3 and C-5).

(d) Synthesis of tert-butyl 2-(tributylstannyl)piperidine-1-carboxylate[25]

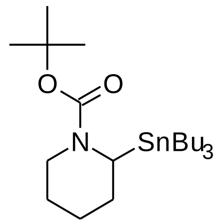

50b

sec-Butyllithium (1.2 M in cyclohexane, 21.6 ml, 25.9 mmol) was added dropwise over 45 min *via* cannula to a solution of TMEDA (3.0 mL, 26 mmol) in dry Et_2O (100 mL) at -78°C. After 20 min, *tert*-butyl piperidine-1-carboxylate (**49b**, 4.0 g, 22 mmol) was added. The mixture turned milky yellow during the addition and was stirred for 4 h. Tributyltin chloride (11.7 mL, 43.2 mmol) was added and the mixture warmed to room temperature while being stirred for 12 h. The mixture was washed with water (2 x 50 mL) and then with 50 mL of 2% H_3PO_4(aq). The aqueous layer was extracted with petroleum ether (2 x 10 mL). The combined organic layers were dried over anhydrous $MgSO_4$, filtered, evaporated and purified by column chromatography eluting with 10% ethyl acetate in hexane, to give *tert-butyl 2-(tributylstannyl)piperidine-1-carboxylate*, **50b**, as a colourless oil (5.78 g, 56.4 %). IR (film) ν_{max}/cm^{-1} 2924, 2875, 1672 (C=0), 1427 (C-N), 1270 (C-O) cm^{-1}; δ_H NMR (400 MHz, C_6D_6) 3.82-3.80 (1H, m, 6-C$H_A$$H_B$), 3.02-3.01 (2H, m, 2-$CH_2$), 2.88-2.85 (1H, m, 6-$CH_A$$H_B$), 1.78-1.69 [7H, m, 3-C$H_A$$H_B$ and (2'-CH_2)$_3$], 1.67-1.57 (1H, m, 3-$CH^A$$H^B$), 1.56-1.44 [7H, m, 5-C$H_A$$H_B$ and (3'-CH_2)$_3$], 1.39 (3H, s, $COCH_3$), 1.38-1.18 (3H, m, 4-CH_2 and 5-$CH^A$$H^B$), 1.16-1.05 [6H, m, (1'-CH_2)$_3$], 1.00 [9H, t, *J* 7.3 (4'-CH_3)$_3$]; δ_C NMR (100 MHz, C_6D_6) 156.2 (C=O), 79.2 (C-9), 47.5 (C-6), 47.3 (C-2), 31.1 (C-3), 29.9 (C-2'), 28.4 (3 x CH_3), 28.2 (C-3'), 27.1 (C-5), 26.7 (C-4), 14.1 (C-4'), 12.1 (C-1').

3.3. Synthesis of Fischer Carbenes

3.3.1. Simple Fischer Carbenes

(a) Synthesis of 1-methoxy-1-ethylidene pentacarbonyl chromium(0)[53]

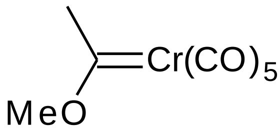

52

Chromium hexacarbonyl (2.51 g, 11.4 mmol) was crushed into a fine powder and added to a flame-dried Schlenk flask containing freshly dried Et_2O (40 ml) under argon. MeLi (1.0 M in hexane, 22.8 ml, 22.8 mmol) was added dropwise over 15 min and the mixture was stirred at room temperature for 1 hour, during which time the solution turned from yellow to dark brown. The solvent was removed *in vacuo* and the dark brown residue was taken up in degassed water. Trimethyloxonium tetrafluoroborate (6.75 g, 45.7 mmol) was added over 5 min and this mixture was left to stir for 1 hour. The product was extracted with 3 x 10 ml portions of dry Et_2O which were then removed *in vacuo* to give a yellow solid. Purification was by flash column chromatography using distilled hexane under argon pressure, and allowing crystals to form as the hexane evaporated. The desired product, *1-methoxy-1-ethylidene pentacarbonyl chromium(0)*, **52**, was obtained as yellow crystals (1.61 g, 56.4%). IR (film) v_{max}/cm^{-1} 2060, 1923, 1451, 1259; δ_H NMR (400 MHz, $CDCl_3$) 4.73 (3H, br s, OCH_3), 2.96 (3H, s, CH_3); δ_C NMR (100MHz, $CDCl_3$) 360.5 (Cr=C), 223.3 (CO_{trans}), 216.4 (CO_{cis}) 67.5 (OCH_3) 49.8 (CH_3)

(b) Synthesis of 1-methoxy-1-butylidene pentacarbonyl chromium(0)[53]

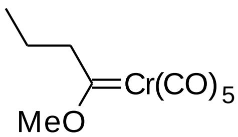

53

Chromium hexacarbonyl (2.50 g, 11.3 mmol) was crushed into a fine powder and added to a flame-dried Schlenk flask containing freshly dried Et_2O (40 ml) under argon. *n*BuLi (2.5 M in hexane, 9.1 ml, 22.75 mmol) was added dropwise over 15 min and stirred at room temperature for 1 hour, during which time the solution turned from yellow to dark brown. The solvent was removed *in vacuo* and the dark brown residue was taken up in degassed water. Trimethyloxonium tetrafluoroborate (6.72 g, 45.4 mmol) was added over 5 min and this mixture was left to stir for 1 hour. The product was extracted with several 10 ml portions of dry Et_2O until no further colour was observed in the organic layer. The solvent was then removed *in vacuo* to give a yellow solid. Purification was by flash column chromatography using distilled hexane under argon pressure, and allowing crystals to form as the hexane evaporated. The desired product, *1-methoxy-1-butylidene pentacarbonyl chromium(0)*, **53**, was obtained as yellow crystals (0.83 g, 25.0 %). δ_H NMR (400 MHz, $CDCl_3$) 4.51 (3H, br s, OCH_3), 3.53 (2H, t, CH_2), 1.30 (2H, m, CH_2), 0.94 (3H, t, CH_3); δ_C NMR (100 MHz, $CDCl_3$) 360.1 (Cr=C), 225.0 (CO_{trans}), 216.9 (CO_{cis}), 68.6 (OCH_3), 46.6 (CH_2), 19.5 (CH_2), 13.6 (CH_3)

(c) Synthesis of 1-methoxy-prop-2-yn-1-ylidene pentacarbonyl chromium(0)[53]

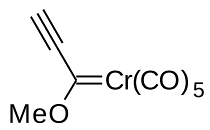

55

Chromium hexacarbonyl (2.51 g, 11.4 mmol) was crushed into a fine powder and added to a flame-dried Schlenk flask containing freshly dried Et_2O (40 ml) under argon. Lithium acetylide, ethylenediamine complex (1.89 g, 20.5 mmol) was added carefully over 5 min and stirred at room temperature for 1 hour, during which time the solution turned from light yellow to dark brown. The solvent was removed *in vacuo* and the dark brown residue was taken up in degassed water. Trimethyloxonium tetrafluoroborate (6.75 g, 45.6 mmol) was added over 5 min and this mixture was left to stir for 1 hour. The product was extracted with several 10 ml portions of dry Et_2O, until no further colour was observed in the organic layer. The solvent was then removed *in vacuo* to give a dark purple/brown solid of *1-methoxy-prop-2-yn-1-ylidene pentacarbonyl chromium(0)*, **55** (0.93 g, 31.3 %). δ_H NMR (400 MHz, $CDCl_3$) 4.31 (3H, br s, OCH_3), 5.26 (H, s, CH); δ_C NMR (100MHz, $CDCl_3$) 359.9 (Cr=C), 224.1 (CO_{trans}), 216.2 (CO_{cis}), 115.2 (CH), 80.0 (C), 67.1 (OCH_3).

3.3.2. Alkoxy-derived Fischer Carbenes

(a) Synthesis of 1-methoxy-2-methoxymethoxy-1-butylidene pentacarbonyl chromium(0)[53]

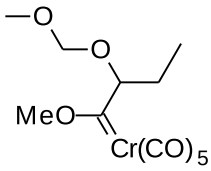

57a

Tributyl[1-(methoxymethoxy)butyl]stannane (**43a**, 1.0 g, 2.5 mmol) was dissolved in dry Et_2O (20 mL) at 0°C. TMEDA (0.38 ml, 2.5 mmol) was added to the cold solution, followed by the dropwise addition of *n*BuLi (1.8 M in hexane, 1.41 ml, 2.5 mmol). The solution was left to stir for 20 min. Chromium hexacarbonyl (0.50 g, 2.3 mmol) was crushed into a fine powder and added in small portions over 10 min and left to stir for 30 min in the cold and then a further 3 h at room temperature. The solvent was removed *in vacuo* and degassed water (20 mL) added to the residue. Trimethyloxonium tetrafluoroborate (1.50 g, 10.1 mmol) was added and the mixture was then left to stir for 30 min at room temperature. The carbene was extracted from the aqueous layer with dry Et_2O in small portions (5 x 5 mL) and placed into a Schlenk flask, where the solvent was removed *in vacuo* to afford **57a**, *1-methoxy-2-methoxymethoxy-1-butylidene pentacarbonyl chromium(0)*, as a yellow oil in combination with unreacted chromium hexacarbonyl and tetrabutyl tin as a side-product (0.26 g crude mass). δ_C NMR (100 MHz, C_6D_6) 362.8 (Cr=C), 223.1 (CO_{trans}), 216.8 (CO_{cis}), 96.0 (OCH_2), 78.6 (CH), 68.2 (OCH_3), 62.7 (OCH_3), 27.1 (CH_2), 19.3 (CH_3).

(b) Synthesis of 1-methoxy-2-methoxymethoxy-1-pentylidene pentacarbonyl chromium(0)[53]

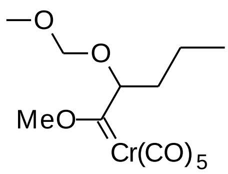

57b

Tributyl[1-(methoxymethoxy)pentyl]stannane (**43b**, 1.0 g, 2.5 mmol) was dissolved in dry Et_2O (20 mL) at 0°C. TMEDA (0.37 ml, 2.5 mmol) was added to the cold solution, followed by the dropwise addition of *n*BuLi (1.7 M in hexane, 1.44 ml, 2.5 mmol). The solution was left to stir for 20 min. Chromium hexacarbonyl (0.49 g, 2.2 mmol) was crushed into a fine powder and added in small portions over 10 min. The solution was left to stir for 30 min in the cold and then a further 3 h at room temperature. The solvent was removed *in vacuo* and degassed water (20 mL) was added to the residue. Trimethyloxonium tetrafluoroborate (1.45 g, 9.82 mmol) was added and the mixture left to stir for 30 min at room temperature. The carbene was extracted from the aqueous layer with dry Et_2O in several 10 ml portions which were placed into a Schlenk flask, where the solvent was removed *in vacuo* to afford **57b**, *1-methoxy-2-methoxymethoxy-1-pentylidene pentacarbonyl chromium(0)*, as a yellow oil in combination with unreacted chromium hexacarbonyl and tetrabutyl tin as a side-product (0.45 g crude mass). δ_C NMR (100 MHz, C_6D_6) 363.1 (Cr=C), 223.0 (CO_{trans}), 216.8 (CO_{cis}), 95.2 (OCH_2), 79.7 (CH), 68.2 (OCH_3), 62.7 (OCH_3), 39.2 (CH_2), 22.8 (CH_2), 14.3 (CH_3)

(c) Synthesis of 1-methoxy-2-methoxymethoxy-3-methyl-1-butylidene pentacarbonyl chromium(0)[53]

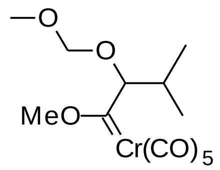

57c

Tributyl[1-(methoxymethoxy)-2-methylpropyl]stannane (**43c,** 1.0 g, 2.5 mmol) was dissolved in dry Et_2O (20 mL) at 0°C. TMEDA (0.37 ml, 2.5 mmol) was added to the cold solution, followed by the dropwise addition of *n*BuLi (1.7 M in hexane, 1.36 ml, 2.5 mmol). The solution was left to stir for 20 min. Chromium hexacarbonyl (0.49 g, 2.2 mmol) was crushed into a fine powder and added in small portions over 10 min. The solution was left to stir for 30 min in the cold and then a further 3 h at room temperature. The solvent was removed *in vacuo* and degassed water (20 mL) was added to the residue. Trimethyloxonium tetrafluoroborate (1.45 g, 9.82 mmol) was added and the mixture left to stir for 30 min at room temperature. The carbene was extracted from the aqueous layer using dry Et_2O in several 10 ml portions and placed into a Schlenk flask, where the solvent was removed *in vacuo* to afford **57c**, *1-methoxy-2-methoxymethoxy-3-methyl-1-butylidene pentacarbonyl chromium(0)*, as a yellow oil in combination with unreacted chromium hexacarbonyl and tetrabutyl tin as a side-product (0.31 g crude mass). δ_C NMR (100 MHz, C_6D_6) 362.8 (Cr=C), 224.8 (CO_{trans}), 216.8 (CO_{cis}), 97.7 (OCH_2), 87.8 (CH), 68.0 (OCH_3), 62.7 (OCH_3), 39.2 (CH), 24.2 (CH_3), 23.4 (CH_3).

3.3.3. Amino-derived Fischer Carbenes

*(a) Attempted synthesis of 1-methoxy-2'-[*N*-(tert-butoxycarbonyl)pyrrolidin]-methylidene pentacarbonyl chromium(0)*[53]

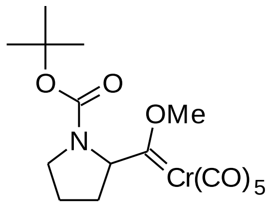

60a

tert-Butyl 2-(tributylstannyl)pyrrolidine-1-carboxylate (**50a**, 1.2 g, 2.6 mmol) was dissolved in dry Et_2O (20 mL) at 0°C. TMEDA (0.39 ml, 2.6 mmol) was added to the cold solution, followed by the dropwise addition of *n*BuLi (1.8 M in hexane, 1.45 ml, 2.6 mmol). The solution was left to stir for 20 min. Chromium hexacarbonyl (0.52 g, 2.3 mmol) was crushed into a fine powder and added in small portions over 10 min and the solution was left to stir for 30 min in the cold and then a further 3 h at room temperature. The solvent was removed *in vacuo* and degassed water (20 mL) was added to the residue. Trimethyloxonium tetrafluoroborate (1.54 g, 10.4 mmol) was added and the mixture then left to stir for 30 min at room temperature. The carbene was extracted from the aqueous layer with dry Et_2O in several 10 ml portions and placed into a Schlenk flask, where the solvent was removed *in vacuo* to afford a yellow residue. NMR analysis confirmed that the desired product, **60a**, *1-methoxy-2'-[N-(tert-butoxycarbonyl)pyrrolidin]-methylidene pentacarbonyl chromium(0)*, was not present.

(b) Attempted synthesis of 1-methoxy-2'-[N-(tert-butoxycarbonyl)piperdin]-methylidene pentacarbonyl chromium(0)[53]

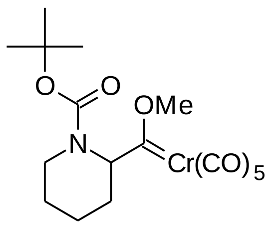

60b

tert-Butyl 2-(tributylstannyl)piperidine-1-carboxylate (**50b**, 1.2 g, 2.5 mmol) was dissolved in dry Et_2O (20 mL) at 0°C. TMEDA (0.38 ml, 2.5 mmol) was added to the cold solution, followed by the dropwise addition of *n*BuLi (1.8 M in hexane, 1.41 ml, 2.5 mmol). The solution was left to stir for

20 min. Chromium hexacarbonyl (0.50 g, 2.3 mmol) was crushed into a fine powder and added in small portions over 10 min and left to stir for 30 min in the cold and then a further 3 h at room temperature. The solvent was removed *in vacuo* and degassed water (20 mL) added to the residue. Trimethyloxonium tetrafluoroborate (1.50 g, 10.1 mmol) was added and then left to stir for 30 min at room temperature. The carbene was extracted from the aqueous layer with dry Et_2O in several 10 ml portions and placed into a Schlenk flask, where the solvent was removed *in vacuo* to afford a yellow residue. NMR analysis confirmed the desired product, **60b**, *1-methoxy-2'-[N-(tert-butoxycarbonyl)piperdin]-methylidene pentacarbonyl chromium(0)*, was not present.

(c) Attempted synthesis of 1-methoxy-2'-[N-(tert-butoxycarbonyl)piperdin]-methylidene pentacarbonyl chromium(0) without the use of stannanes

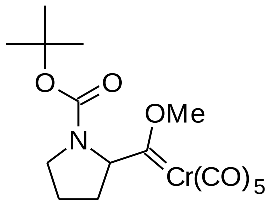

60a

*sec*BuLi (1.8 M in cyclohexane, 9.7 ml, 18 mmol) was added dropwise over 45 min *via* cannula to a solution of TMEDA (2.6 mL, 16 mmol) in dry Et_2O (30 mL) at -78°C. After 20 min, *tert*-butyl pyrrolidine-1-carboxylate (**49a**, 3.0 g, 18 mmol) was added. The mixture turned milky yellow during the addition and was stirred for 6 h. Chromium hexacarbonyl (3.47 g, 15.8 mmol) was crushed into a fine powder and added in small portions over 10 min and left to stir for 30 min in the cold and then a further 3 h at room temperature. The solvent was removed *in vacuo* and degassed water (20 mL) added to the residue. Trimethyloxonium tetrafluoroborate (10.4 g, 70.1 mmol) was added and then left to stir for 30 min at room temperature. The carbene was extracted from the aqueous layer with dry Et_2O in several 10 ml portions and placed into a Schlenk flask, where the solvent was removed *in vacuo* to afford a yellow residue. NMR analysis confirmed the desired product, **60a** *1-methoxy-2'-[N-(tert-butoxycarbonyl)piperdin]-methylidene pentacarbonyl chromium(0)*, was not present.

3.4. Imine Synthesis

(a) Synthesis of N-(phenylmethylidene)aniline

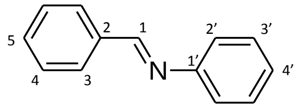

Benzaldehyde (4.85 g, 45.6 mmol), aniline (5.0 g, 53.7 mmol) and catalytic amounts of acetic acid (0.31 ml, 5.4 mmol) were added to a microwavable vial. This was irradiated in a microwave for 20 minutes at 50°C, at 150 W, to afford the desired product, *N-(phenylmethylidene)aniline* (8.00 g, 96.7%). δ_H NMR (400 MHz, $CDCl_3$) 8.49 (H, s, N=CH), 7.2-7.5 (9H, m,2x(3-CH), 2x(4-CH), 5-CH, 2x(2'-CH), 2x(3'-CH), 6.71 (H, t, 4'-CH); δ_C NMR (100 MHz, $CDCl_3$) 160.1 (C-1), 152.1 (C-1'), 136.2 (C-2), 131.5 (C-5), 129.3 (C-3), 128.9 (C-4), 128.9 (C-3'), 126.0 (C-4'), 120.1 (C-2').

Chapter 4: References

1. *Organometallics:* http://pubs.acs.org/page/orgnd7/about.html (accessed 08-02-2012)

2. Seyferth, D. *Organometallics*, **2001**, *20*, 1488-1498

3. Garst, J. F.; Ungvary, F., *Grignard Reagents*, John Wiley & Sons: New York, **2000**, pp 185-275, ISBN 0-471-99908-3.

4. The Official Website of the Nobel Prize - http://www.nobelprize.org/

5. Kealy, T. J.; Pauson, P. L. *Nature*, **1951**, *168*, 1039-1040

6. Wilkinson, G.; Rosenblum, M.; Whiting, M. C.; Woodward, R. B. *J. Am. Chem. Soc.*, **1952**, *74*, 2125-2126

7. Hoff, R.; Mathers, R. T., *Handbook of Transition Metal Polymerization Catalysts,* John Wiley & Sons, **2010**, ISBN 9780470504437

8. Heck, R. F.; Nolley, Jr., J. P. *J. Org. Chem.*, **1972**, *37*, 2320-2322

9. Crabtree, R. H. *The Organometallic Chemistry of the Transition Metals*, **2009**, Wiley, Wiley & Sons, Inc.. Hoboken, New Jersey, USA

10. McNaught, A. D.; Wilkinson, A. *IUPAC. Compendium of Chemical Terminology, 2nd ed. (the "Gold Book")*, **2006**, Oxford: Blackwell Scientific Publications

11. Hill, R. H.; Puddaphatt, R. J. *J. Am. Chem. Soc.*, **1985**, *107*, 1218-1225

12. Frankland, E. *J. Chem. Soc.*, **1849**, *2*, 263

13. Buckton, G. B. *Phil. Trans.*, **1859**, *149*, 417

14. Pope, W. J.; Peachey, S. J. *Proc. Chem. Soc.*, **1903**, *19*, 290.

15. Kuivila, H. G.; Menapace, H. G.; Warner, C. R. *J. Am. Chem. Soc.*, **1962**, *84*, 3584

16. Davies, A. G. *Organotin Chemistry*, **2003**, Wiley, Verlag GmbH & Co. KGaA, Weinheim, chpt 4

17. Koscheshkov, K. A. *Ber. Deutsch. Chem. Gesell.*, **1926**, *62*, 996

18. Luijten, J. G. A.; van der Kerk, G. J. M. *Investigations in the Field of Organotin Chemistry*, Tin Research Institute, Greenford, **1955**

19. Rosenberg, S. D.; Gibbons, A. J.; Ramsden, H. E. *J. Am. Chem. Soc.*, **1957**, *79*, 2137

20. Seyferth, D.; Harvey, H. M. *Inorg. Chem.*, **1963**, *2*, 652

21. Kocheshkov, K. A.; Nadi, M. M.; Aleksandrov, A. P. *Ber.*, **1934**, *67B*, 1348

22. Still, W. C., *J. Am. Chem. Soc.*, **1978**, *100*, 1481-1487

23. Still, W. C.; Sreekumar, C. *J. Am. Chem. Soc.*, **1980**, *102*, 1201

24. Beak, P.; Zajdel, W. J.; Reitz, D. B. *Chem. Rev.*, **1984**, *84*, 471-523

25. Beak, P.; Kerrick, S. T.; Wu, S.; Chu, J., *J. Am. Chem. Soc.* **1994***, 116*, 3231-3239.

26. Santiago, M.; Low, E.; Chambournier, G.; Gawley, R. E. *J. Org. Chem.*, **2003**, *68*, 8480-8484

27. Gawley, R. E.; Zhang, Q.; McPhail, A. T. *Tetrahedron: Asymm*, **2000**, *11*, 2093-2106

28. Beak, P.; Lee, W. K. *Tetrahedron Lett.*, **1989**, *30*, 1197-1200

29. Beak, P.; Lee, W. K. *J. Org. Chem.*, **1993**, *58*, 1109-1117

30. (a) Kitching, W.; Olszowy, H.; Waugh, J.; Doddrell, D., *J. Org. Chem.* **1978***, 43*, 898-906. (b) Clayden, J.; Greeves, N.; WarrGen, S.; Wathers, P. *Organic Chemistry*, Oxford University Press: New York, United States, **2001**

31. Granã, P.; Paleo, M. R.; Sardina, F. J. *J. Am. Chem. Soc.*, **2002**, *124*, 12511-12514

32. Clayden, J. *Organolithiums: Selectivity for Synthesis*; Tetrahedron Organic Chemistry Series; Elsevier Science LTD. Oxford, **2002**

33. Peterson, D. J. *J. Organomet. Chem.*, **1970**, *21*, 63

34. Peterson, D. J. *J. Am. Chem. Soc.*, **1971**, *93*, 4027

35. Peterson, D. J.; Ward, J. F. *J. Organomet. Chem.*, **1974**, *66*, 209

36. Burchat, A. F.; Chong, J. M.; Park, S. B. *Tetrahedron Lett.*, **1993**, *34*, 51

37. Chambournier, G.; Gawley, R. E. *Org. Lett.*, **2000**, *1*, 653

38. Gawley, R. E.; Zhang, Q. *Tetrahedron*, **1994**, *50*, 6077

39. Iula, D.; Gawley, R. E. *J. Org. Chem.*, **2000**, *65*, 6196

40. Coldham, I.; Dufour, S.; Haxell, T. F. N.; Howard, S.; Vennall, G. P. *Angew. Chem. Int. Ed.*, **2002**, *41*, 3887

41. Gawley, R. E.; Zhang, Q.; Campagna, S. *J. Am. Chem. Soc.*, **1995**, *117*, 11817

42. Coldham, I.; Fernandez, J.-C.; Snowden, D. J. *Tetrahedron Lett.*, **1999**, *40*, 1819

43. Tsunoda, T.; Fujuwara, K.; Yamamoto, Y.; Itô, S., *Tetrahedron Lett.*, **1991**, *32*, 1975-1978

44. Gawley, R. E.; Zhang, Q., *J. Am Chem. Soc.*, **1993**, *115*, 7515-7516

45. Gawley, R. E.; Klein, R.; Ashweek, N. J.; Coldham, I., *Tetrahedron*, **2005**, *61*, 3271-3280

46. Chambournier, G.; Gawley, R. E., *Org. Lett.*, **2000**, *2*, 1561-1564

47. Klein, R.; Gawley, R. E., *J. Am. Chem. Soc.*, **2007**, *129*, 4126-4127

48. Fürstner, A. *Chem. Rev.*, **1999**, *99 (4)*, 991-1046

49. Jolly, P. W. *Acc. Chem. Res.*, **1996**, *29 (11)*, 544-551

50. Zeiss, H. H.; Tsutsui, M. *J. Am. Chem. Soc.*, **1957**, *79 (12)*, 3062-3066

51. Wilke, G. *Angewandte Chemie*, **1963**, *75*, 10-20

52. Frémont, P.; Marion, N.; Nolan, S. T., *Coord. Chem. Rev*., **2009**, *253*, 862-892

53. Fischer, E. O.; Maasböl, A., *Angew. Chem.,* **1964**, *76*, 645

54. Fischer, E. O.; Maasböl, A. *Chemische Berichte*, **1967**, *100*, 2445-2456

55. Dötz, K. H. *Angew. Chem.*, **1975**, *87*, 672; *Angew. Chem., Int. Ed. Engl.*, **1975**, *14*, 644;

56. Reviews:
(a) Dötz, K. H. *Angew. Chem.,* **1984**, *96*, 573; *Angew. Chem., Int. Ed. Engl.,* **1984**, *23*, 587;
(b) Dötz, K. H.; Stendel, J. Jr., In *Modern Arene Chemistry*; Astruc, D., Ed.; Wiley-VCH: Weinheim, Germany, **2002**; pp 250–296;
(c) Ito, T.; Minato, M. In *Compounds of Groups 7–3, (Mn..., Cr..., V..., Ti..., Sc..., La..., Ac...) Science of Synthesis: Houben-Weyl Methods of Molecular Transformations*; Imamoto, T., Ed.; Thieme: Stuttgart, Germany, **2002**; pp 333–380. Vol. 2;
(d)Dötz, K. H.; Wenzel, B. Jr.; Jahr, H. C., *Top. Curr. Chem.,* **2005**, 248, 63;
(e) Waters, M. L.; Wulff, W. D., *Org. React*., **2008**, 70, 121;
(f) Couladouros, E. A.; Stromgilos, A. T., In *Quinones and Heteroatom Analogues Science of Synthesis Houben-Weyl Methods of Molecular Transformations*; Griesbeck, A. G., Ed.; Thieme: Stuttgart: Germany, **2006**; vol. 28, pp 217–322.

57. Mieusset, J.-L.; Brinker U. H., *J. Org. Chem.,* **2008**, *73*, 1553-1558

58. Schrock, R. R., *J. Am. Chem. Soc.*, **1974**, *96*, 6796

59. (a) Dewar, M. J. S., *Bull. Soc. Chim. Fr.,* **1951**, *18*, 79
(b) Chatt, J.; Duncanson, L. A., *J. Chem. Soc.*, **1953***,* 2929

60. Frenking, G.; Solà, M.; Vyboishchikov, S. F., *J. Organomet. Chem.,* **2005**, *690*, 6178-6204

61. Poater, J.; Cases M.; Fradera, X.; Duran, M.; Solà, M., *Chem. Phys.*, **2003**, *294*, 129-139

62. Ehlers, A. W.; Dapprich, S.; Vyboishchikov, S. F.; Frenking, G., *Organometallics*, **1996**, *15*, 105.

63. Cases, M.; Frenking, G.; Duran, M.; Solà, M., *Organometallics*, **2002**, *21*, 4182

64. Torrent, M; Duran, M.; Solà, M., *Organometallics,* **1998**, *17*, 1492

65. Vyboishchikov, S. F.; Frenking, G., *Chem. Eur. J.*, **1998**, *4*, 1428

66. Wang, C.-C.; Wang, Y.; Liu, H.-J.; Lin, K.-J.; Chou, L.-K.; Chan, K.-S., *J. Phys. Chem.*, **1997**, *101*, 8887

67. Block, T. F.; Fenske, R. F., *J. Am. Chem. Soc.*, **1977**, *99*, 4321

68. Dötz, K. H., *Angew. Chem. Int. Ed. Engl.*, **1975**, 14, 644

69. Bernasconi, C. F.; Perez, G. S., *J. Am. Chem. Soc.*, **2000**, *122*, 12441

70. Bernasconi, C. F.; Ali, M.; Lu, F., *J. Am. Chem. Soc.*, **2000**, *122*, 1352

71. Harrison, J. F.; Liedtke, C. R.; Liebman, J. F., *J. Am. Chem. Soc.*, **1979**, *101*, 7162

72. Irikura, K. K.; Goddard, W. A.; Beauchamp, J. L., *J. Am. Chem. Soc.*, **1992**, *114*, 48

73. (a) Öfele, K., *J. Organometallic Chem.*, **1968**, *12*, 42;
(b) Öfele, K.; Roos, E.; Herberhold, M., *Naturforsch*, **1976**, *31*, 1070

74. Wanzlick, H.-W.; Schönherr, H.-J., *Angew. Chem.*, **1968**, *80*, 154; *Angew. Chem., Int. Ed. Engl.*, **1968**, *7*, 141

75. Herrmann W. A.; Köcher, C., *Angew. Chem.*, **1997**, *109*, 2257; *Angew. Chem., Int. Ed. Engl.*, **1997**, *36*, 2162

76. Arduengo A. J. III; Harlow, R. L.; Kline, M., *J. Am. Chem. Soc.*, **1991**, *113*, 361

77. Crudden, C. M.; Allen, D. P., *Coord. Chem. Rev.*, **2004**, *248*, 2247

78. Barluenga, J.; Vicente, R.; López, L. A.; Tomás, M., *J. Organometallic Chem.*, **2006**, *691*, 5642

79. Sierra, M. A.; Mancheño, M. J.; Gómez-Gallego, M., *Acc. Chem. Res.*, **2005**, *37*, 44

80. Göttker-Schnettmann, I.; Aumann, R.; Bergander, K., *Organometallics*, **2001**, 3574

81. Sander, W.; Kötting, C.; Hübert, R., *J. Phys. Org. Chem.*, **2000**, *13*, 561.

82. (a) Bach, R. D.; Su, M.-D.; Aldabbagh, E.; Andrés, J. L.; Schlegel, H. B., *J. Am. Chem. Soc.*, **1993**, *115*, 10237
(b) Ulman, M.; Grubbs, R. H., *Organometallics*, **1998**, *17*, 2484
(c) Volland, M. A. O.; Hansen, S. M.; Rominger, F.; Hofmann, P., *Organometallics*, **2004**, *23*, 800

83. (a) Occhipinti, G.; Jensen, V. R., *Organometallics,* **2011**, *30*, 3522–3529
(b) Occhipinti, G.; Bjørsvik, H.-R.; Jensen, V. R., *J. Am. Chem. Soc.*, **2006**, *128*, 6952.

84. Hoye, T. R.; Chen, K.; Vyvyan, J. R., *Organometallics*, **1993**, *12*, 2806-2809

85. Fischer, E. O.; Kollmeier, H.-J., *Chem. Ber.*, **1971**, *104*, 1339

86. Fischer, E. O.; Leupold, M.; Krieter, C. G.; Müller, J., *Chem. Ber.*, **1972**, *105*, 150

87. Casey, C. P.; Burkhardt, T. J., *J. Am. Chem. Soc.*, **1973**, *95*, 5833

88. Semmelhack, M. F.; Lee, G. R., *Organometallics*, **1987**, *6*, 1839-1844

89. Dötz, K. H.; Stendel, J. Jr., *Chem. Rev.,* **2009**, *109*, 3227-3274

90. (a) Barluenga, J.; Vicente, R.; López, L. A.; Rubio, E.; Tomás, M.; Álvarez-Rúa, C., *J. Am. Chem. Soc.*, **2004**, *126*, 470;
(b) Barluenga, J.; Vicente, R.; Barrio, P.; López, L. A.; Tomás, M., *J. Am. Chem. Soc.*, **2004** , *126*, 5974;
(c) Barluenga, J.; Vicente, R.; Barrio, P.; López, L. A.; Tomás, M.; Borge, J., *J. Am. Chem. Soc.*, **2004**, *126*, 14354;
(d) Barluenga, J.; Vicente, R.; Barrio, P.; López, L. A.; Tomás, M., *J. Am. Chem. Soc.*, **2006**, *128*, 7050;
(e) Barluenga, J.; Barrio, P.; López, L. A.; Tomás, M.; Garcıá-Granda, S.; Álvarez-Rúa, C., *Angew. Chem. Int. Ed.*, **2003**, *42*, 3008

91. Romero, P. E.; Whited, M. T.; Grubbs, R. H., *Organometallics*, **2008**, *27*, 3422-3429

92. Matsuyama, H.; Nakamura, T.; Iyoda, M., *J. Org. Chem.* **2000**, *65*, 4796-4803

93. McGuire, M. A.; Hegedus, L. S., *J. Am. Chem. Soc.*, **1982**, *104* , 5538

94. (a) Schwindt, M. A.; Miller, J. R.; Hegedus, L*., J. Organometallic Chem*., **1991**, *413*, 143–153.
(b) Hegedus, L. S., In *Comprehensive Organometallic Chemistry II*; Abel, E. W., Stone, F. G. A., Wilkinson, G., Eds.; Pergamon: Oxford, **1995**; *Vol. 12*, p 549.
(c) Hegedus, L., *Acc. Chem. Res*., **1995**, *28*, 299–305.
(d) Hegedus, L., *S. Tetrahedron,* **1997**, *53*, 4105–4128.

95. Hegedus, L. S.; de Weck, G.; D'Andrea, S., *J. Am. Chem. Soc.*, **1988**, *110*, 2122

96. Köbbing, S.; Mattay, J., *Tetrahedron Lett.*, **1992**, *33*, 927-930

97. Fernández, I.; Cossio, F. P.; Sierra, M. A., *Acc. Chem. Res.,* **2011**, *44*, 479-490

98. Lage, M. L.; Fernández, I.; Mancheño, M. J.; Sierra, M. A., *Inorg. Chem.,* **2008**, *47*, 5253-5258

99. Fernández, I.; Sierra, M. A.; Mancheño, M. J.; Gómez-Gallego, M.; Cossio, F. P., *J. Am. Chem. Soc.*, **2008**, *130*, 13892-13899

100. Wrighton, M. *Chem. Rev.,* **1974**, *74,* 401-430

101. Arrieta, A.; Cossio, F. P.; Fernández, I.; Gómez-Gallego, M.; Lecea, B.; Mancheño, M. J.; Sierra, M. A., *J. Am. Chem. Soc.,* **2000**, *122*, 11509-11510

102. Turro, N. J., in *Modern Molecular Photochemistry*, University Science Books, Sausalito, CA, **1991**

103. Barluenga, J.; Fañanás-Mastral, M.; Aznar, F.; Valdés, C., *Angew. Chem.*, **2008**, *120*, 6696–6699; *Angew. Chem. Int. Ed.*, **2008**, *47*, 6594–6597

104. Barluenga, J.; Fañanás-Mastral, M.; Fernández, A.; Aznar, F., *Eur. J. Org. Chem.*, **2011**, 1961–1967

105. Srivastava, P.; Sarkar, A.; Sawoo, S.; Chakraborty, A.; Dutta, P.; Bouloussa, O.; Méthivier, C.; Pradier, C. M.; Boujday, S.; Salmain, M., *J. Organometallic Chem.,* **2011**, *696,* 1102-1107

106. Samanta, D.; Faure, N.; Rondelez, F.; Sarkar, A., *Chem. Commun*., **2008**, 1186-1187

107. Sawoo, S.; Dutta, P.; Chakraborty, A.; Mukhopadhyay, R.; Bouloussa, O.; Sarkar, A., *Chem. Commun.*, **2008**, 5957-5959

108. Maiorana, S.; Licandro, E.; Perdicchia, D.; Baldoli, C.; Vandoni, B.; Giannini, C.; Salmain, M., *J. Mol. Cat A: Chem.*, **2003**, *204-205*, 165-175

109. Salmain, M.; Licandro, E; Baldoli, C.; Maiorana, S.; Tran-Huy, H.; Jaouen, G., *J. Organometallic Chem.*, **2001**, *617-618*, 376

110. Fernandes, R. A.; Chaven V. P., *Tetrahedron: Asymmetry*, **2011**, *22*, 1312-1319

111. (a) Ushiyama, K.; Tanaka, N.; Ono, H.; Ogata, H., *J. Antibiot*., **1971**, *24*, 197;
(b) Tanaka, N.; Ogata, H.; Ushiyama, K.; Ono, H., *J. Antibiot*., **1971**, *24*, 222.

112. Mukherjee, S.; Roy, P.; Ghorai, B. K., *Synthesis*, **2011**, *9*, 1419-1426

113. Kim, S.; Choi, S. Y.; Lee, Y. T.; Park, K. H.; Sitzmann, H.; Chung, Y. K., *J. Organomet. Chem.*, **2007**, *692*, 5390-5394

114. Artillo, A.; Sala, G. D.; de Santis, M.; Llordes, A.; Ricart, S.; Spinella, A., *J. Organometallic Chem.*, **2007**, *692*, 1277-1284

115. Lee, H-S.; Tuckerman, M. E. *J. Phys. Chem.*, **2006**, *61*, 3259-3267

116. Hehre, W. J.; Yu, J.; Kluzinger, P. E.; Lou, L. *A Brief Guide to Molecular Mechanics and Quantum Chemical Calculations*; Wavefunction, Inc.: Irvine, **1998**

117. *Roadmap for Computational Chemistry*, **1999**, Council for Chemical Research (final version accessible at http://www.chemicalvision2020.org/pdfs/compchem.pdf)

118. McWeeny, R.; Sutcliffe, B. T., in *Methods of Molecular Quantum Mechanics*, Acad. Press, London, **1969**

119. Fermi, E. *Z. Phys*, **1928**, *48*, 73

120. Thomas, L. H. *Proc. Camb. Phil. Soc.*, **1927**, *23*, 542

121. Hohenberg, P.; Kohn, W. *Phys. Rev.*, **1964**, *136 (3B)*, B864-B871

122. Kohn, W.; Sham, L. J. *Phys. Rev, **1965**, 140, 1133*

123. Harrison, N. M. *Introduction to* DFT:
http://www.ch.ic.ac.uk/harrison/Teaching/DFT_NATO.pdf (Accessed 27-02-2012)

124. Capelle, K. *A bird's-eye view of density-functional theory, v6, Braz. J. Phy.*, **2006**, accessible at: http://arxiv.org/abs/cond-mat/0211443

125. Hood, R. Q.; Chou, M. Y.; Williamson, A. J.; Rajagopal, R.; Needs, R. J.; Foulkes, W. M. C. *Phys. Rev. Lett.,* **1997**, *78*, 3350

126. Perdew, J. P. *et al*., *Phys. Rev.,* **1992**, *46*, 6671-6687

127. Moruzzi, V. L.; Janek, J. F.; Williams, A. R., in *Calculated Electronic Properties of Metals*, Pergamon, New York, **1978**

128. Kurth, S.; Perdew, J. P.; Blaha, P. *Int. J. Quant. Chem.*, **1999**, *75*, 889

129. Adamo, C.; Ernzerhof, M.; Scuseria, G. E. *J. Chem. Phys.*, **2000**, *112*, 2643

130. Perdew, J. P.; Burke, K.; Ernzerhof, M. *Phys. Rev. Lett.*, **1996**, *77*, 3865

131. Becke, A. D. *Phys. Rev. A*, **1988**, *38*, 3098

132. Lee, C. T.; Yang, W. T.; Parr, R. G. *Phys. Rev. B*, **1998**, *37*, 785

133. Becke, A. D. *J. Chem. Phys.*, **1993**, *98*, 5648

134. Heyd, J.; Scuseria, G.; Ernzerhof, M. *J. Chem. Phys.*, **2003**, *118*, 8207

135. Cancio, A.; Chou, M. Y.; Hood, R. O. *Phys. Rev. B*, **2002**, *64*, 115112

136. García-González, P. *Phys. Rev. A*, **2000**, *62*, 2321

137. Kurth, S.; Perdew, J. P.; Blaha, P. *Int. J. of Quant. Chem.*, **2000**, *75*, 889

138. Adamo, C.; Ernzerhof, M.; Scuseria, G. E. *J. Chem. Phys.*, **2000**, *112*, 2643

139. IUPAC. Compendium of Chemical Terminology, 2nd ed. (the "Gold Book"). Compiled by A. D. McNaught and A. Wilkinson. Blackwell Scientific Publications, Oxford (1997). XML on-line corrected version: http://goldbook.iupac.org (2006-) created by M. Nic, J. Jirat, B. Kosata; updates compiled by A. Jenkins. ISBN 0-9678550-9-8. doi:10.1351/goldbook.

140. Pauling, L. *J. Am. Chem. Soc.*, **1947**, *69*, 542

141. Wiberg, K. A. *Tetrahedron*, **1968**, *24*, 1083

142. Mayer, I. *Chem. Phys. Lett.*, **1983**, *97*, 270

143. Mayer, I. *Int. J. Quantum Chem.*, **1984**, *26*, 151

144. Bridgeman, A. J.; Cavigliasso, G.; Ireland, L. R.; Rothery, J. *J. Chem. Soc., Dalton Trans.*, **2001**, *14*, 2095

145. Bridgeman, A. J.; Halcrow, A.; Jones, M.; Krausz, E.; Solanki, N. K. *Chem. Phys. Lett.*, **1999**, *314*, 176

146. Coulson, C. A. *Proc. R. Soc. London*, *Ser. A*, **1939**, *169*, 413

147. Mulliken, R. S. *J. Chem. Phys.*, **1955**, *23 (10)*, 1833-1831

148. Fu, Z.-W.; Qin, Q.-Z. *J. Electrochem. Soc.*, **2000**, *147*, 4610

149. Vayenas, C. G.; Conway, B. E.; White, R. E. *Modern Aspects of Electrochemistry, Volume 36*, Kluwer Academic/Plenum Publishers, New York, **2003**

150. Kohn, W., *Rev. Mod. Phys.,* **1999**, *71*, 1253

151. Pople, J., A. *Rev. Mod. Phys.,* **1999**, *71*, 1267

152. Jones, R. O.; Gunnarsson, O., *Rev. Mod. Phys.,* **1989**, *61*, 689-746

153. Segall, M. D., *Phys. Rev.,* **1998**, *57*, 4618-4621

154. Shah, R.; Payne, M. C.; Lee, M.-H.; Gale, J. D., *Science*, **1996**, *271*, 1395-1397

155. Rutter, M. J.; Heine, V., *J. Phys.: Cond. Matter*, **1997**, *9*, 2009-2024

156. Zend, W.-S.; Heine, V.; Jepson, O., *J. Phys.: Cond. Matter*, **1997**, *9*, 3489-3502

157. Kirchhoff, F., *J. Phys.: Cond. Matter*, **1996**, *8*, 9353-9357

158. Kohn, W.; Becke, A. D.; Parr, R. G., *J. Phys. Chem.*, **1996**, *100*, 12974-12980

159. Payne, M. C., *Rev. Mod. Phys.,* **1992**, *64*, 1045-1097

160. Chen, Y.; Zhao, L.; Xu, C. M.; Liu, Z. C.; Frenking, G. *J. Mol. Struct.*, **2009**, *905*, 40-43

161. Ducéré, J. M.; Goursot, A.; Berthomieu, D. *J. Phys. Chem. A.*, **2005**, *109*, 400-408

162. Vogel, A. I.; Tatchell, A. R.; Furnis, B. S.; Hannaford, A. J.; Smith, P. W. G., *Vogel's Textbook of Practical Organic Chemistry*, (5^{th} Ed), Pearson Education Limited England, **1996**, ISBN-13: **978-0582462366**

163. Behling, J. R.; Ng, J. S.; Babiak, K. A.; Campbell, A. L.; Elsworth, E.; Lipshutz, B. H., *Tetrahedron Lett.*, **1989**, *30*, 27

164. Farina, V.; Farina, V. *J. Org. Chem.* **1991***, 56*, 4985.

165. Wrackmeyer, B. *J. Organometal. Chem.*, **1978**, *145*, 183-188

166. Hani, R.; Geanangel, R. A. *Coordination Chem. Rev.*, **1982**, *44*, 229-246

167. McManus, J.; Cunningham, D.; Hynes, M. J. *J. Organometal. Chem.*, **1994**, *468*, 87-92

168. Kofron, W. G.; Yeh, M. K., *J. Org. Chem.*, **1976**, *41*, 438

169. Kofron, W. G.; Baclawski, L. M., *J. Org. Chem.*, **1976**, *41*, 1879-1880

170. Sawyer, J. S.; Kucerovy, A.; Macdonald, T. L; McGarvey, G. J., *J. Am. Chem. Soc.*, **1988**, *110*, 842-853

171. Brückner, R.; Wender, P. *Organic Mechanisms: Reactions, Stereochemistry and Synthesis*, Springer-Verlag Berlin Heidelberg, **2010**, ISBN: 978-3-642-03650-7

172. Meyer, A. Masters Thesis, Rhodes University, Department of Chemistry, **2011**

173. Lötz, S.; Crause, C.; Olivier, A. J.; Liles, D. C.; Görls, H.; Landman, M.; Bezuidenhout, D. I., *Dalton Trans.,* **2009**, 697–710

174. Hegedus, L. S.; McGuire, M. A.; Schultze, L. M., *Org. Synth.,* **1987***, 65*, 140-144

175. Danheiser, R. L.; Romines, K. R.; Koyama, H.; Gee, S. K.; Johnson, C. R.; Medich, J., *Org. Syn.,* **1993***, 71*, 133-138.

176. (a) Guzen, K. P.; Guarezemini, A. S.; Orfao, A. T. G.; Cella, R.; Pereira, C. M. P.; Stefani, H. A., *Tetrahedron Lett.*, **2007**, *48*, 1845
(b) Tabatabaee, M.; Heravi, M. M.; Sharif, M.; Esfandiyari, F., *E-J. of Chem.*, **2011**, *8*, 535-540
(c) Saini, A. K.; Carlin, C. M.; Patterson, H. H., *J. Polym. Sci. A Polym. Chem.*, **1993**, *31*, 2751–2758

177. Fu, N.; Tidwell, T. T. *Tetrahedron*, **2008**, *64*, 10465

178. Ashworth, I. W.; Cox, B. G.; Meyrick, B., *J. Org. Chem.*, **2010**, *75*, 8117-8125

179. (a) Basavaiah, D.; Rao, A. J.; Satyanarayana, T., *Chem. Rev.*, **2003**, *103*, 811-891
(b) Basavaiah, D.; Rao, V. K.; Reddy, R. J., *Chem. Soc. Rev.*, **2007**, *36*, 1581-1588

180. Perdew, J. P.; Wang, Y., *Phys. Rev. B.*, **1992**, *45*, 13244-13249